THE UNIVERSITY *of* EDINBURGH

Redox regulation of Salicylic acid biosynthesis by S-nitrosylation

Samuel Casasola Zamora

THE UNIVERSITY *of* EDINBURGH

Thesis submitted for the degree of

Doctor of Philosophy

University of Edinburgh

School of Biological Science

2019

Declaration

I hereby declare that the work presented here is my own except where explicitly stated in the text* and has not been submitted in any form for any degree at this or any other university.

Samuel Casasola Zamora

* The first and second round screening of mutagenized *PR1::LUC par2-1* lines shown in **Figure 7.3** were conducted in collaboration with Akmal Adilah Idris.

Abstract

A general outcome of plant-pathogen interactions is the oxidative and nitrosative burst, characterized for the accumulation of reactive oxygen and nitrogen species (ROS and RNA) which coordinate signalling cascades. Among RNS, Nitric oxide (NO) stands as a key signalling molecule in different physiological processes including plant immunity. An established mechanism for the transfer of NO bioactivity is S-nitrosylation (SNO), the reversible binding of a NO molecule to the thiol group of a susceptible cysteine, allowing specific proteins to respond to changes in the cellular REDOX state.

The first genetic evidence about the role of NO in plant immunity was noted in *Arabidopsis thaliana* plants carrying a loss-of-function mutation of the *S-nitrosoglutathione (GSNO) reductase 1 (GSNOR1)* gene. This mutation resulted in increased total cellular S-nitrosylation and compromised basal, non-host and R-gene mediated immunity, and impaired synthesis and accumulation of the immune activator salicylic acid (SA). SA plays a pivotal role in the regulation of basal and systemic resistance. It is mainly produced by the activity of the enzyme Isochorismate Synthase 1 (ICS1) in response to pathogens.

To date, significant progress has been achieved in understanding the mechanisms by which S-nitrosylation regulates SA signalling. However, the molecular mechanisms by which NO regulates SA biosynthesis remains elusive.

To investigate if NO mediates transcriptional or posttranscriptional regulation over *ICS1* expression we generated the reporter line *ICS1::GUS.* Our data suggest that *ICS1* is subjected to transcriptional repression by S-nitrosylation. In agreement with previous observations about inhibition of the DNA-binding of SARD1 to the *ICS1* promoter upon S-nitrosylation of SARD1 at Cysteine 438. We observed a significant reduction in the binding affinity of recombinant wild type (WT) SARD1 but not in SARD1 with a Cystein 438 to Serine mutation. To expand this observations and investigate the biological relevance of S-nitrosylation of Cys438 we generated transgenic lines expressing a C-terminal HA and Nano luciferase SARD1 and SARD1C438S fusion proteins.

We showed that SARD1 can be S-nitrosylated *in vivo.* We did not observe any difference in local immunity against *Pseudomonas syringae* infection between the WT and C438S lines. Interestingly, the SARD1C438S lines showed impaired activation of

systemic acquired resistance (SAR) compared to the WT. In addition, we observed that SARD1 protein level follows a circadian rhythm after SA treatment, which was impaired in the C438S mutant, suggesting that S-nitrosylation of SARD1 is necessary for optimal activation of SAR. It is possible that S-nitrosylation of SARD1 coordinates protein-protein interactions between SARD1 and other SAR activators.

We developed a strategy to express and purify recombinant SARD1 for structural studies. Solving the three-dimensional structure of SARD1 can foster our understanding on the molecular interactions behind the regulation of SARD1. Finally, we designed a forward mutant screening to search for second-site mutations that can suppress the *gsnor1* phenotype, which we speculate could be related with a novel mechanism for GSNO-turnover or NO metabolism. Collectively, our work can contribute to integrate NO cues in the regulation of SA biosynthesis and suggests a role for S-nitrosylation of SARD1 in systemic immunity.

Lay Summary

Through their lifetime, plants interact with a diverse collection of potentially pathogenic microorganisms. Plant disease represents one of the main threats to crop productions. However, plants have evolved sophisticated defence mechanisms to prevent microbial infection. In response, some few specialised microorganisms have developed strategies to overcome plant defences and promote disease. The activation of plant defences encompasses the production and accumulation of signalling molecules, such as reactive oxygen and nitrogen species (ROS and RNS) and salicylic acid (SA), to activate the expression of defence genes at the infection site. SA is a plant hormone considered as a master activator of plant defences against biotrophic microorganisms, including local defence and priming defences in uninfected leaves allowing plants to respond faster in the case of a secondary infection. SA is produced in response to pathogens via the activity of the enzyme isochorismate synthase 1 (ICS1). Given its importance in immunity, plants must ensure that SA is produced rapidly after the infection occurs, and its accumulation is stopped after the infection has been contained.

To do this, plants incorporate ROS and RNS mediated posttranslational protein modifications (PTMs) into the signalling events during plant immunity. Among the PTMs, S-nitrosylation, the addition of a Nitric Oxide (NO) molecule to a protein, stands as a central mechanism to regulate plant immunity. It is well documented that S-nitrosylation plays a significant role in controlling the expression of defence genes downstream of SA accumulation. However, the mechanism by which S-nitrosylation controls SA biosynthesis remains poorly understood. Our research suggests that S-nitrosylation can contribute to regulating SA biosynthesis by controlling the activity of the protein SARD1 (Systemic Acquired Resistance 1), one of the main proteins that promote the expression of *ICS1*. We observed that upon S-nitrosylation the ability of SARD1 to bind to its target DNA is reduced, potentially influencing the timing and the extent of SA accumulation during the immune response. The tight regulation of SA accumulation allows plants to efficiently fight infections without significantly compromising development. Further research is needed to understand if S-nitrosylation of SARD1 is required to prime defences in systemic leaves after a primary infection. Our work can contribute to expanding our understanding of how plants regulate the activation of plant immunity, potentially allowing us to engineer crops that can respond faster to bacterial infections in the future.

Contents

Chapter 1 Introduction

Introduction

During their lifetime, plants encounter a vast number of potentially pathogenic microorganisms. However, plants have evolved a sophisticated and efficient network of defence mechanisms resulting in plant disease being a rare outcome (Spoel & Dong, 2012).

Plant defences are organised as sequential layers of protection. As a first layer, plants develop physical barriers to prevent the entrance of microbial pathogens into the plants. In the second level of defence, plants incorporated pathogen recognition receptors (PRR) that recognise highly conserved pathogen/microbe-associated molecular patterns (PAMPs or MAMPs). The activation of the PRR by the recognition of a potential pathogen induces PAMP-triggered immunity (PTI), which encompass the expression of defence genes and the accumulation of antimicrobial compounds to prevent further colonisation of the pathogen (Dodds & Rathjen, 2010).

In response, some specialised pathogens evolved effector proteins aimed to highjack PTI and promote infection. Plants have counteracted this threat by developing a third layer of defence, consisting of R-proteins, which are cytoplasmic receptors that can recognise effectors directly or effectors' activity indirectly. The recognition of an effector initiates effector-triggered immunity (ETI) characterised by a stronger immune response accompanied by the hypersensitive response (HR) that results in localised cell death at the infection site to prevent further spread. As an additional level of defence, plants developed systemic acquired resistance (SAR) that provides a long-lasting and broad-spectrum immunity allowing plants to initiate a faster and stronger response against secondary infections (Kachroo & Kachroo, 2018; Fu & Dong, 2013).

The activation of immune responses depends on a complex network of physiological changes and molecular interactions mediated in a significant part by the production of reactive oxygen and nitrosative species (Mittler, 2017). Also, the immune activator salicylic acid (SA) plays a central role in mediating resistance against biotrophic pathogens and in the establishment of (SAR) (Fu & Dong, 2013).

Plant defences are very effective at repelling potential infections, with only a small subset of highly specialised pathogens being able to overcome plants defences and promote disease. Significant progress has been made in understanding the molecular mechanisms behind the activation of plant immunity (Spoel & Dong, 2012). Recent research highlights the importance of redox-based post-translational modification in the fine-tuning and regulation of immune responses (Mittler, 2017). Among these modifications, S-nitrosylation, the reversible binding of a nitric oxide (NO) molecule to a rare, highly reactive protein Cysteine (Cys) thiol (SH) group to form an S-nitrosothiol (SNO), enables a protein to function as a molecular switch mediating signalling cascades in response to changes in the redox state (Yu *et al*, 2012; 2014).

The first genetic evidence of S-nitrosylation modulating plant immunity was noted in *Arabidopsis* plants with a knock-out mutation of the *S-nitrosoglutathione reductase 1 (gsnor1)* gene. These plants exhibited increased cellular S-nitrosylation and compromised basal, non-host, and *R-gene* mediated immunity, linked with reduced and delayed SA-biosynthesis and signalling (Feechan *et al*, 2005).

To date, the development of molecular and biochemical techniques for the identification of S-nitrosylation such as the biotin-switch assay (Jaffrey & Snyder, 2001) have contributed to insights into how NO mediates SA-signalling via S-nitrosylation. However, the mechanisms by which this post-translational modification regulates SA-biosynthesis remain unexplored.

This chapter will focus on introducing the current knowledge on the role of NO and SA in the regulation of plant immunity and the establishment SAR.

Nitric Oxide

NO is a highly active gaseous molecule recognised as an essential signalling regulator in both plants and animals. It has been associated with the regulation of different physiological and cellular responses (Hancock & Whiteman, 2016). In mammals, NO is mainly produced by the activity of the enzyme nitric oxide synthase (NOS). In humans, the NOS family consists of three main isoforms. The neuronal (nNOS/NOS1) and endothelial (eNOS/NOS3) isoforms are expressed constitutively, and their activity relies on intracellular calcium (Ca^{2+}) levels.

In contrast, inducible NOS (iNOS/NOS2) ACTIVITY IS Ca^{2+}-independent. The structural analysis of the three mammalian isoforms showed that they share a similar

overall structure, consisting of an N-terminal oxygenase domain (NOSoxy) and a C-terminal reductase domain (NOSred) linked by a calmodulin-binding motif. The N-terminal domain mediates homodimerization and protein-protein interactions. The binding of calmodulin promotes conformational changes of the homodimer required for the enzymatic activity (Jeandroz *et al*, 2016; Santolini *et al*, 2017).

The NOS enzymes catalyse the conversion of L-arginine to L-citrulline and NO in a two-step oxidation reaction. During catalysis, the NOSoxy domain binds a heme prosthetic group and the redox factor tetrahydrobiopterin (BH4). The NOSred domain transfer electrons provided by NADPH to the heme group via the cofactors Flavin mononucleotide (FMN) and Flavin adenine dinucleotide (FAD) in the presence of oxygen.

NO production in plants

Given the physiological importance of NO, intensive work has been undertaken to identify the mechanisms for NO production in plants. However, the precise molecular mechanisms for NO production in plants are not fully understood. The evidence suggests that NO can be produced by two main routes; a reductive route via the reduction of nitrites to NO and an oxidative route via the oxidation of aminated molecules (Astier *et al*, 2017).

Reductive pathway for NO production

Nitric oxide can be produced from different routes and different substrate in non-enzymatic reactions under specific conditions. For instance, the reduction of nitrite (NO_2^-) to NO can occur under actively reducing or under low pH environments in the presence of a high nitrite concentration (Astier *et al*, 2017).

Nitrate Reductase (NR)

In addition, different enzymes have been reported to mediate the reduction of NO_2^- to NO. The cytoplasmic enzyme nitrate reductase (NR) catalyses the reduction of nitrate (NO_3^-) to NO_2^- in an NADH dependent reaction, also using molybdopterin, heme and FAD as cofactors. NR represents the first rate-limiting step for nitrate assimilation. Notably, this enzyme can also exhibit NO_2^- to NO reductase (Ni-NR) activity. Under normal conditions, the alternative Ni-NR activity occurs with lower efficiency compared to the NO_3^- to NO_2^- conversion, exhibiting a K_m of 100 µM for NO_2^-

compared with 10 µM for NO_3^-. However, the Ni-NR activity can be increased under low oxygen or an acidic environment.

In *Arabidopsis,* the genes *NIA1* and *NIA2* code for NR, with *NIA2* playing a more significant role for the NR activity. The genetic evidence for the importance of NR in the production of NO comes from the fact that the *nia1, nia2* and the *nia1nia2* plants are severely impaired in NO production in different physiological processes, including stomatal movement, hormonal responses, abiotic stress responses and floral and root development (Wilkinson & Crawford, 1991; Astier *et al*, 2017).

NO:NOFNiR mechanism in *Chlamydomonas reinhardtii*

An additional mechanism for NO production by NR was discovered recently in the microalgae *Chlamydomonas reinhardtii.* It was observed that NR could interact with the partner protein NOFNiR (nitric oxide-forming nitrite reductase) and catalyse the reduction of NO_2^- to NO in an NADPH dependent reaction using electrons supplied by the diaphorase activity of NR (NADPH -> NR -> electron acceptor). The NOFNiR enzyme belongs to the family of the amidoxime reducing component (ARC) protein family. Currently, two mitochondrial *Arabidopsis* ARC genes have been identified (Chamizo-Ampudia *et al*, 2016), with mARC isoform 2 exhibiting *in-vitro* NO-producing activity when incubated with NO_2^- in a reducing environment (Yang *et al*, 2015). Currently, a NO:NOFNiR mechanism similar to that present in *C reinhardtii* has not been described in higher plants. However, further research may demonstrate the role of this mechanism to fine-tune NO production in plants (Chamizo-Ampudia *et al*, 2016, 2017).

Ni:NOR plasma membrane-bound NR

Additional to the cytoplasmic NR enzyme, a nitrite to NO reduction activity was observed in membrane fractions obtained from *Nicotiana tabacum* roots. The putative enzyme was defined as plasma membrane-bound nitrite:NO reductase (NiNOR) and was proposed to reduce NO_2^- to NO using cytochrome *C* as an electron donor and showed maximum activity at low oxygen concentrations and under acidic conditions (Stöhr *et al*, 2001). The underlying mechanism suggests that NiNOR would reduce NO_2^- produced from NO_3^- by an apoplastic membrane-bound nitrate reductase (PM-NR). However, the identity of NiNOR remains unknown (Astier *et al*, 2017; Santolini *et al*, 2017).

Molybdoenzymes

A common feature between NR and NOFNiR is the existence of a molybdenum cofactor (Moco) in their structure, which acts as a redox chromophore (Yang *et al*, 2015). In plants, different Moco containing enzymes have been described with a potential NO-producing activity (Astier *et al*, 2017; Santolini *et al*, 2017).

Xanthine oxidases (XO)

The enzyme xanthine oxygenase (XO) was first described in mammals and is the enzyme responsible for purine catabolism, the conversion of hypoxanthine to xanthine and subsequently xanthine into urea. Plants contain two *XO* genes which are proposed to contribute to REDOX homeostasis during immune reactions by promoting the production of superoxide anions (O_2^-) during the ROS burst and ureic acid-mediated hydrogen peroxide removal in chloroplasts (Ma *et al*, 2016). Notably, phosphorus deprived white lupin (*Lupinus albus*) roots showed increased NO production which was reduced when the samples were treated with the XO and NOS inhibitors, but not with a NR inhibitor. Furthermore, it was also observed that the gene *LaXDH* was overexpressed in phosphorus deprivation, suggesting that the XO pathway was involved in NO production under these conditions (Wang *et al*, 2010). However, evidence of the role of XO in NO production in other plants is limited and the *in vitro* experiments to produce NO by recombinant XO were unsuccessful (Astier *et al*, 2017).

Aldehyde oxidases (AOs) and Sulphite oxidases (SOs)

The AO enzymes exhibit significant structural similarity with XOs; they participate in the production of O_2^- by catalysing the oxidation of aldehydes into carboxylates. Additionally, their NO_2^- into NO reduction activity has been reported in mammalian systems. In plants, they participate in abscisic acid (ABA) and indole-3-acetic acid (IAA) synthesis and ROS production. However, no direct evidence has been reported about their capacity to produce NO in plants (Astier *et al*, 2017).

Similarly, SOs catalysed the oxidation of sulphite to sulphate in an O_2-dependent mechanism, and the mammalian isoform has been shown to reduce NO_2^- into NO *in vitro* under low oxygen conditions. No evidence about its participation in NO-production in plants is available, and its role is thought to be in the sulphate assimilation pathway (Yarmolinsky *et al*, 2012; Astier *et al*, 2017).

Mitochondrial electron transport chain

In addition, Gupta *et al*, (2005) described an alternative NO_2^- to NO production mechanism involving the mitochondrial electron transport. They observed that root segments of *NR* knockout plants could produce NO under anoxic conditions, which was blocked by the addition of mitochondrial electron transport inhibitors. Further characterisation of the mechanism showed that the reaction occurred at the mitochondrial membrane but not at the mitochondrial matrix and was restricted to root tissue, considering that the reaction is inhibited by oxygen (Gupta & Kaiser, 2010; Gupta & Igamberdiev, 2011). The production of NO from mitochondria electron transport components has been shown to occur in different higher plant species, including *Arabidopsis,* barley, pea and tobacco and may play a role in signalling regulation processes (Astier *et al*, 2017).

Oxidative pathway for NO production

In mammals, NOS plays a significant role in NO production. Pioneering work using plant extracts in a reaction containing all the NOS cofactors and using radiolabelled arginine as a substrate to measure the conversion of arginine into citrulline suggested the existence of NOS-like activity in plants. A protein displaying NOS-like activity was isolated from tobacco extracts by this biochemical approach. Further characterisation of the protein demonstrated that the protein belongs to the glycine decarboxylase complex and that it is not involved in NO production (Santolini *et al*, 2017; Astier *et al*, 2017).

Guo F.Q. *et al*, (2003) used a genetic approach and identified a gene with sequence similarity to a protein implicated in NO biosynthesis from the snail *Helix pomatia*. They observed that an *Arabidopsis* line carrying a T-DNA insertion in the second exon of the target gene showed impaired NO production and named the gene as *NOS1.* Further characterisation of the gene revealed that the gene belonged to the GTPase family and was renamed as *NO-associated 1 (NOA1)*. In subsequent experiments, a *NOS* gene was identified from the marine unicellular algae *Ostreococcus tauri* which exhibit significant sequence similarity to the human eNOS. *Arabidopsis* plants expressing the *OtNOS* gene under the control of the inducible promoter of the sunflower *Hahb-4* gene displayed higher NO accumulation compared with plants transformed with the empty vector, suggesting that higher plants contain all the necessary cofactors to support NOS-like activity (Foresi *et al*, 2015).

The evidence mentioned above demonstrates the existence of NOS-like activity in plants. However, significant debate arises from the approaches used to measure NOS-like activity. For instance, the arginine assay is based on measuring the reduction of the radiolabelled arginine and not in the formation of radiolabelled citrulline as a product. The inaccuracy of the arginine assay was later demonstrated by the fact that the arginine-dependent activity measured from *Arabidopsis* extract produced argininosuccinate (AS) instead of citrulline. In subsequent experiments, the production of NO was measured using chemiluminescent methods and electron paramagnetic resonance, demonstrating the existence of NOS-like activity in plants extract, strictly dependent on the presence of arginine, NADPH and different NOS cofactors. These observations, together with the finding of a *NOS* gene from *O. tauri* suggests the existence of a *NOS* gene in the plant lineage, however, no homologous gene has been found in higher plants (Santolini *et al*, 2017; Astier *et al*, 2017)

In a recent study, Jeandroz *et al*, (2016) used the datasets generated from the 1000 Plants international consortium (1KP) to search for transcripts coding for plant NOS-like proteins. From their analysis, no related NOS-like sequence was identified from the 1080 sequenced transcriptomes of land plants, and only 15 out of 265 of the analysed algal genomes contained NOS-like sequences. This fact suggests that instead of producing NO through NOS-like enzymes, land plants may have evolved regulated NO_3^- assimilation and reduction mechanisms for NO production. Additionally, the possibility of a protein, or complex of proteins with NOS-like activity conformed by the interactions of different protein domains, not evident at the sequence level, cannot be discarded (Jeandroz *et al*, 2016; Santolini *et al*, 2017).

Evidence for oxidative NO-production pathway

The existence of NOS-like activity in plants has been described by different approaches and for different plant species. For instance, the measurement of NO produced by chemiluminescent means rather than on arginine reduction provides a more accurate visualisation of the NOS-like enzymatic activity. Additionally, different reports using a pharmacological approach based on the use of NOS inhibitors, mainly arginine analogues such as NG-Nitro-L-arginine methyl ester (L-NAME), convey in the general conclusion of impaired NO production mediated by NOS inhibition (Astier *et al*, 2017).

Arginine mediated NO-production

The observed reduction of NO production upon NOS inhibition suggests the existence of a possible arginine-mediated route for NO-production. Interestingly, the *Arabidopsis* mutant *nox1*, which exhibits high NO production, carries a loss-of-function mutation in a chloroplast phosphoenolpyruvate/phosphate translocator, which results in higher arginine accumulation (Frungillo *et al*, 2014). In plants, arginine metabolism involves the activity of arginase, which catalyse the conversion of arginine into ornithine and urea. Interestingly, *Arabidopsis* plants with reduced arginase activity displayed higher NO production, while overexpression resulted in impaired NO accumulation (Flores *et al*, 2008; Shi *et al*, 2013).

Additionally, arginine can be decarboxylated into agmatine by the activity of the enzyme arginine decarboxylase (ADC). In *Arabidopsis*, agmatine is the primary precursor for the biosynthesis of polyamines (PA), and two *ADC* genes of chloroplastic origin have been reported. The overexpression of the pepper *ADC* gene in tobacco cells resulted in increased PA accumulation and higher NO production. Conversely, the *Arabidopsis adc2.1* mutant, impaired in PA synthesis, showed impaired NO accumulation in response to iron deficiency (Zhou *et al*, 2016). The central PAs found in plants are spermine, spermidine and putrescine. Previous research has shown that exogenous spermine application can induce NO production in *Arabidopsis* seedlings, consistent with the genetic evidence regarding PA synthesis. Furthermore, the compiled data supports the existence of an oxidative pathway for NO production in plants, connected to arginine metabolism. However, the precise molecular mechanism remains elusive (Santolini *et al*, 2017; Astier *et al*, 2017).

NO Signalling

RNS and ROS interactions

NO has been the focus of intensive research over the past decades. However, the molecular mechanisms behind its production, sensing and signal transduction remain poorly characterised. A hallmark of aerobic metabolism is the formation of oxygen and nitrogen derived free radicals (ROS and RNS, respectively), which play a critical role in signalling during different physiological processes. The interplay between ROS and RNS, together with the source of ROS/RNS, cellular localisation and the turnover of

ROS/RNS pools determine the specificity of REDOX signalling (Foyer & Noctor, 2015).

The interactions of RNS, ROS and other reactive groups form the cornerstone to address the complexity of NO signalling. For instance, O_2^- and NO interact with each other to form peroxynitrite ($ONOO^-$), the reaction of NO with a thiol group (SH) forms an S-nitrosothiol (SNO), and glutathione (GSH) and NO react to form S-nitrosoglutathione (GSNO). The products of these reactions have potential signalling activities on their own, and the individual forming components are removed from the cell during the reaction (Hancock *et al*, 2018).

The spatial and temporal distribution of the reactive molecules in the cell promotes the formation of specific signalling products that determine a specific cellular outcome. Commonly, NO and SNO are present in minimal concentrations in the cell under basal conditions; their concentrations increase in response to different stimuli. Importantly, other reactive molecules, such as hydrogen sulphide (H_2S), can suppress NO/ROS-mediated signalling, suggesting that the signalling event is arrested until a threshold level is achieved (Hancock, 2019).

Hancock, (2019) describes the consideration of REDOX chemistry to determine how NO impacts on REDOX state and the REDOX state influence NO signalling. The outcome of ROS and NO interaction depends on which reactive species are present at a specific time. NO can exist in the radical form (NO) but also as nitroxyl (NO^-), and nitrosonium (NO^+) and the cellular REDOX state can influence the presence of an isoform of NO.

The cellular REDOX state can be estimated from the total concentration of glutathione, taking as input both the reduced (GSH) and oxidised (GSSG) glutathione concentration expressed as an oxidised:reduced (ox:red) ratio.

The redox status of an experimental solution (E_h) can then be estimated using the ox:red ratio and the mid-point potential (E_m) of the reactive species being studied. These values are subsequently used in the Nernst equation to calculate the REDOX potential E_h (Hancock, 2019).

$$\mathrm{E_h} = \mathrm{E}_{m\ (pH\ 7.4)} + \frac{RT}{\mathrm{nF}} \times 2.303\ \mathrm{Log}\frac{[\mathrm{OX}]}{[\mathrm{Re\,d}]}$$

Where:

E_h = Redox potential
$E_{m(pH7.4)}$ = Midpoint potential of the REDOX couple at pH 7.4
R = Gas constant
T = Temperature (Kelvin)
F = Faraday constant
n = number of electrons used in oxidation/reduction

The cellular REDOX potential estimated from GSH concentrations indicates that the cellular state is modified depending on the increase or decrease of GSH concentrations. Also, signalling molecules can modify the GSH ratio. For instance, the formation of GSNO from NO and GSH will reduce the GSH availability, affecting and the overall REDOX ratio (Hancock *et al*, 2018; Hancock, 2019). Various signalling molecules, including NO, can exist as REDOX couples in an oxidised/reduced state in response to the cellular environment. Each redox couple has an E_m associated with their interconversion and the change between states allow them to exert their biological function. The cellular REDOX state can favour the formation of one member of the REDOX couple over the other.

An example of how the REDOX state can influence RNS couples comes from the NO^- /NO^- singlet couple, with an estimated E_m of -350 mV. The cellular REDOX status has been estimated in different systems with a cellular average of -242 mV. Interestingly, the cellular environment was observed to become more oxidising during cell differentiation (-200 mV) and apoptosis (-170 mV). Therefore, the change from -242 mV to – 200 or -170 mV during the transition from normal to differentiation or apoptosis REDOX state of the cell will promote the NO state, which is considered to be the signalling form of this molecule, suggesting that a more oxidising state promotes NO signalling to drive differentiation and apoptosis (Hancock, 2019).

Additionally, cells have evolved specialised buffering systems to regulate the cellular REDOX homeostasis, including the GSH:GSSG, the ascorbate: dehydroascorbate (AsA:DHA) system, and also other low molecular weight (LMW) thiols, all present in millimolar cellular concentrations. The high concentrations of GSH, AsA and LMW thiols suggest that ROS alone will not be sufficient to generate a significant impact in the global REDOX state. A possibility to explain the oxidising environment in

differentiation and apoptosis can be as a mechanism to promote the existence of a partner in a REDOX couple over the other (Hancock *et al*, 2018).

Cells maintain a highly reduced cellular state to allow physiological functions and stabilise cofactors, such as NADH, and to allow REDOX signalling. Driving the cellular fate toward an oxidising environment is commonly recognised as oxidative stress. Also, the formation of NO and RNS under reducing conditions will shorten NO/RNS half-life further.

The fact that different intracellular pathways are compartmentalised suggests that the REDOX status can also be compartmentalised (Hancock, 2019). Therefore, a small increase in REDOX amount in a specific cellular compartment (organelle or a cytoplasmic section) can have a significant effect on the proteins and molecules in the proximity, despite it representing a minimum effect in the global cellular REDOX state (Hancock, 2019). Therefore, the compartmentalisation of NO and interacting partners could play a critical role in triggering signalling events and aiding signalling specificity (Hancock, 2019).

NO bioactivity

A proposed mechanism by which plants interpret these RNS and ROS cues, and transfer their bioactivity to trigger specific responses is through REDOX bases post-translational modifications (PTMs) (Umbreen *et al*, 2019). Generally, amino acids containing sulphur, such as cysteine (Cys) are targets for PTMs. The hydrogen atom in the sulfhydryl (-SH) of Cys residues facilitates the interaction of this amino acid with other reactive groups. For instance, the interaction of two SH groups forms a disulphide (S-S) bond, which helps to stabilise protein structure (Umbreen *et al*, 2019).

The three-dimensional structure of proteins is determined by the interaction of the amino acid sequence and their intrinsic hydrophilic/hydrophobic properties. As a result, most Cys residues are embedded within the secondary protein structure, and only a small subset of proteins contain rare surface exposed Cys residues that exhibit a low pKa SH group to support REDOX modifications. This characteristic allows specific proteins to act as molecular switches, sensing the cellular REDOX state (Yu *et al*, 2014; Spadaro *et al*, 2010).

Likewise, both ROS and RNS can promote PTMs targeting the SH group of the susceptible cysteine residues. For example, H_2O_2 can oxidise the SH group to sulfenic

acid (SOH), sulfinic acid (SO_2H) and sulfonic acid (SO_3H) depending on the H_2O_2 concentration, with SO_3H being an irreversible modification (Yu *et al*, 2014). Also, the SH group can be targeted by NO (S-nitrosylation), glutathione (S-glutathionylation) and H_2S (S-sulfhydration), resulting in a competition between the reactive molecules for the susceptible thiol groups. Each modification will trigger a different outcome, potentially altering the protein function. However, a particular modification can be favoured by the cellular REDOX state, the concentration and the proximity of the reactive partners (Hancock *et al*, 2018; Hancock, 2019).

S-nitrosylation

Among these modifications, S-nitrosylation stands as a central mechanism to transfer NO bioactivity. S-nitrosylation refers to the covalent and reversible binding of a NO molecule to the SH group of a susceptible Cys to form an S-nitrosothiol (SNO), consistently altering protein function (Frederickson Matika & Loake, 2014). Growing evidence highlights the importance of S-nitrosylation mediating NO bioactivity. It has been shown to regulate diverse protein functions. For instance, it can promote protein translocation (Tada *et al*, 2008), regulate DNA binding (Tavares *et al*, 2014; Cui *et al*, 2018), enzymatic activity (Wang *et al*, 2009b; Yun *et al*, 2011), repress signalling (Feng *et al*, 2013), modify transcriptional dynamics (Chaki *et al*, 2015; Begara-Morales *et al*, 2014; Hussain *et al*, 2016), among other activities (Feng *et al*, 2019).

Interestingly, the S-nitrosylated/reduced state of a protein (R-SNO:R-SH) couple has an estimated E_m of -400 mV. An increasing cellular oxidising state will favour the R-SNO form, potentially driving S-nitrosylation signalling under cellular events such as cell differentiation, apoptosis or other physiological processes. Taken together, it is suggested that an increase in NO levels in response to an increasing oxidising state and compartmentalised NO and interacting protein partners can promote SNO signalling, driving a specific cellular outcome (Hancock *et al*, 2018; Hancock, 2019).

NO and GSNO

NO is a molecule with a relatively short half-life. The formation of SNO can increase its half-life and mediate the establishment of cellular SNO pools to aid signalling specificity. For instance, S-nitrosylation of the tripeptide GSH produces S-nitrosoglutathione (GSNO). GSH is considered as the most abundant source of thiol groups in the cell. Upon S-nitrosylation, GSNO acts as stable storage and transporter

of NO bioactivity by significantly extending its half-life, and allowing diffusion to different cellular compartments (Espunya *et al*, 2012). Additionally, GSNO can act as a selective *trans*-nitrosylating agent by transferring the SNO group to other susceptible proteins (Frungillo *et al*, 2014; Hancock *et al*, 2018).

Nitric Oxide in Plant immunity

The first genetic evidence about a link between plant immunity and S-nitrosylation came from the identification by a reverse genetic approach of the gene *GSNOR1* which controls the global cellular turnover of GSNO. GSNO is formed by S-nitrosylation of the antioxidant compound GSH, and it comprises a stable reservoir of NO bioactivity. Previous reports have shown that NR-derived NO inhibits GSNOR1 function through S-nitrosylation, which may be necessary to amplify the NO signal. Also, GSNO can act as a NO-donor and *trans*-nitrosylate other proteins (Feechan *et al*, 2005; Frungillo *et al*, 2014).

Interestingly, a loss-of-function mutation in *GSNOR1* resulted in an increased total cellular level of GSNO, comprising multiple aspects of plant immunity, including PTI and ETI. Furthermore, it was noted that the absence of GSNOR1 negatively affected the immune activator salicylic acid (SA) accumulation and produced delayed and reduced expression of SA-dependent genes (Feechan *et al*, 2005).

SABP3 carbonic anhydrase activity

Currently, molecular techniques such as the biotin-switch have allowed expanding our understanding of the molecular mechanism by which SNO regulated SA downstream signalling. For instance, S-nitrosylation of Cys280 of the SA binding protein 3 (SABP3) blocks the binding of SA to SABP3 and inhibits its carbonic anhydrase activity, required for lipid synthesis and the expression of defence genes. Therefore, S-nitrosylation of SABP3 can act as a negative feedback loop to modulates defence response (Wang *et al*, 2009b).

NPR1

Additionally, the central regulator of plant immunity response Non-expresser of pathogenesis-related genes 1 (NPR1) is proposed to localise to the cytoplasm under basal conditions, existing as an oligomer stabilised by disulphide bonds, presumably via Cys82 and Cys216. Upon pathogen infection, changes in the REDOX status promotes the reduction of the disulphide bonds by thioredoxin (TRX-*h5*) and allows monomerisation of NPR1 and its translocation into the nucleus to help drive SA-

dependent gene expression. Moreover, S-nitrosylation of Cys156 of NPR1 is thought to promote the formation of disulphide bonds and favour oligomer conformation, helping to maintain oligomer-monomer homeostasis of NPR1 (Tada *et al*, 2008; Spoel & Dong, 2012; Yu *et al*, 2014).

TGA1

Upon translocation into the nucleus, NPR1 interacts with the TGACG (TGA) transcription factors to drive the expression of *PR* genes. TGA1 has been shown to be S-nitrosylated at Cys260 and S-glutathionylated ay Cys266, which is thought to protect TGA from oxidative damage. *In vitro* characterisation of TGA1 in ab=n electromobility shift assay (EMSA) after treatment with GSNO, suggests the formation of disulphide bonds between Cys172 and Cys287. Additionally, enhanced DNA binding was observed upon GSNO treatment. Further experiments expressing TGA1 with Cys to serine (Ser) substitution of Cys172 and Cys287 in *Arabidopsis* plants *tga1 tga4* double mutants exhibited enhanced expression of *PR* genes, indicating that a reduced state of TGA1 is necessary for bioactivity and that GSNO-mediated modification positively affects its DNA binding (Lindermayr *et al*, 2010).

RBOH

During ETI, plants exhibit localised cell death (hypersensitive response) at the infection site to prevent further biotrophic pathogen growth. This outcome is supported by increased ROS accumulation via the activity of NADPH oxidases (*At*RBOH). The observation that *gsnor1-3* plants, with high GSNO accumulation, showed accelerated HR formation and also increased resistance to the avirulent pathogen *Hyaloperonospora arabidopsidis* Emwa1 as a result of the enhanced HR, indicating that NO can modulate cell death. The enzyme RBOH was found to be S-nitrosylated *in vivo* at Cys890. It is predicted that this modification prevents the interaction with the cofactor Flavin adenine dinucleotide (FAD) reducing ROS production and acting as a negative feedback regulation loop during late stages of the hypersensitive response (Yun *et al*, 2011).

SRG1

A recent publication has shown that the zinc finger transcription factor SRG1 can be S-nitrosylated both *in vitro* and *in vivo* preferentially at Cys87. SRG1 expression is induced by NO accumulation. Subsequently, SRG1 binds to the promoter region of its target genes, where it recruits the repressor TOPLESS, blocking gene expression.

Upon S-nitrosylation at Cys87, SRG1 binding affinity for its target promoters is reduced, removing the transcriptional repression. S-nitrosylation of SRG1 may participate in a negative feedback loop to regulate the extent of the immune response (Cui *et al*, 2018).

Significant progress has been made in understanding the role of S-nitrosylation in the modulation of SA-signalling and in regulating the activation and duration of the immune response (Fig 1.1). However, the molecular mechanisms by which this modification regulates SA biosynthesis remains poorly understood.

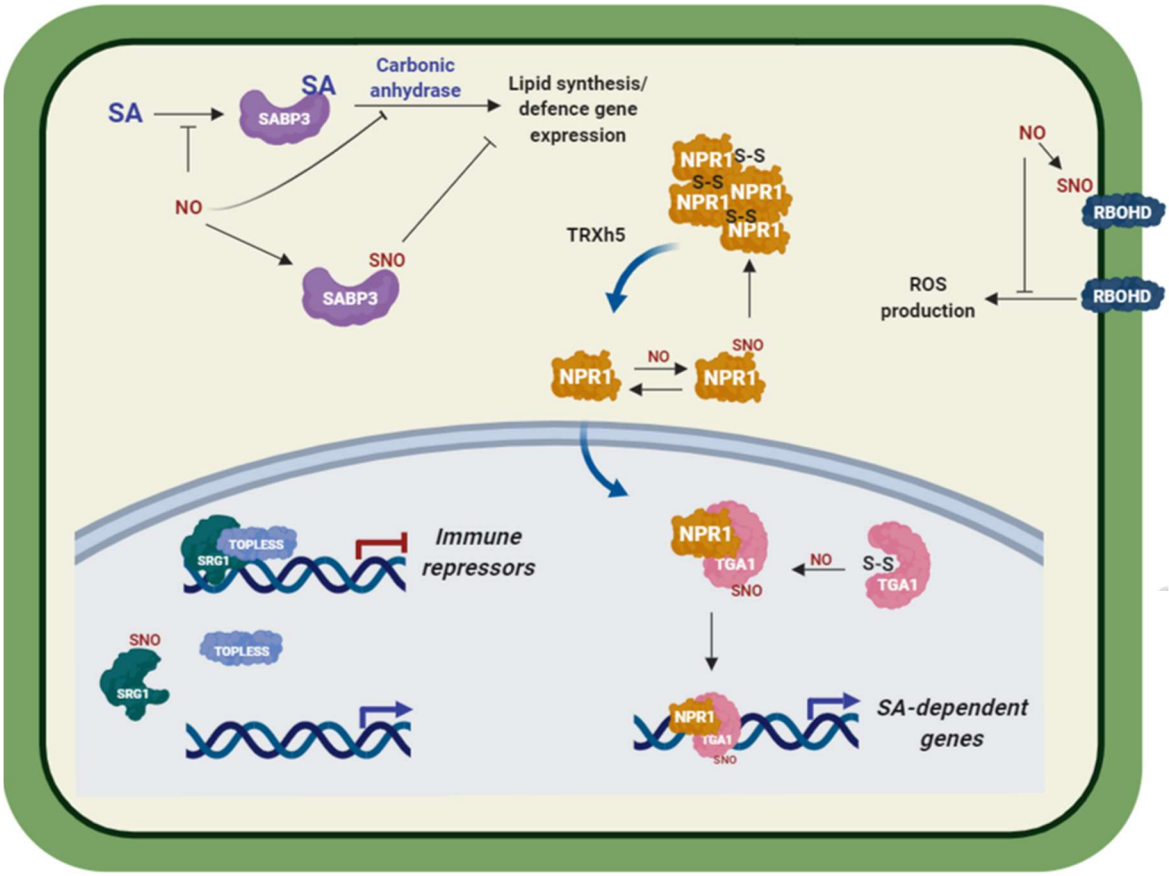

Figure 1.1. S-nitrosylation in plant immunity. The figure summarisea the role of S-nitrosylation in plant immunity. S-nitrosylation of the SA-binding protein 3 (SABP3) inhibits its carbonic anhydrase activity, preventing defence gene expression. Additionally, S-nitrosylation of NPR1 promotes its oligomer conformation. After pathogen challenge, SA-mediated REDOZ changes promote the reduction of NPR1 allowing its translocation into the nucleus, where NPR1 interacts with TGA TF to drive *PR* expression. S-nitrosylation of TGA1 enhances DNA binding to its target promoters. Additionally, S-nitrosylation of RBOHS prevents the interaction with cofactors and inhibits ROS production. Furthermore, SRG1 binds to its target promoters and recruits the repressor TOPLESS to transcriptionally repress its target genes. Upon S-nitrosylation of SRG1 its DNA-binding is reduces allowing the expression of immune repressors.

Salicylic acid

SA is a key hormone in plants, it is known to participate in the regulation of diverse physiological processes, involving development and defence (Vlot *et al*, 2009; Dempsey & Klessig, 2017). In plant immunity, SA mediates resistance against biotrophic pathogens. Upon pathogen infection, SA accumulation is required to induce the expression of *PR* genes and the biosynthesis of defence compounds.

In previous studies, *Arabidopsis* plants expressing the bacterial *salicylate hydroxylase (nahG)* gene which encodes an enzyme that hydrolases SA, are unable to accumulate SA and show enhances susceptibility to virulent and avirulent pathogens (Delaney *et al*, 1994). Interestingly, exogenous application of SA to these plants restores resistance against pathogen infection. Further, it has been shown that exogenous application of SA promotes the expression of SA-dependant defence genes and the establishment of systemic acquired resistance (SAR), providing broad-spectrum protection against different pathogens (Zhang *et al*, 2010).

SA biosynthesis in plant immunity

SA can be synthesised by two different metabolic pathways, from cinnamic acid via the enzyme Phenylalanine ammonia lyase (PAL) and from chorismate by the activity of the enzyme isochorismate synthase 1 (ICS1) (Dempsey *et al*, 2011; Wildermuth *et al*, 2001).

Also, it has been reported that some bacteria such as the *Pseudomonas aeruginosa* and *Pseudomonas fluorescence* can synthesise SA from chorismate in a two steps reaction involving the isomerisation of chorismate into iso-chorismate by the enzyme ICS and the consecutive processing into SA and pyruvate by the enzyme pyruvate lyase (IPL). Likewise, in *Yersinia enterocolitica* and *Mycobacterium tuberculosis* SA is produced directly from chorismate in a single coupled reaction catalysed by the bi-functional enzyme SA synthase (SAS) (Dempsey *et al*, 2011; Vlot *et al*, 2009).

In plants, chorismate is produced in the plastid (Fig 1.2). The fact that some plastid derived-pathways have a prokaryotic endosymbiotic origin suggested the possibility of the existence of a plant *ICS* gene. Wildermuth et al, (2001) identified two *ICS* genes (*ICS1* and *ICS2*) in the *Arabidopsis* genome by genetic analysis. The ICS genes share 83% sequence similarity (Dempsey et al, 2011). Further, the expression of *ICS1* was increased after infection with the pathogen *Golovinomyces orontii* and *P. syringae pv*

maculicula (Psm). It was also noted that the *ICS1* expression correlated with the expression of the *PR1* gene and with the accumulation of SA (Wildermuth *et al,* 2001).

Moreover, the *Arabidopsis* mutants *SA induction-deficient 2 (sid2-1)* and *enhanced disease susceptibility 16 (eds16)* accumulated only 5 to 10% SA after induction with virulent or avirulent pathogens relative to wild-type plants. These plant lines were shown to contain mutations in the *ICS1* gene. This evidence suggested that a significant proportion of SA produced in response to pathogen occurs through the ICS1 pathway (Wildermuth *et al*, 2001; Kumar, 2014; Zheng *et al*, 2012a; Dempsey *et al*, 2011).

Interestingly, the plant ICS1 contains a sixty-six N-terminal amino acid extension absent in the bacterial isoforms. This N-terminal peptide shows identity with the typical chloroplast transit sequence and is followed by a putative cleavage site, consistent with the proposed plastid origin of SA (Wildermuth *et al*, 2001). Significant efforts have been made to identify an enzyme exhibiting isochorismate pyruvate lyase activity to complete the metabolic pathway downstream of isochorismate for SA biosynthesis. However, despite the exhaustive search, no gene or enzyme had been identified (Dempsey & Klessig, 2017).

Different genetic evidence suggested an essential role for the MATE-transporter Enhanced Disease Susceptibility 5 (EDS5) and AvrPphB Susceptible 3 (PBS3) for SA accumulation in response to pathogens. EDS5 is localised on the chloroplast envelope and was thought to mediate the export of SA from the chloroplast to the cytoplasm (Serrano *et al*, 2013), while PBS3, which belongs to the GH3 acyl-adenylase enzyme family (Nobuta *et al*, 2007).

It was recently reported by two independent groups that EDS5 mediates the export of isochorismate to the cytoplasm and PBS3 promotes the conjugation of glutamate to isochorismate yielding isochorismate-9-glutamate. Notably, the product of this reaction was shown to decompose spontaneously into SA and enolpyruvyl-N-glutamate both *in vitro* and *in vivo*, completing the pathway for SA biosynthesis from chorismate (Fig 2.1) (Rekhter *et al*, 2019; Torrens-spence *et al*, 2019).

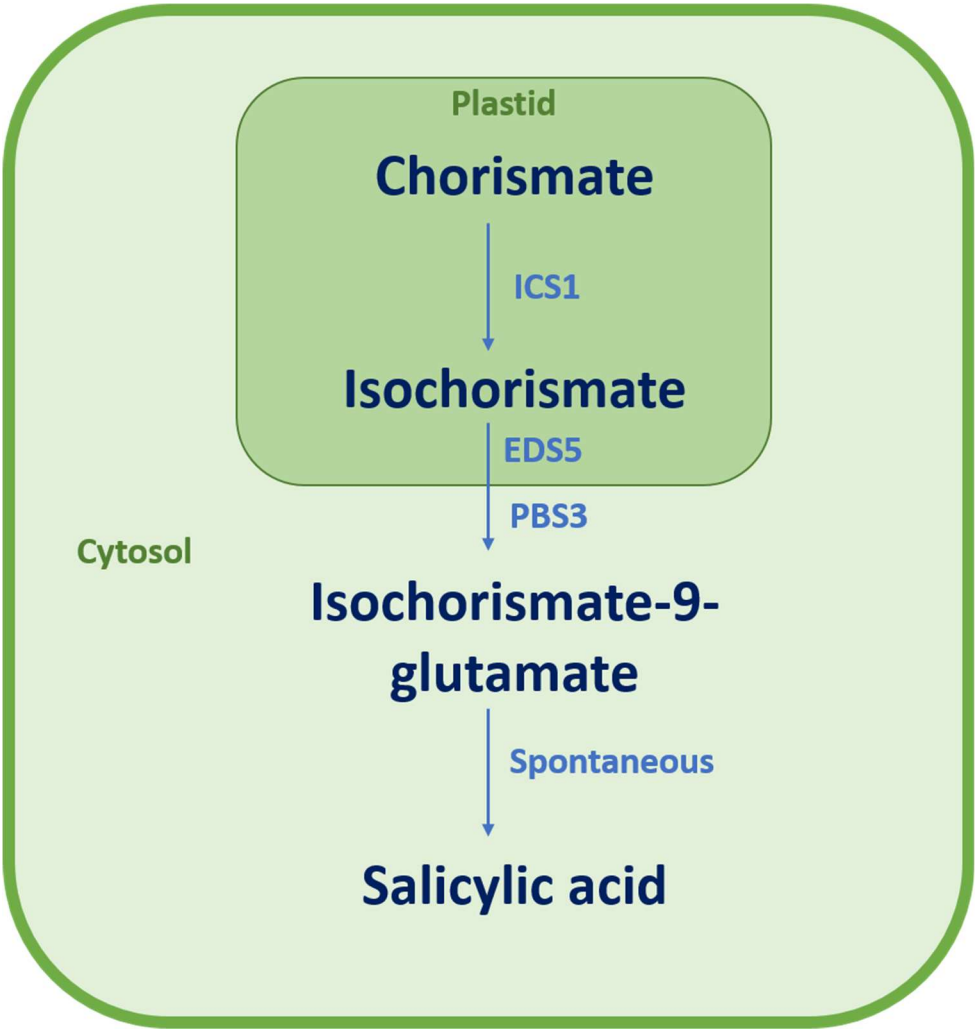

Figure 1.2. Schematic representation of Salicylic acid biosynthesis in plants in response to pathogens. Isochorismate Synthase 1 (ICS1), Enhanced Disease Susceptibility 5 (EDS5) and *avrPphB* susceptible 3 (PBS3). Adapted from Rekhter *et al,* 2019

Regulation of ICS1 expression for SA biosynthesis

To date, the critical role of ICS1 on SA biosynthesis and accumulation in response to pathogens has led to an intense search to identify transcription factors that can regulate *ICS1* expression.

Upstream SA biosynthesis

Different studies using *Arabidopsis* mutants have led to the identification of molecular components of SA-mediated signalling. The proteins enhanced disease susceptibility 1 (EDS1) and non-specific disease resistant 1 (NDR1) have been proposed to act upstream of SA accumulation preferentially during R-protein mediated immunity. EDS1 is associated with toll-interleukin-1 (TIR) receptor pathway and NDR1 with coiled-coil (CC) R-proteins (Aarts *et al*, 1998). EDS1, a putative lipase, physically

interacts with phytoalexin deficient 4 (PAD4) and senescence-associated gene 101 (SAG101) (Feys *et al*, 2001; Feys, 2005). EDS1 and PAD4 are proposed to act upstream of SA accumulation, *eds1* and *pad4* plants showed compromised SA accumulation in response to *Pseudomonas* infection, which could be reversed by exogenous SA application (Feys *et al*, 2001). Additionally, *ndr1* plants showed impaired *PR1* expression and SAR in response to avirulent *Pseudomonas* infection (Fig 1.3) (Shapiro & Zhang, 2001).

SARD1/CBP60g

The transcription factors SAR-Deficient 1 (SARD1) and Calmodulin Binding Protein 60g (CBP60g) stand as critical players driving *ICS1* expression. SARD1 was identified from a mutant screen of over 200 T-DNA insertion mutants looking for compromised systemic acquired resistance. Two SALK lines with an insertion in the gene *At1g73805* showed compromised SAR and was named as *SAR-Deficient 1 (SARD1)*. Overexpression of *SARD1* led to enhanced resistance to pathogens and increased free, and total SA. *SARD1* belongs to the ACBP60 protein family. It was noted that *cbp60g* plants also showed impaired SAR development, which was further increased in the *sard1cbp60g* double mutant, linked with a dramatic reduction in both free and total SA accumulation. Both proteins were shown to bind to the GAAATT motif in the *ICS1* promoter *in vitro*, and the binding to the *ICS1* promoter was confirmed *in vivo* (Zhang *et al*, 2010). These proteins are also suggested to be involved in the regulation of different aspects of plant immunity on the grounds of their ability to bind to the promoter of different genes related to both positive and negative regulation of plant immunity (Sun *et al*, 2015).

WRKY

The transcription factors WRKY28 and WRKY46 were identified to coexpress with *ICS1* under certain conditions in a coexpression analysis using 372 publicly available microarray data sets (van Verk *et al*, 2011a). It was later shown that WRKY28 and WRKY46 were able to induce the expression of *GUS* under the control of the *ICS1* promoter in a transactivation assay using *Arabidopsis* protoplasts. The binding site of WRKY28 was mapped to two WK-like boxes (TGAC) located at position -445 and -460 in the *ICS1* promoter (van Verk *et al*, 2011b).

TCP8 and TCP9

Wang *et al* (2015) performed a yeast one-hybrid approach to screen for *ICS1* regulators. They identified the transcription factor teosinte branched1/cycloidea/PCF 8 (TCP8) as a potential regulator if *ICS1* expression. The binding of TCP8 to the *ICS1* promoter was confirmed by EMSA and chromatin immunoprecipitation (ChIP) assays. Another member of the TCP family, TCP9 was observed to coexpress with *TCP8* and *ICS1* during plant immunity. Additionally, the *tcp8 tcp9* double mutant showed reduced *ICS1* expression together with higher susceptibility to *Pseudomonas syringae* infection (Wang *et al*, 2015).

NTL9 and CHE

In a similar experiment, Zheng *et al* (2015) identified the transcription factors NTM-like 9 (NTL9), and Circadian Clock Associated 1 (CCA1) hiking expedition (CHE/TCP21) as regulators of *ICS1* expression during specific immune responses following a yeast one-hybrid approach. NTL9 was related to *ICS1* expression in guard cells, mediating stomata closure during PTI. The *ntl9* mutant plants showed compromised stomata function, which could be rescued upon exogenous application of SA, linking NTL9 with *ICS1* expression in PTI. Additionally, CHE was found to participate in the circadian regulation of SA levels, which serves as a mechanism to prime defences at times of the day where pathogens show higher activity (Karapetyan & Dong, 2018). Also, CHE was proposed to regulate *ICS1* expression in distal leaves during SAR. Interestingly, the *che* mutant showed reduced *SARD1* and *CBP60g* expression, suggesting that the molecular mechanisms behind CHE regulation of *ICS1* could occur probably by modulating SARD1 and CBP60g expression. Interestingly, no TCP *cis*-elements are found within the promoter region of *SARD1* and *CBP60g*, suggesting an indirect regulatory mechanism (Zheng *et al*, 2015).

EIN3 and EIL1

In addition, different transcription factors involved in *ICS1* repression have been described. For instance, the ethylene insensitive 3 (EIN3) and EIN3-like 1 (EIL1) which are involved in the regulation of ethylene (ET)-dependent gene expression were found to repress *ICS1* expression. The *Arabidopsis* double mutant *ein3 eil1* showed constitutive activation of immune responses in the absence of a pathogen, whereas overexpression of these proteins increased susceptibility to bacterial infection. Additionally, both EIN3 and EIL1 were shown to bind to the *ICS1* promoter

in vitro and *in vivo*, together with higher *ICS1* expression and accumulation of free and total SA in the double mutant (Chen *et al*, 2009a).

ANAC019, ANAC055 and ANAC072

A study aiming to elucidate the coronatine-mediated virulence mechanisms of some virulent *Pseudomonas* strains led to the identification of the NAC (NAM/ATAF1, ARAF2/CUC2) family members ANAC019, ANAC055 and ANAC072 as negative regulators of *ICS1* expression. A common virulent strategy of adapted pathogens is to highjack hormonal signalling pathways to favour infection. It was observed that coronatine treatment induce the expression of ANAC019, 055 and 072, and plants showed reduced accumulation of SA via repression of *ICS1*. Additionally, the *nac019/055/072* triple mutant showed higher *ICS1* expression under basal conditions, and NAC019 was shown to bind to the *ICS1* promoter in vivo (Zheng *et al*, 2012).

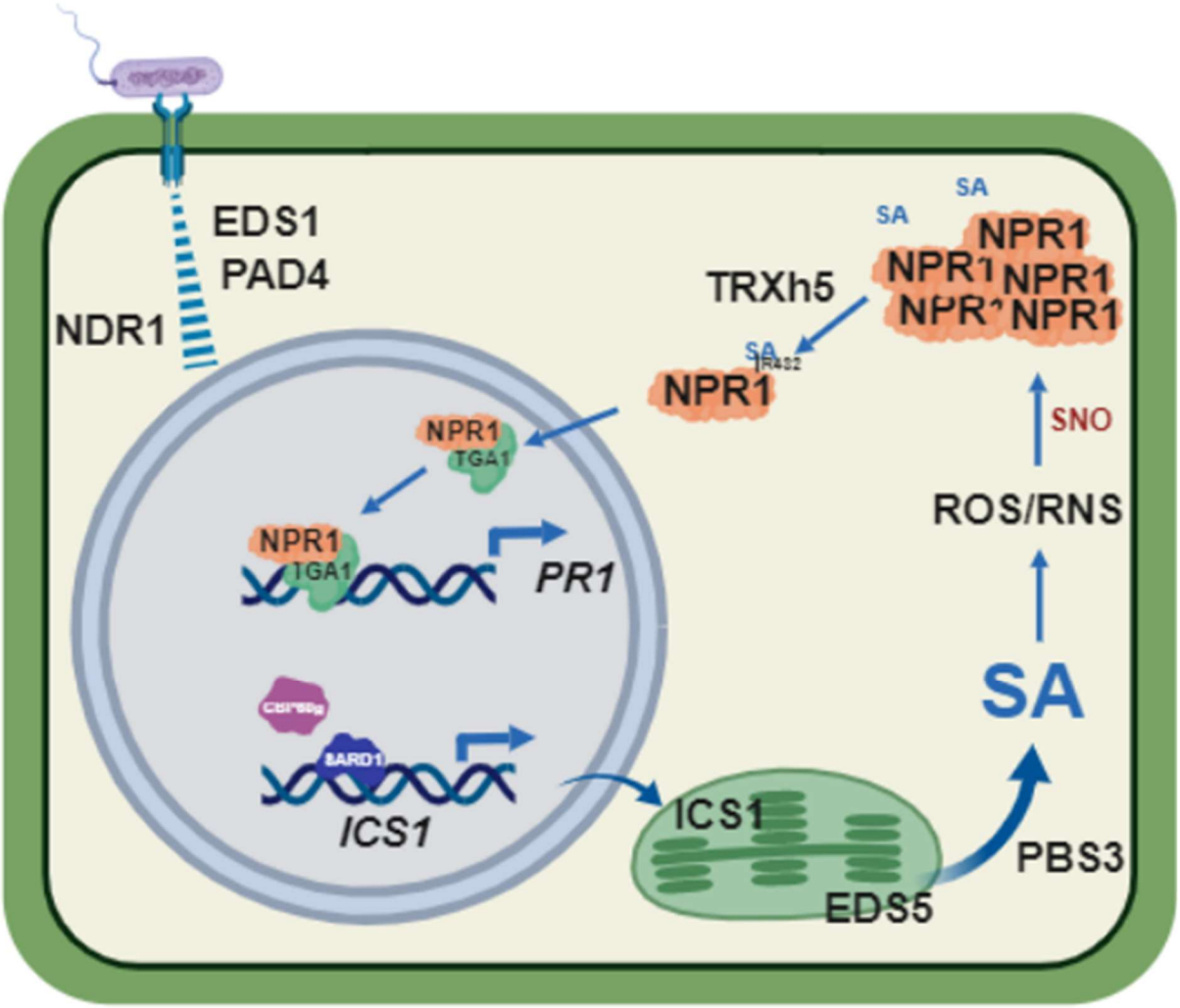

Figure 1.3. Schematic representation of SA-mediated signalling. The detection of a pathogen by pathogen recognition receptors triggers a signalling cascade that induces SA biosynthesis via the activity of ICS1. After accumulation of SA, SA mediates REDOX changes that promote the reduction of NPR1 oligomer and its translocation into the nucleus where it interacts with TGA TFs to drive SA-mediated gene expression.

SA signalling

The best characterised mechanism for SA-dependent gene expression is the NPR1-dependent pathway. Notably, *npr1 Arabidopsis* plants are impaired to activate immune responses in response to pathogen infection or exogenous SA-treatment, indicating that NPR1 acts downstream of SA accumulation. NPR1 contains two protein-protein interaction domains, ankyrin repeat and BTB/POZ domains, and a C-terminal nuclear localisation and trans-activation domain (Cao *et al*, 1997; Mou *et al*, 2003). Under basal conditions, NPR1 localises in the cytoplasm in an oligomeric conformation, stabilised by disulphide bonds. Upon infection, SA-mediated REDOX changes promote monomerisation of NPR1 via the activity of (TRX*h*5) and translocation into the nucleus where NPR1 acts as a cofactor for TGA TFs to drive the expression of SA-dependent genes (Fig 1.3) (Tada *et al*, 2008; Kneeshaw *et al*, 2014).

Additionally, NPR1 and its homologue proteins NPR3 and NPR4 are proposed as SA receptors and show opposite transcriptional roles. NPR1 acts as a transcriptional activator and NPR3/4 as a transcriptional repressor of defence genes. NPR1, NPR3 and NPR4 bind SA through the conserved arginine (Arg) residue 432, 428 and 419, respectively. The mutation of this amino acid renders the NPR proteins unable to bind SA and compromise its transcriptional activity. It was shown that NPR3 and NPR4 repress the expression of important SA-signalling components such as SARD1 via interaction with TGA2, 5 and 6, and the transcriptional repression is released upon SA binding. Similarly, NPR1 and SA binding is a critical requirement for the expression of SA-mediated genes (Ding *et al*, 2018). The transcriptional dynamics mediated by NPR1/3/4 help fine-tune SA-mediated immunity.

ICS1 network

Different studies suggest a complex network of interaction and overlapping/complementary functions between these transcription factors to precisely modulate *ICS1* expression. For instance, SARD1 and CBP60g play a central role in *ICS1* expression in response to pathogens and SAR. Additionally, both proteins can bind to the promoter of regulators of different nodes of plant immunity, covering both positive and negative regulators (Sun *et al*, 2015). Also, TCP8 was found to interact with SARD1, WRKY28, TCP8, TCP9, TCP20, and also with the negative regulator ANAC019 (Wang *et al*, 2015). CHE is proposed to regulate the circadian oscillation

of *ICS1* expression and SAR induction by modulating SARD1 and CBP60g expression (Zheng *et al*, 2015).

Additionally, changes in the Ca^{2+} signature contribute to regulating the timing of *ICS1* expression. Ca^{2+} is thought to activate CBP60g through calmodulin binding and WRKY28 via phosphorylation mediated by Ca^{2+} -dependent protein kinases (CPK), linking calcium influxes with SA biosynthesis (Wang *et al*, 2009a; Gao *et al*, 2013). NTL9 is thought to mediate stomatal closure during PTI and is expressed mainly in guard cells, implying a tight regulation depending on the desired cellular outcome (Zheng *et al*, 2015). The negative regulators of *ICS1* expression are involved in the signalling pathways of other plant hormones. The repression of *ICS1* by these TF may mediate cross-talk between SA, ET and JA pathways fine-tuning the immune response (Dempsey & Klessig, 2017).

Project Aims

The fact that the loss-of-function *gsnor1 Arabidopsis* mutant exhibit increased cellular S-nitrosylation levels and reduced SA biosynthesis and accumulation in response to pathogens suggests the possibility of a NO-mediated regulatory mechanism of SA biosynthesis. Current findings have helped to elucidate the molecular mechanisms by which S-nitrosylation regulates SA-signalling. However, our understanding of how S-nitrosylation regulates SA biosynthesis during plant immunity is limited.

In previous work, Li (2015) observed delayed *ICS1* expression in *gsnor1-3 Arabidopsis* plants. We speculated that *ICS1* could be subjected to transcriptional or posttranscriptional regulation. In addition, Li (2015) observed that the TF SARD1 can be S-nitrosylated at Cys438 and that SARD1 binding to the *ICS1* promoter was reduced upon S-nitrosylation. Investigate the extent of S-nitrosylation of Cys438 on SARD1 binding-affinity.

Project goals

Differentiate between transcriptional and posttranscriptional repression of *ICS1* expression by S-nitrosylation using the reporter line *ICS1::GUS par2-1.*

Investigate the extent of S-nitrosylation on SARD1 activity *in vitro* using a quantitative approach

Generate *Arabidopsis* transgenic lines to investigate if SARD1 can be S-nitrosylated *in vivo* and investigate what is the biological relevance of this modification.

Design a genetic screening using the *PR1::LUC* line to search for second-site mutations that can regulate GSNO-turnover or reduce total cellular S-nitrosylation in the *gsnor1* background.

Chapter 2 Materials and Methods

Plant material

The *Arabidopsis thaliana* accessions used (Columbia (Col-0), *gsnor1-3, par2-1, sard1-1 (SALK_138476), sard1-2 (SALK_052422), Landsberg erecta (Ler-0) and Ler1-3*) were grown in long day conditions, consisting in 16 hours light at 22°C and 8 hours darkness at 18°C. Plants were grown in soil mix containing Levington F2 + sand (150L), horticultural sand (40L), Sinclair standard grade Perlite (60L) and Everris Exemptor (75g). The F2+S is a peat, sand mix with fertiliser, pH 6.5.

For growth in sterile conditions, seeds were surface sterilised with 75% ethanol for 5 minutes, followed by 20% bleach + 0.02% Tween 20 and five subsequent washes in sterile water. The seeds were stratified for four days at 4°C. The seeds were grown in half-strength MS (2.2 gL^{-1} MS basal salts, 1% sucrose and 0.8% agar).

Generation of transgenic lines

For the generation of the *SARD1::SARD1-HA* and *SARD1:SARD1-nLUC* genomic DNA was extracted from Col-0 plants. The primers used to isolate the native *SARD1* promoter and terminator were used by Zhang *et al* (2010) before. For the genetic constructions, the sequences of interested were amplified with gene-specific primers adding BpiI restriction sites plus compatible overhangs for modular cloning using the MOCLO toolkit (Engler *et al*, 2014).

Bacterial growth conditions.

The bacterial strains used were grown in lysogeny broth (LB) at 37°C media unless stated differently. General cloning and plasmid propagation were done in *Escherichia coli* DH5 α.

Bacterial strains for recombinant protein expression
BL21 (DE3) Competent *E. coli* NEBC2527I
BL21 Shuffle T7 express *E. coli* NEBC3029J -Growth at 30°C

Pseudomonas strains grown on LB media supplemented with 10mM magnesium chloride + corresponding antibiotics, grown at 28°C
Pseudomonas syringae p.v. maculicula ES4326 Strep 100mg/L

Pseudomonas syringae p.v. maculicula ES4326 *(avrB)* Strep 100 mg/L + Kan 50mg/L
Pseudomonas syringae p.v. tomato DC3000 Rif 100mg/L
Pseudomonas syringae p.v. tomato DC3000 *(avrB)* Rif 100 mg/L + Kan 50mg/L

Pathogen infiltration

Psm ES4326 were grown overnight at 30°C and diluted to a final OD_{600} of 0.0002 in 10 mM $MgCl_2$. The leaves were infiltrated by pressure infiltration using a 1ml needleless syringe against the abaxial part of the leave.

RNA extraction and cDNA synthesis

RNA was extracted using the Trizol™ method according to the manufacturer protocol. Briefly, 100 mg of grounded tissue was resuspended in 1 ml of Trizol™ and was incubated for 10 minutes at room temperature. The suspension was centrifuged at 12,000 g for 5 minutes, and the supernatant was transferred to a fresh tube, all centrifugations were performed at 4°C. 200 µL of chloroform per ml of Trizol™ used were added to the supernatant and were shaken by hand for 20 seconds and incubated at room temperature for 2 minutes. After incubation, the samples were centrifuged for 15 min at 12,000g. The aqueous phase was transferred to a new 1.5 ml Eppendorf tube, and the RNA was precipitated with 500 µL of isopropanol. Samples were shaken and incubated for 10 minutes at room temperature followed by centrifugation at 12,000 g for 10 minutes. The supernatant was discarded, and the pellet was washed twice with 1 ml of 75% ethanol in DEPC water, mixed briefly by vortex and centrifuged at 7,500 g for 5 minutes. Next, the pellet was air-dried and resuspended in 50 µL of RNase free water and incubated for 10 minutes at 55°C. Finally, the RNA concentration and purity were determined by absorbance at 260nm, and the integrity was evaluated in 1% agarose gel stained with ethidium bromide.

The first cDNA strand was synthesised using the High-capacity cDNA reverse transcription Kit from Applied Biosystems. 1.5 µg of pure RNA was used in a 20 µl reaction, incubated for 2 hr at 37°C. The enzyme was inactivated at 85°C for 5 minutes, and samples were stored at -20°C until use.

Semi-quantitative PCR and competitive PCR

The differences in gene expression were determined by semi-quantitative PCR in a 25 µL reaction (1X Crimson buffer, 200µM dNTPs, 1 µM forward primer, 1 µM reverse primer, 1.25 units Crimson TAQ DNA polymerase, 1 µM template DNA) using 25-28 cycles of 94°C for 40 sec, 57°C for 1 minute and 72°C for 40 seconds, followed by a final extension of 72°C for 5 minutes. The genes *ACTIN2* and *UBIQUITIN10* were used as internal standards. The primers used are listed in table 2.

GUS staining

For histological GUS staining, seedlings or three-week-old plants were sprayed with SA solution or infiltrated with a virulent/avirulent *Pseudomonas* suspension. The plant tissue was harvested 24, 48 and 72 hours after treatment. The plant tissue was rinsed in staining buffer without X-gluc (20 mM NaPO4 pH 7.2, 0.2 mM EDTA, 0.1% Triton X-100, 1 mM potassium ferrocyanide (K4[Fe(CN)6]·3H2O) and 1 mM potassium ferricyanide). Subsequently, the samples were submerged and vacuum infiltrated in staining buffer containing 1 mM X-gluc substrate. After infiltration, the samples were incubated at 37ºC for 24 or 48 hours. Finally, the chlorophyll was washed with serial 95% EtOH washes and leaves stored in EtOH at 4ºC until imaging.

Quantitative GUS activity assay

GUS activity was quantified from intact plant tissue following the protocol described by Blazquez (2007). The protocol is based on the hydrolysis of the substrate 4-methylumbelliferyl β-D-glucuronide (4-MUG) by GUS to produce 4-methylumbelliferone (4-MU). 4-MU is a fluorescent compound with excitation and emission at 365 and 455 nm, respectively. To measure GUS activity, leaf discs from induced *ICS1::GUS* Col 0 and *ICS1::GUS par2-1* plants were placed at the bottom of the well of a 96-well plate. The tissue was covered with 100 µL of GUS extraction buffer (50 mM NaPO4 pH 7.2, 10 mM EDTA, 0.1% SDS, 0.1% Triton X-100 and 1 mM PMSF) including 1 mM 4-MUG. The samples were incubated at 37ºC for 16 hours. After incubation, 50 µL of stop reagent (1 M sodium carbonate) was added to each well. A 4-MU standard curve covering a range from 0 to 500 nM was prepared in stop reagent. Finally, 100 µL per each sample were transferred to a new 96-well

plate well, and the fluorescence was measured using excitation 365 nm and emission at 455 nm with a 430 nm filter. The GUS activity was quantified by linear regression from the standard curve and reported as nmol 4-MU per surface area.

Recombinant protein expression, extraction and purification

MBP-SARD1: *E. coli* BL21 strain (DE3) cells carrying the plasmid pDEST0his-MBP with the SARD1 insert were grown overnight at 37°C in 5ml of LB media containing 100µg/ml ampicillin. 1 ml of the overnight culture was used to inoculate 100 ml of LB media in a 250 ml flask. The culture was grown at 37°C with constant agitation until it reached an OD600 between 0.6 - 0.7. Protein expression was induced by adding IPTG to a final concentration of 0.5 mM and incubated at room temperature for 3 hours.

The MBP-SARD1 fusion protein was purified using amylose resin (NEB E8021S). 1 ml of amylose resin was loaded into a 5 ml Pierce™ centrifugation column. The resin was equilibrated with 5 column volumes of column buffer (20 mM Tris-HCl, 200 mM NaCl, 1 mM EDTA). The crude extract was then loaded into the column. The resin was washed with six volumes of column buffer. The fusion protein was eluted with 3 ml of 10 mM maltose in column buffer. Finally, 0.5 ml fractions were collected and stored at 4°C until use.

Western Blot

The protein concentration in the fractions was calculated by Bradford assay (Bradford, 1976). The protein containing fractions were loaded in an SDS- PAGE gel (10% Acrylamide resolving gel, 5% stacking gel, run at 90V). The gels were transferred overnight to a nitrocellulose membrane at a constant current of 0.13 A in 20% methanol transfer buffer. The transfer was verified by Ponceau stain. The membrane was then blocked with 5% milk in PBS-T for 20 minutes, followed by a 1-hour incubation with 1/10,000 anti-MBP-HRP conjugated antibody, or anti-HA 1/2,000 mouse primary antibody followed by 1/3,000 anti-mouse-HRP conjugated secondary antibody. The membrane was washed at least three times with fresh PBS-T. 1 ml of Thermo Scientific Supersignal West Pico Chemiluminescent Substrate was added to the membrane. X-ray films were exposed to the membrane for specific time intervals.

In vivo Imaging

Arabidopsis plants containing the PR1::LUC transgene was grown as previously described. 1-week old plants were sprayed with a 5 mM luciferin solution in distilled water plus 0.01% Triton X-100 and screened for LUC activity using an EM-CCD ultra-low-light imaging camera system (Hamamatsu C9100-1). Images were collected over 10 seconds exposition and processed for background subtraction (Murray *et al*, 2002).

In vivo luminometer assay

Arabidopsis seedlings expressing the *SARD1::SARD1 Nano luciferase* construction were germinated in 96-well plates. Each well contained 100 µL of half-strength MS media plus 50 µg/ml Kanamycin. The seedlings were germinated in long day conditions. 1-week old seedlings were sprayed with a 10 mM salicylic acid solution and 1:50 furimazine in 0.01% Triton X100 solution. Bioluminescent measures were collected every hour for a total of 7 days.

Pathogen challenge and SAR assay

Pseudomonas syringae a) p.v. Tomato DC300 or b) p.v. Maculicula ES4326 were grown overnight in LB supplemented with 10mM $MgCl_2$ and the appropriate antibiotics. Cells were harvested by centrifugation at 5000 G for 10 minutes and washed with sterile 10mM $MgCl_2$. The $O.D._{600}$ was adjusted to 0.0002 for the virulent pathogen, 0.002 for avirulent growth assay and 0.025 for avirulent SAR induction. To induce SAR, one bottom leaf was infiltrated with a high dose of avirulent *Pseudomonas.* Three days afterwards, three distal leave were infiltrated with 0.0002 virulent solutions. For control, the initial infiltration was done with 10 mM $MgCl_2$.

After the defined incubation time, two leaf discs from independent leaves were ground together in 500 mL of 10mM $MgCl_2$ for a total of six independent samples per genotype. Following homogenisation, six serial dilutions were prepared for each sample, and 10 uL were plated per dilution for a total of six repetitions of each dilution per plate. When the plates contain well-defined colonies, the colonies were counted and analysed according to the protocol described by Liu *et al*, (2015).

Biotin Switch

To detect S-nitrosylated proteins. The protein samples were incubated with GSNO or CysNO 1 mM for 20 minutes in the dark. The NO-donor was removed by gel filtration using a Zeba column. Subsequently, free thiols were blocked with 25 mM NEM with continuous mixing for 30 minutes at 50°C. The proteins were precipitated with a 2X volume of 100% acetone and centrifuged at 15,000 G for 10 minutes. Following precipitation, the samples were resuspended in labelling buffer and 0.45 µM Biotin HPDP and ascorbate. The biotin labelled proteins were mixed with SDS-loading buffer and boiled for 10 min at 95°C. Subsequently, the fractions were resolved by SDS-PAGE and the nitrosylated proteins detected by western blot.

In vivo S-nitrosylation.

SARD1::SARD1-HA plants were induced with 1mM SA for 12 hours. Upon induction, the leaves were infiltrated with 1mM GSNO in 10mM $MgCl_2$. Following 1 hours incubation, the samples were harvested in liquid nitrogen and ground to a fine powder. All this process was done in the dark. The tubes were covered with foil. The samples were resuspended in HEN buffer + 1mM PSMF + 0.5% Triton X100 + 25 mM NEM. After resuspension, the samples were incubated at 50°C for 30 minutes with constant mixing. For negative control, the samples were incubated for 30 minutes with 50mM DTT. After incubation, the samples were centrifugated at 15,000 G for 10 minutes and the supernatant transferred to a new tube. The protein samples were then precipitated with acetone 100% and resuspended in labelling buffer with 1 mM Biotin HPDP. After Labelling, with 1mM Biotin-HPDP the biotinylated proteins were pulled down using an agarose streptavidin resin and blotted against HA or pulled down HA and blotted against biotin.

Electrophoretic Mobility Shift Assay (EMSA)

To evaluate the effect on the DNA-binding of SARD1 to the *ICS1* promoter upon S-nitrosylation we used EMSA, following the protocol described by Zhang *et al*., (2010) with minor modifications. A 25 bp forward and reverse fragments of the *ICS1* promoter containing the GAAATTT motif and a fragment with a mutation in the binding site GAAGGGT (Sun *et al*, 2015) were ordered from Integrated DNA Technologies (IDT). The double-stranded probe was annealed by incubating equimolar concentrations of the forward and reverse strands at 95 ºC for 20 min and reducing temperature to room

temperature at a rate of 0.5ºC per minute. The probe was end-labelled in a 40 µL reaction containing ten pmol of double-stranded DNA, 100 units of T4 polynucleotide kinase (NEB) and 40 µCi of [γ-32P] ATP (PerkinElmer) incubated at 37ºC for 30 minutes. The unincorporated labelled nucleotides were removed using an illustra MicroSpin G-50 Spin Column (GE healthcare). The probe was diluted to a final concentration of 0.1 pmol/ µL.

For the binding reaction, 100 ng of purified MBP-SARD1 or MBP-SARD1C438S were mixed with 4 µL of 5X binding buffer (50 mM HEPES pH 7.7, 375 mM KCL, 6.25 mM $MgCl_2$, 25% glycerol and 100 ng of poly[dI-dC] (LightShift Pierce) and 5 mM DTT), the volume was adapted to 19 µL with sterile water and the reaction was incubated on ice for 20 min. Subsequently, 1 µL of the labelled probe (0.1pmol) was added per reaction and mixed by pipetting up and down. The reaction was incubated for 30 min at 37ºC. The mix was loaded into a 5% polyacrylamide gel in 1X TGE buffer (25 mM Tris pH 8.3, 190 mM glycine, 1 mM EDTA). After electrophoresis, the gel was dried for 2 hours at 60ºC under vacuum. Finally, an X-ray film was exposed to the gel in the dark at -80ºC overnight (different exposure times) and developed afterwards.

EMSA after S-nitrosylation

To evaluate the changes of DNA binding of the recombinant protein after S-nitrosylation, we first diluted the recombinant SARD1 or SARD1C438S fractions to 100 ng/µL and transferred 9 µL into seven 0.2 mL PCR tubes. The NO donor was diluted in the 1X binding buffer to final 1, 2.5, 5, 10 and 50 mM concentrations. Two different 5X binding buffer were prepared, containing + DTT or – DTT. Subsequently, 1 µL of each NO donor dilution was added to each independent protein tube to obtain a final concentration of 0.1, 0.25, 0.5, 1.0 and 5.0 mM. The reaction was incubated for 20 min at room temperature in the dark. Finally, 9 µL of the reaction mix (4 µL of 5X DNA binding buffer, 1 µL poly[dI-dC] and 4 µL water) were added to each protein-NO-donor tube to obtain a final volume of 19 µL. Finally, 1 µL of 0.1 pmol DNA probe was added to each tube, and the reaction was incubated at room temperature for 20 min and loaded for electrophoresis separation as mentioned above.

Equilibrium dissociation constant

To calculate the equilibrium dissociation constant before and after S-nitrosylation of SARD1, we titrated increasing protein concentrations covering a range from 30 to 600

nmol of protein under NO-donor treatment and control conditions. Briefly, 49 µL of quantified protein fractions were placed into two independent test tube. For the NO-donor treatment, 1 µL of 50 mM GSNO was added to the 49 µL of the protein fraction (1 mM GSNO), and 1 µL of water was added to the control. After mixing, the S-nitrosylated/control protein was transferred in increasing volumes into seven 0.2 mL PCR tube and the volume adjusted to 10 µL with sterile water to obtain the desired concentrations (covering from 30 to 600 nmol). Simultaneously, we prepared a master mix consisting of 5X DNA- binding buffer (without DTT), poly [dI-dC] and 0.1 pmol of fluorophore-labelled DNA probe. 10 µL of the master mix was added to each reaction tube. After mixing, the reaction was incubated for 20 min at room temperature following gel electrophoresis as described above. After running, the gel was scanned using a LiCOR Odyssey system. The intensity of the DNA-protein and free probe bands was quantified using the software ImageJ. The fraction of DNA-bound and unbound were plotted following the protocol described by Heffler, Walters, & Kugel, (2012).

Chapter 3 Transcriptional Regulation of *ICS1* expression by S-nitrosylation

Introduction

Salicylic acid

Salicylic acid (SA) is a vital defence hormone in plants. Upon pathogen infection, SA accumulation in leaves is a critical requirement to induce the expression of pathogenesis-related genes and the biosynthesis of defence compounds (Loake & Grant, 2007; Vlot *et al*, 2009; Dempsey & Klessig, 2017). Plants can produce SA by two independent metabolic pathways. The first one derived from cinnamate catalysed by the enzyme phenylalanine ammonia lyase (PAL) and the other pathway via chorismate catalysed by the activity of the enzyme Isochorismate Synthase I (ICSI). It is now known that the major proportion of SA produced in response to pathogen infection occurs via the ICS1 pathway, considering that the *Arabidopsis thaliana ics1* mutant plants exhibit dramatically reduced SA accumulation after pathogen infection (Lawton *et al*, 1995; Wildermuth *et al*, 2001).

Our current understanding of the molecular mechanisms underlying SA-mediated immunity suggests that the proteins Enhanced Disease Susceptibility 1 (EDS1) and Phytoalexin Deficient 4 (PAD4) act upstream of SA accumulation, promoting *ICS1* expression during basal and Pathogen Associated Molecular Pattern (PAMP) Triggered Immunity (PTI) (Cui *et al*, 2017). After accumulation, SA mediates transcriptional reprogramming via direct interaction with Non-Expresser of Pathogenesis-Related Genes 1 (NPR1) and TGA transcription factors (Tada *et al*, 2008) to promote the expression of defence genes.

ICS1-Associated transcription factors

To better understand how SA coordinates these mechanisms, numerous studies have focused on identifying transcription factors (TFs) that regulate *ICS1* expression, finding proteins that have been shown to bind to the *ICS1* promoter *in vivo* and exert a positive or negative transcriptional effect on *ICS1* expression. For instance, the absence of the TF SAR-deficient 1 (SARD1) and its homologue, calmodulin-binding protein 60g (CBP60g), drastically compromises *ICS1* expression in response to pathogen infection and severely increases the susceptibility to *Pseudomonas* infection (Zhang *et al*, 2010). Also, the TF WRKY28 was reported to bind and upregulate the activity of the *ICS1* promoter in a protoplast assay (van Verk *et al*,

2011b). The teosinte branched1/cycloidea/PCF 8 (TCP8) and TCP 9 were found to co-express with *ICS1* and bound to the *ICS1* promoter *in vivo*. Further, the *tcp8 tcp9* double mutant exhibited a significant reduction in *ICS1* expression during immune responses (Wang *et al*, 2015). Similarly, the TF NTM-like 9 (NTL9) was found to drive *ICS1* expression in guard cells to mediate stomatal closure during plant immunity and the CCA1-hiking expedition (CHE/TCP21) TF was shown to control *ICS1* expression in association with the circadian oscillation of SA concentrations (Zheng *et al*, 2015). Interestingly, the *che* mutant also showed reduced *ICS1* expression and compromised expression of *SARD1* and *CBP60g*, suggesting that CHE regulation of *ICS1* may depend on modulation of SARD1 and CBP60g (Zheng *et al*, 2015).

TFs reported to exert transcriptional repression of *ICS1* include Ethylene Insensitive 3 (EIN3) and EIN3-like 1 (EIL1), which are known to regulate ethylene (ET)-dependent gene expression. Constitutive SA accumulation and expression of SA-dependent gene expression have been observed in the *ein3 eil1* double mutant (Chen *et al*, 2009a). Likewise, the NAC (NAM/ATAF1, ARAF2/CUC2) family members ANAC019, ANAC055 and ANAC072, which are involved in jasmonic acid (JA)-mediated signalling were reported to repress *ICS1* expression and promote stomatal re-opening in response to the bacterial toxin, coronatine (Zheng *et al*, 2012b). Further, the spatial and temporal interactions of these TF's are thought to mediate cross-talk between SA, ET and JA pathways (Dempsey & Klessig, 2017).

Transcriptional and posttranscriptional regulation of gene expression

The transcriptional reprogramming is regulated at different levels. Transcriptional regulation occurs mainly through the binding of gene-specific TFs to *cis*-regulatory elements located within the promoter region of certain genes (Lee *et al*, 2006; Hong *et al*, 2003). The process is coordinated by the enzyme RNA polymerase II (RNAPII) which binds to the promoter of target genes assisted by general transcription factors (GTFs). The Mediator complex interacts with gene-specific transcription factors and binds to RNAP11 to mediate its transcriptional activity and specificity (Li *et al*, 2016). The Mediator core is composed of over twenty subunits, organised into three modules named head, middle and tail. The head and middle modules interact with GTFs and RNAPII, and the tail interacts gene-specific TF. Additionally, the mediator core contains a separable cyclin-dependent kinase 8 (CDK8) module which blocks the interaction with RNAPII leading to transcriptional repression, allowing the Mediator to

act as a transcriptional activator or repressor depending on the subunit composition (Zhang *et al*, 2013c; Shaikhali & Wingsle, 2017).

In *Arabidopsis,* the mediator has been associated with the transcriptional regulation of different signalling processes including plant immunity (Shaikhali *et al*, 2015). The mediator subunits MED15, MED16 and MED14, were identified as critical regulators of SA and systemic acquired resistance (SAR) signalling pathways. The *med14* mutation resulted in reduced and delayed expression of central genes for SA biosynthesis and signalling, including *ICS1, PBS3, EDS5, NPR1/3/4,* and *PR1*, together with higher susceptibility to *Pseudomonas* infection and reduced accumulation of free and total SA (Zhang *et al*, 2013c). Contrary, *Arabidopsis med16* plants showed normal SA accumulation but compromised in SAR and SA-dependant genes expression, including *NPR1* and *PR1* (Zhang *et al*, 2012).

After transcription, the expression profile can be modified by different posttranscriptional regulatory mechanisms which include microRNA-mediated degradation, nonsense-mediated mRNA decay, nuclear export control, translation efficiency control, intracellular protein trafficking, and regulated nuclear localisation (Lee *et al*, 2006). Both transcriptional and posttranscriptional mechanisms are regulated by RNA binding proteins (RBPs), which participate in mRNA export from the nucleus to the cytoplasm by interacting with the nuclear pore complexes (NPCs) (Staiger et al, 2013).

S-nitrosoglutathione in plant immunity

In *Arabidopsis*, the absence of the enzyme S-nitrosoglutathione reductase 1 (GSNOR1) resulted in increased total cellular S-nitrosylation and compromised basal, non-host, and *R*-gene mediated immunity. Furthermore, *atgsnor1-3* plants showed reduced SA-mediated gene expression and reduced SA biosynthesis and accumulation (Feechan *et al*, 2005). This observation suggests the possibility of a regulatory mechanism of SA biosynthesis mediated by S-nitrosylation, potentially by transcriptional repression of *ICS1* expression, control of *ICS1* mRNA stability or translation or alternatively, the post-translational regulation of ICS1 activity.

A well-established method to study temporal and spatial gene expression in plants is the application of the bacterial reporter gene, *β-glucuronidase (GUS)*. GUS catalyses the hydrolysis of β-O-glycosidic linkages from a broad range of substrates, allowing histological and quantitative analysis of the associated plant promoter activity in

different situations. In addition, plants lack endogenous GUS activity, making this approach reliable to assess qualitatively or quantitatively gene expression patterns in plants (Kim *et al*, 2005).

To determine if SNO accumulation in *gsnor1* plants reduces SA levels by repressing the transcription of *ICS1*, rather than an alternative post-transcriptional mechanism we prepared an *Arabidopsis* line possessing a *GUS* reporter gene under the control of the *ICS1* promoter (*ICS1::GUS*) (Li, 2015). The reporter line was subsequently crossed into the *par2-1* genetic background, which is an ethane methyl sulphonate (EMS) mutant containing a G to A mutation in the *GSNOR1* gene, that renders the corresponding protein inactive. Importantly, the *par2-1* mutants exhibit an indistinguishable phenotype to the *gsnor1-3* line (Chen *et al*, 2009b). Both lines exhibit increased overall S-nitrosylation, short roots, loss of apical dominance and reduced SA accumulation and signalling, compromising different modes of plant immunity (Feechan *et al*, 2005; Yun *et al*, 2016). The application of the *par2-1* line enabled us to avoid generating a line with more than one transgene because this might result in gene silencing (Gelvin, 2003).

Results

Characterisation of *ICS1::GUS* transgenic lines

In previous work undertaken in our lab, a 1,500 bp fragment of the *ICS1* promoter including the 5'-untranslated region and sequences including the binding sites for most of the TF known to regulate *ICS1* expression was amplified from *Arabidopsis* Colombia 0 genomic DNA and cloned into the pGWB3 vector to transcriptionally fuse *GUS* to the *ICS1* promoter. The pGB3 *ICS1::GUS* plasmid was introduced into *Agrobacterium tumefaciens* GV3101 strain and subsequently used to transform *Arabidopsis* plants by floral dipping (Li, 2015). From the 24 T1 plants obtained, we selected four lines that express *GUS* in response to *Pseudomonas syringae* pv maculicula ES4326 (*Psm* ES4326) infection for further screening.

To characterise these lines, we compared the expression profile of transgene expression to that of the endogenous *ICS1* gene, following inoculation with *Psm* ES4326. Thus, we inoculated *ICS1::GUS* T3 homozygous plants with *Psm* ES4326 and compared transcript levels by semi-quantitative PCR. The expression of the *ICS1* gene steadily increased from 3 hours post inoculation (HPI), reaching a maximum expression level between 12 and 24 HPI. The temporal expression of the transgene

was found to be congruent with the expression of the endogenous *ICS1* gene (Fig 3.1A).

We then analysed the spatial kinetics of transgene expression following pathogen challenge or induction by exogenous SA application. Thus, we inoculated a single leaf of a 3-week-old *ICS1::GUS* plant with a high concentration of *Psm* ES4326 (*avrB)* or sprayed this line with a SA solution. Subsequently, we performed histological GUS staining of whole plants at 24 and 72 hours post-inoculation / treatment.

The challenged leaves showed strong GUS induction flanking the infection site and interestingly, displayed GUS accumulation in areas surrounding the vascular tissue at 24 HPI (Fig 3.1B). In the distal leaves, localised GUS activity spots were observed at this time point. Interestingly, we observed less GUS activity at 72 HPI than at 24 HPI (Fig 3.1C), in agreement with the temporal dynamics of *ICS1* expression following *Psm* inoculation, in which the *ICS1* transcript accumulation decreases after 48 HPI (Li, 2015).

The plants treated with exogenous SA showed GUS activity regions that resemble the *GUS* expression pattern in distal leaves (Fig 3.1 D). Interestingly, we observed localisation of GUS activity in the vascular tissue mainly in the leaves from primary infection and only in some specific leaves after SA treatment, including the first two true leaves from the rosette (Fig 3.2 A to E). The spatial and temporal profile we observed is compatible with the *ICS1::GUS* spatial kinetics described in previous reports (Hunter *et al*, 2013; Lv *et al*, 2015). Collectively, these experiments suggest that transgenic *ICS1::GUS* lines function as a robust reporter of the expression of the endogenous *ICS1* gene.

Transcriptional repression of *ICS1* by S-nitrosylation

The fact that the a*tgsnor1-3* plants showed reduced total SA levels (Feechan *et al,* 2005) suggests the existence of regulatory mechanisms for SA biosynthesis resulting from increased GSNO levels. Further, it has been shown that *ICS1* transcript levels are reduced in *gsnor1* plants, implying increased GSNO levels result in reduced *ICS1* transcription, increased *ICS1* turnover or perhaps both. To differentiate between these possibilities, we crossed the *ICS1::GUS* transgene into *par2-1* plants, as a reduction in *GUS* transcription and by extension, GUS activity, would indicate increased GSNO levels in *gsnor1* plants impact transcription from the *ICS1* promoter.

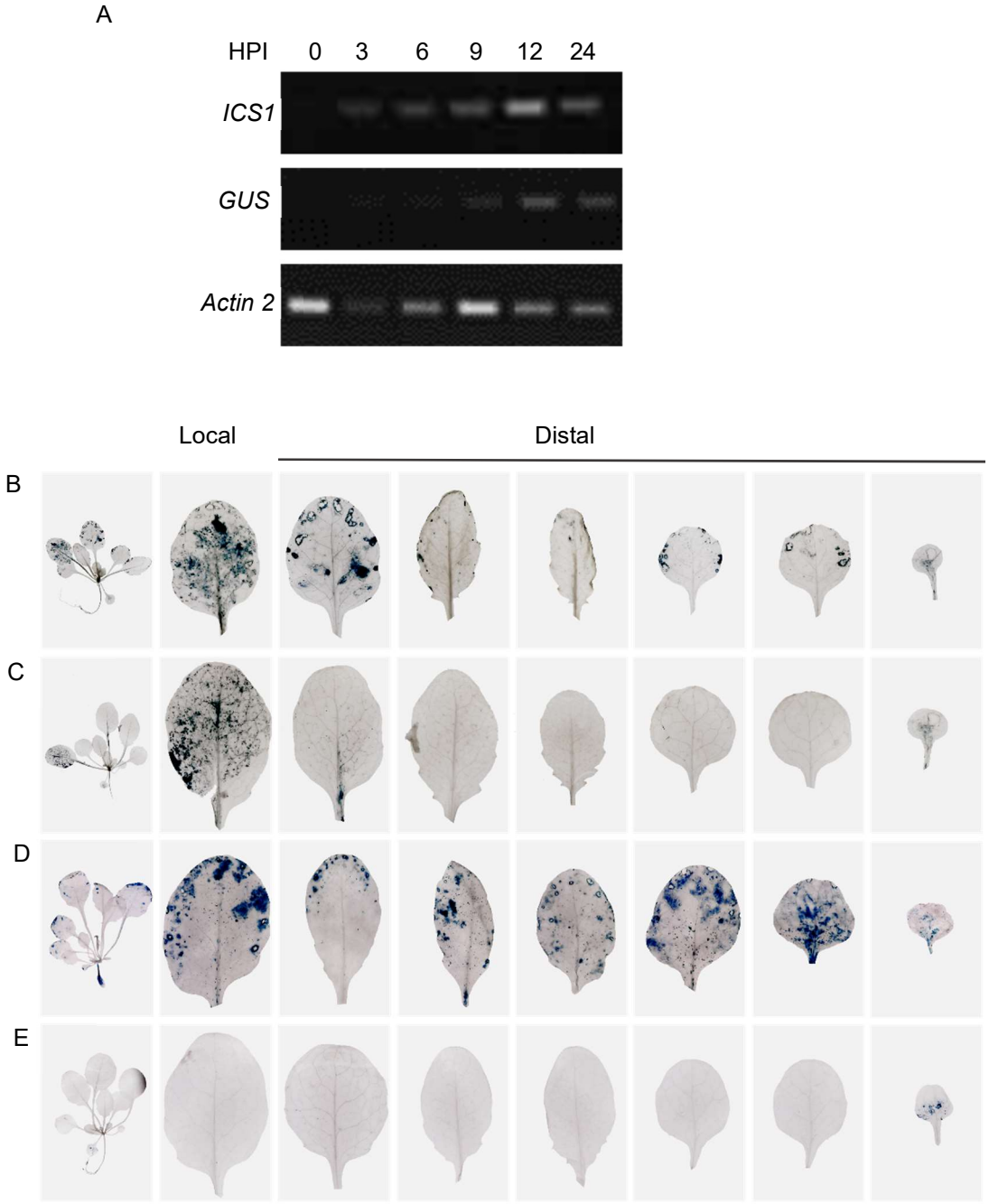

Figure 3.1. Characterisation of *ICS1::GUS* transgenic Col-0 plants. A) Semi-quantitative PCR to compare *ICS1* and *GUS* transcript levels in T3 homozygous *ICS1::GUS* Col 0 plants. Samples were collected at the stated hours post-infection (HPI) with *Pseudomonas syringae* pv maculicula ES4326 (*Psm)* ($O.D._{600}$ = 0.002). B to E) Histological GUS staining of *ICS1::GUS* Col 0 plants at B) 24 HPI and C) 72 HPI of a single leaf with *Psm* ES4326 (*avrB*), D) 24 hours after foliar application of salicylic acid 1 mM and E) mock treatment.

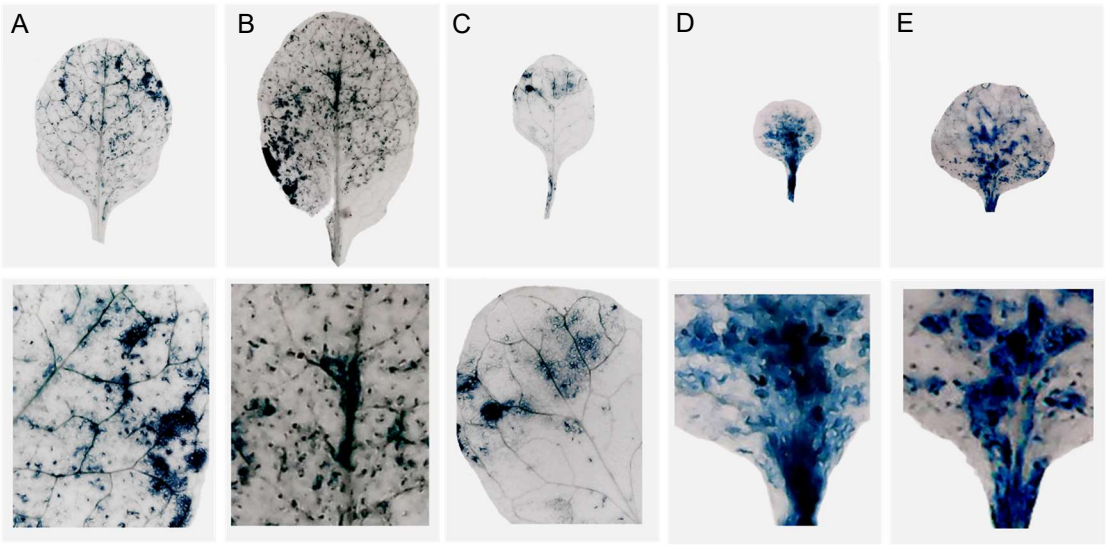

Figure 3.2 Spatial profile of *ICS1::GUS* transgene expression. Histological GUS staining of *ICS1::GUS* Col-0 plants after: A) local leaf at 24 HPI or B) 72 HPI, C) distal leaf at 24 HPI with *Pseudomonas syringae* ES4326 (*avrB*) $O.D._{600}$ = 0.025 and D, E) exogenous SA 1mM treatment.

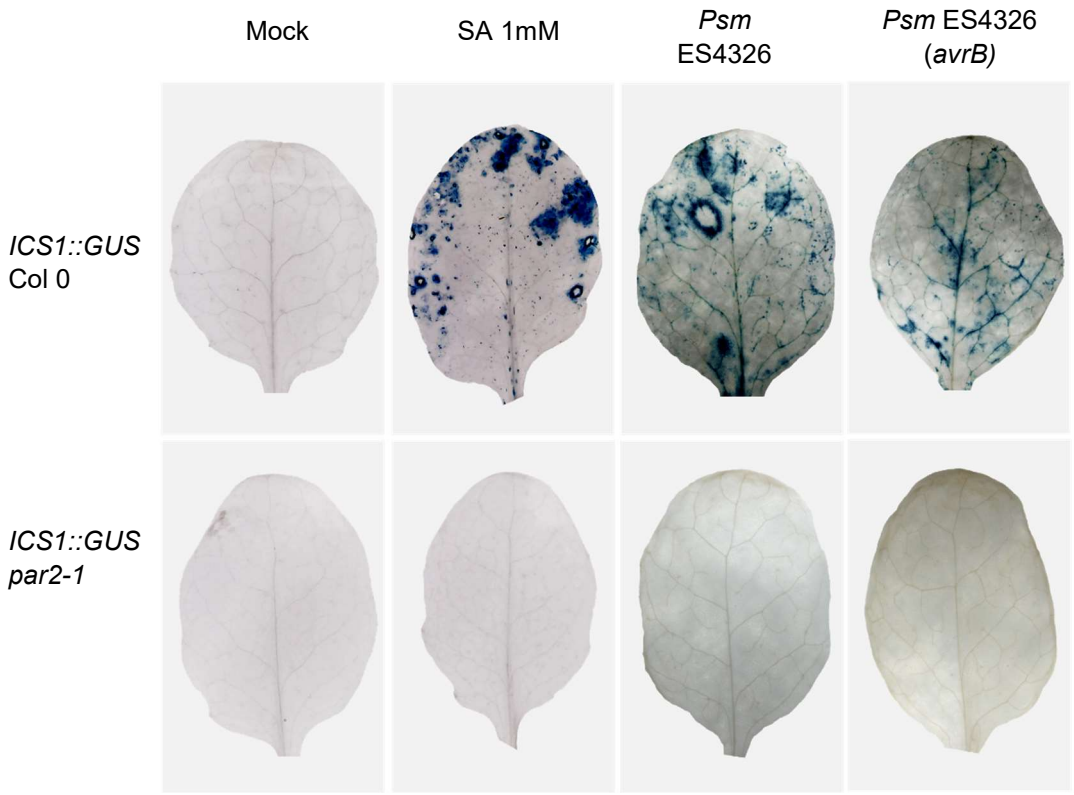

Figure 3.3. Transcriptional repression of *ICS1* in *par2-1* plants. Histological GUS staining of *ICS1::GUS* Col-0 and *ICS1::GUS par2-1* plants. Leaves were harvested and stained with 2 mM X-Gluc solution 24 hours after treatment with 1 mM SA and 24 HPI with *Psm* ES4326 and *Psm* ES4326 (*avrB).*

As expected, the heterozygous F1 *ICS1::GUS par2-1* plants showed a wild-type (WT) phenotype as a single functional *GSNOR1* allele from the WT parental is enough to mask the *par2-1* phenotype. The F2 seeds were then screened on selective MS plates, and seeds from homozygous *par2-1* plants exhibiting the *gsnor1* phenotype were collected. We then identified F3 double homozygous *ICS1::GUS par2-1* plants by scoring for kanamycin resistance and confirmed their identity by genotyping the *ICS1::GUS* insertion and monitoring the *gsnor1* phenotype.

Subsequently, we induced *ICS1* expression in the resulting *ICS1::GUS* Col-0 and *ICS1::GUS par2-1* plants by exogenous application of 1 mM SA. Following histological GUS staining with X-gluc, we observed strong *ICS1* induction in the wild-type background, but no GUS activity was visible in *par2-1* plants (Fig 3.3).

To confirm and extend these results, we challenged both reporter lines with *Psm* ES4326 and with a *Psm* ES4326 (*avrB)*. We observed strong GUS activity in Col-0 in response to both virulent and avirulent pathogens, but no GUS activity was detected in the *par2-1* genetic background. We also performed a quantitative GUS assay, a fluorometric method with higher sensitivity than X-gluc staining. The analysis of GUS activity from leaf discs of Col-0 and *par2-1* plants 24 hrs after induction with SA 1 mM showed similar results to our previous observations; wild-type plants exhibited significantly higher GUS activity than *gsnor1* plants after SA treatment. However, no significant GUS induction was detected in *par2-1* plants (Fig 3.4).

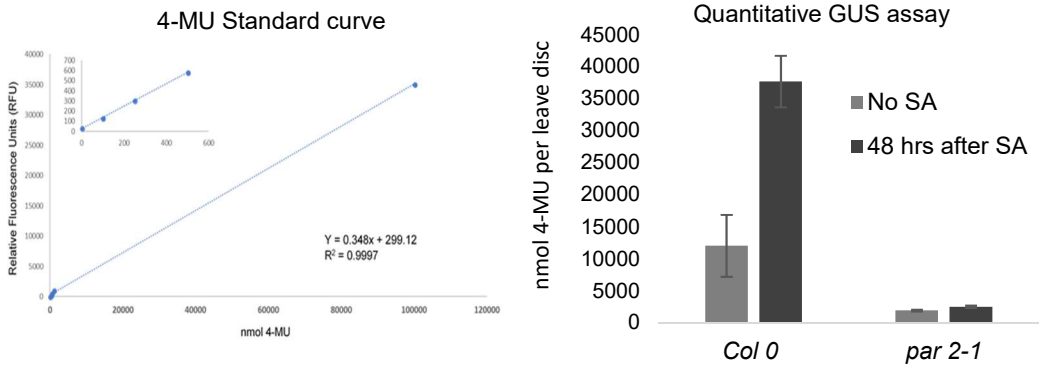

Figure 3.4. Quantitative of *ICS1* expression in Col-0 and *par2-1* plants. GUS extraction from 1cm^2 leaf discs from *Arabidopsis ICS1::GUS* Col-0 and *par2-1* lines 48 hrs after induction with 1 mM SA and incubated with the substrate 4-MUG for 16 hr at 37 ºC. GUS activity represented as equivalent nmol of 4-MU per leaf disc. Bars show the mean value of 3 leaf discs from 9 different plants in two independent experiments. Error bars represent the standard error.

Discussion

Robust reporter of *ICS1* expression

Here we report the utility of an *ICS1::GUS* transgenic line to investigate the molecular mechanism by which increased GSNO levels regulates SA biosynthesis in *gsnor1* plants. The full-length of the *ICS1* promoter region extends over 3,173 bp. Our construction contains a 1,500 bp fragment of the promoter (Li, 2015), covering the 5'UTR and the binding site for the transcription factors reported to drive *ICS1* expression, as shown in Table 3.1.

Different *ICS1::GUS* constructions have been described previously. For instance, Van Verk *et al*, (2011) used a 1,000 bp fragment of the *ICS1* promoter to investigate WRKY transcription factors related to SA biosynthesis in a protoplast assay. In different experiments, Lewsey *et al*, (2010) and Hunter *et al.*, (2013) used a 1,500 bp fragment of the *ICS1* promoter to study plant viral-defence mechanisms in relation to SA. This same construction was used by Lv *et al.*, (2015) looking at the role of β-cyclocitral and SA in excessive light acclimation. Additionally, Tedman-Jones *et al*, (2008) conducted a forward mutant screening using 2,500 bp of the *ICS1* promoter (*ICS::LUC)* to identify constitutive *ICS1* expression in a mutagenized *Arabidopsis* population, finding that the *constitutive ICS1 expression 1 (cie1)* mutant exhibit enhanced resistant to *Hyalonperonospora parasitica*, correlating with higher SA accumulation. The *cie1* mutation was mapped to the xyloglucan galactosyltransferase *MUR3* gene involved in cell wall biosynthesis. This mutant also showed deregulation of *ICS1* expression, identified using an *ICS1::GUS* construction employing the same sequence of the *ICS1* promoter. These reports highlight the utility of the *ICS1::GUS* transgene and that a 1,500 bp fragment of the *ICS1* promoter contains the core regulatory elements for *ICS1* expression.

Also, we observed congruent *ICS1* temporal and spatial expression patterns as those in previous reports, showing significant *ICS1* accumulation 24 hrs after *Psm* infection and reduction in transcript levels toward 72 HPI (Wildermuth *et al*, 2001; Wang *et al*, 2015).

ICS1 expression in vascular tissue

We observed strong GUS activity in the vasculature of the infected leaves at 24 HPI which could relate with priming of SAR upon infection. Additionally, we observed a different *ICS1* spatial profile in distal leaves to that of the primary infected leaves,

characterised by lower GUS activity and localised GUS spots. A similar spatial profile was observed in plant leaves treated with exogenous SA, which mimics the SA spatial profile during SAR. The pattern observed in distal leaves is consistent with SA accumulated during SAR, which has been described to occur at lower rates than at the primary infection site (Dempsey & Klessig, 2017; Singh *et al*, 2017).

Mounting evidence highlight the importance of the vascular tissue in the transport and amplification of SAR-associated signals. Specifically, phloem loading of SAR signals can occur via the apoplast or the symplast. SAR signals are rapidly generated within four to six hours after infection and translocate presumably via the phloem to distal tissue (Shine *et al*, 2018).

Table 3.1. Binding site of *ICS1* related transcription factors

Transcription factor	**Effect on *ICS1***	**Binding motif**	**Number of Cys residues**	**Binding site location (bp)**	**Reference**
SARD1/CBP60g	Positive	GAAATTTTGG	4, 11	-1,217	(Zhang *et al*, 2010)
WRKY 28	Positive	W-Box	4	-445, -460	(van Verk *et al*, 2011b)
TCP8/TCP9	Positive	GGGCCCAC	1, 0	-150	(Wang *et al*, 2015)
NTL9	Positive	NAC-core binding site TTNCGTA	8	-109, -468, -603, -1,072, -1,315, -1,422, -1,703, -1,897	(Zheng *et al*, 2015)
CHE	Positive	Class I TCP binding site GGNCC- CAC	1	-126	(Zheng *et al*, 2015)
ANAC018, 055, 072	Negative	NAC Core binding site CGTAG	3,2,4	-109, -468, -603, -1,072, -1,315, -1,422, -1,703, -1,897	(Zheng *et al*, 2012; Jensen & Skriver, 2014)
EIN3/EIL1	Negative	A(C/T)G(A/T)A(C/T)CT	11 11	-117 to -324	(Chen *et al*, 2009a)

Different mobile SAR inducers have been identified, including SA and its derivative Methyl-SA (MeSA), azelaic acid (AzA), diterpenoid dehydroabietinal (DA), glycerol-3-phosphate (G3P), pipecolic acid (Pip), and the free radicals NO and ROS (Gao *et al*, 2015; Kachroo & Kachroo, 2018). MeSA has been detected in the phloem. However SAR kinetic studies suggest the time frame for MeSA requirement in distal tissue are within 48 to 72 hours (Park *et al*, 2009), suggesting it to be a secondary mobile SAR signal (Singh *et al*, 2017; Dempsey & Klessig, 2017).

ICS1 expression and SA accumulation in both local and distal tissue is a critical requirement for SAR. SA and Pip act synergistically to activate SAR. Pip has been identified in high concentrations in phloem exudates during early SAR events, preceeding SA accumulation in distal leaves. Additionally, *agd2-like defence response protein 1* (*ald1*) mutants, deficient in Pip synthesis, failed to accumulate SA in distal leaves 48 HPI with *Psm* and *ics1* plants could accumulate Pip in local leaves but show compromised Pip accumulation in distal leaves following *Psm* infection (Bernsdorff *et al*, 2016). Suggesting that ICS1 activity is necessary for proper Pip translocation through the vasculature, corresponding with the *ICS1* spatial profile we observed (Navarova *et al*, 2012).

Transcriptional repression of *ICS1* by high GSNO concentrations

We analysed the effect of high total cellular S-nitrosylation on *ICS1* expression. No GUS activity was detected after pathogen infiltration or exogenous SA application on *ICS1::GUS par2-1* plants following histological GUS staining. The GUS protein sequence is composed of 603 amino acids, containing nine cysteines in the sequence. The GUS sequence analysis using the S-nitrosylation prediction tool SNOSITE (Lee *et al*, 2011) identified six cysteines as potential S-nitrosylation targets. Therefore potentially inhibiting GUS activity.

Interestingly, Shi *et al*, (2015) investigated the relationship between auxin signalling and NO using a *DR5::GUS* construct in Col0 and *gsnor1-3* plants. They observed impaired auxin signalling in the *gsnor1-3* background as reported by reduced GUS activity. However, they could observe GUS activity by histological staining in the *gsnor1-3* plants. They confirmed the effect using a *DR5::GFP* construction, indicating that GUS is a suitable tool to study promoter activity under a high S-nitrosylation background. Thus, the observed impairment on *ICS1* expression in *ICS1::GUS par2-1* plants may be due to transcriptional repression of the *ICS1* promoter rather than inhibition of GUS activity by S-nitrosylation.

This observation is consistent with unpublished results from Li (2015) where reduced and delayed *ICS1* transcript accumulation was observed in *gsnor1-3* plants 12 hrs after infection with *Psm* ES4326 compared to wild-type. Further, significantly reduced GUS activity was observed in the GUS quantitative assay. Collectively, these data support the hypothesis of repression of the *ICS1* promoter by enhanced GSNO levels, likely via S-nitrosylation.

One possibility to explain the transcriptional repression of *ICS1* and the reduced and delay expression of SA-dependent genes in the *gsnor1* background could be related to S-nitrosylation modulating the transcriptional activity of the Mediator complex. Notably, MED14 and MED16 which play a central role in the transcriptional regulation of SA-mediated immunity which contain 25 and 27 Cys residues, respectively (Shaikhali *et al*, 2015; Zhang *et al*, 2013c, 2012). The fact that *med14* plants exhibited reduced SA accumulation and downregulation of central SA-biosynthesis genes, including *ICS1, EDS5* and *PBS3,* suggests a direct link of this MED14 with SA biosynthesis (Zhang *et al*, 2013c). Contrary, *med16* plants showed normal SA accumulation but compromised SA-dependent gene expression (Zhang *et al*, 2012). The genetic evidence and the high number of Cys residues within MED14/MED16 amino acid sequence suggests the possibility of a REDOX-based mechanism for transcriptional regulation of SA biosynthesis and signalling. Potentially through modulation of the interaction between the Mediator complex and SA-associated TFs, such as SARD1 and CBP60g.

A similar possibility to explain the transcriptional repression on *ICS1* promoter can be related with modulation of the DNA-binding by S-nitrosylation of the *ICS1*-specific TFs. For instance, the DNA-binding of the *Arabidopsis* zinc finger (ZF) TF SRG1 to the promoter of immune repressors is reduced upon S-nitrosylation preferentially at Cys87. SRG1 is induced by the nitrosative burst after pathogen challenge and binds to its target promoters where it recruits the transcriptional repressor TOPLESS to promote the establishment of the immune response. Accumulation of NO leads to S-nitrosylation of SRG1 and promotes its release from the promoter (Cui *et al*, 2018). Additionally, S-nitrosylation has been shown to regulate the DNA-binding of the plant-specific transcription factors *at*MYB2 and *at*MYB30. These TFs were found to be S-nitrosylated *in vitro* and *in vivo* at the conserved Cys-53 resulting in inhibition of its DNA-binding activity (Serpa *et al*, 2007; Tavares *et al*, 2014). In mammals, the DNA-binding of the ZF-TF Ying Yang 1 (YY1) to the *Fas* promoter was inhibited upon S-

nitrosylation of YY1 (Hongo *et al*, 2005). Similarly, the DNA-binding of the yeast TF LAC9 was also shown to be regulated by S-nitrosylation (Kröncke *et al*, 1994). Therefore, emerging evidence suggests a relationship between S-nitrosylation and the modulation of DNA-binding activity.

To explore these possibilities, it would be interesting to use a yeast-two hybrid approach or Bimolecular Fluorescence Complementation (BiFC) assay to look for MED14/MED16 interacting proteins among the TFs associated with *ICS1* and SA-signalling and evaluate if MED14 and MED16 are targets for S-nitrosylation *in vitro* using the biotin switch assay, followed by characterisation of the effect of S-nitrosylation on these proteins interactions. Additionally, SARD1 and CBP60g play a central role driving *ICS1* expression (Zhang *et al*, 2010). Importantly, they contain 4 and 11 Cys residues within their sequence, respectively. To address if S-nitrosylation can modulate its DNA-binding activity to the *ICS1* promoter, it will be necessary to undertake *in vitro* characterisation of their DNA-binding activity and biotin switch to evaluate if they are targets of S-nitrosylation.

Our data support the possibility of transcriptional repression of the *ICS1* promoter by S-nitrosylation. However, some proteins have been shown to be subjected to transcriptional and posttranscriptional regulation. For instance, the *Arabidopsis* TF NFYA5 which is involved in drought tolerance was found to be subjected to partial transcriptional regulation using a *NFYA5::GUS* reporter line (Li *et al*, 2008). Additionally, the *NFYA5* transcript contains a target site for miRNA169 which mediates posttranscriptional silencing during basal conditions. Downregulation of miRNA169 during drought allows rapid accumulation of NFYA5 in leaves and guard cells to prevent water loss (Li *et al*, 2008).

Interestingly, the RBP-defence related 1 (RBP-DR1) which is associated with posttranscriptional regulation in plants was linked with *ICS1* expression after the observation that *rbp-dr1* plants exhibit enhanced resistance to *Pseudomona syringae* pv *tomato* DC3000 infection together with higher *ICS1*-dependent SA accumulation and increased *PR1* expression (Qi *et al*, 2010). The *at*RBP-DR1 amino acid sequence contains 6 Cys residues, and 5 predicted S-nitrosylation sites according to the SNOSITE prediction tool (Lee *et al*, 2011). Additionally, a quick search on the *Arabidopsis* MPSS Plus Database (Nakano *et al*, 2005) for small-RNA signatures that matches the *ICS1* mRNA sequence showed five potential miRNA that target the *ICS1* transcript. It may be possible that S-nitrosylation of RBP-DR1 in the *gsnor1*

background contributes to additional posttranscriptional mechanisms to repress *ICS1* expression.

To investigate this possibility, it will be necessary to prepare an additional *ICS1::ICS1-GUS* translational fusion and compare GUS activity with the transcriptional fusion *ICS1::GUS* and with mRNA levels in both WT and *gsnor1* backgrounds (Lee *et al*, 2006). A correlation between the mRNA and protein level could represent transcriptional repression of *ICS1. A*lternatively, a mismatch between mRNA and protein levels could hint the activation of posttranscriptional mechanisms (Lee *et al*, 2006). Also, it will be interesting to test if these predicted miRNAs are involved in posttranscriptional repression of *ICS1* and if S-nitrosylation is involved in the expression of these miRNA.

The accumulated evidence highlights the critical role S-nitrosylation plays in modifying transcription dynamics and protein function. Our data suggest the existence of a transcriptional repression mechanism of *ICS1* expression mediated by S-nitrosylation, possibly contributing to explain the significant transcriptional repression of *ICS1* in *gsnor1-3* plants. However, further research is needed to elucidate the molecular mechanism behind this possibility.

Chapter 4 *In vitro* S-nitrosylation of SARD1 impacts its DNA-binding affinity

Introduction

The plant hormone salicylic acid (SA) is known to coordinate different biological processes and its accumulation is an essential requirement for the expression of pathogenesis-related genes and the deployment of systemic acquired resistance (SAR) in uninfected leaves (Loake & Grant, 2007; Spoel & Dong, 2012; Dempsey & Klessig, 2017). Similarly, nitric oxide (NO) is considered as a critical signalling molecule that can regulate gene expression and signalling pathways via post-translational modifications to target proteins (Kovacs *et al*, 2016). S-nitrosylation, the reversible covalent binding of a NO molecule to the thiol group to a rare, highly reactive Cysteine residue can modulate protein bioactivity allowing specific proteins to act as molecular switches sensing changes in the cellular redox state (Yu *et al*, 2014).

GSNOR1

Additionally, S-nitrosoglutathione (GSNO), formed by S-nitrosylation of glutathione (GSH), acts as stable storage of NO bioactivity and can function as a potent NO-donor to *trans*-nitrosylating other proteins. The cellular level of GSNO is governed by the activity of the enzyme GSNO Reductase 1 (GSNOR1), which catalyses the reduction of GSNO into oxidised glutathione (GSSG) and ammonium (NH_3) (Feechan *et al*, 2005 Frungillo *et al*, 2014;).

Arabidopsis plants with impaired GSNOR1 activity showed increased total SNO cellular levels and compromised basal, non-host and *R*-gene resistance and reduced SA biosynthesis and accumulation (Feechan *et al*, 2005). However, the molecular mechanisms by which elevated S-nitrosylation mediates repression of SA biosynthesis is not known. Our previous observations with the *ICS1::GUS* transgene in *gsnor1* impaired plants suggest transcriptional repression of the *ICS1* promoter, probably contributing to explain the reduction of SA accumulation in *gsnor1-3* plants.

SARD1 and CBP60g

To date, several transcription factors (TFs) that modulate *ICS1* expression have been reported. Among these, SARD1 and CBP60g have been linked with a significant role in driving *ICS1* expression. The *sard1 cbp60g* double mutant is severely impaired in

SA biosynthesis and displays reduced basal and systemic immunity (Zhang *et al*, 2010; Wang *et al*, 2011; Sun *et al*, 2015). SARD1 and CBP60g share 39% identity at the protein level and contain a highly conserved DNA-binding domain (DBD) in the middle region and are entirely diverged at the N- and C- terminal domains (Zhang *et al*, 2010). Both proteins share a preference for the binding domain GAAATTT and were shown in a ChIP-SEQ experiment to bind to the promoter region of a vast array of immune-related genes, including positive and negative immune regulators (Sun *et al*, 2015).

Also, It was recently shown that the SARD1 and CBP60g C-terminal domain is targeted by the *Verticillium* secreted effector protein VdSCP41 to promote *Verticillium* wilt disease, suggesting the existence of a *trans*-activation domain located at the C-terminal end of the DBD, compromising the activation of immune responses (Qin *et al*, 2018). One possibility to explain this effect could be a direct alteration of SARD1/CBP60g DNA-binding capabilities upon interaction with the effector protein, possibly mediated by conformational changes at the C-terminal end.

S-nitrosylation

A critical requirement for protein S-nitrosylation to occur is the availability of a surface exposed Cys residue exhibiting a low pKa sulfhydryl group (Yu *et al*, 2014). Both SARD1 and CBP60g contain cysteine residues in their amino acid sequence, 4 and 11 cysteine residues, respectively, making them attractive candidates to investigate the effect of S-nitrosylation on their activity. Moreover, S-nitrosylation has been shown to modulate the DNA-binding capabilities of the plant-specific TF Myb-2, and Myb-30, in which reduced DNA-binding upon S-nitrosylation of a conserved Cys residue was observed (Serpa *et al*, 2007; Tavares *et al*, 2014).

Biotin switch

The Biotin-switch assay is a biochemical technique to identify S-nitrosylation targets *in vitro*. The principle of the assay relies on three main steps. First, the recombinant protein is incubated with a NO-donor to promote S-nitrosylation. Secondly, the un-nitrosylated thiols groups are irreversibly blocked with N-ethylmaleimide (NEM) and finally, the nitrosothiols are reduced with sodium ascorbate and the nascent thiol groups are labelled with a biotin molecule. The biotinylated protein can be detected by western blot (Jaffrey & Snyder, 2001).

In vitro S-nitrosylation of SARD1

In previous work from our lab, Li (2015) expressed recombinant SARD1 with an N-terminal Maltose Binding Protein (MBP) tag (MBP-SARD1) and evaluated its DNA binding activity to a 181 bp fragment of the *ICS1* promoter in an electromobility shift assay (EMSA) after incubation with the NO-donors, CysNO and GSNO. Reduced DNA-binding of SARD1 was observed after the NO-donor treatment. The effect could be reversed by the addition of the reducing agent dithiothreitol (DTT) (Li, 2015), consistent with the reports of S-nitrosylation on Myb-2 and Myb-30 DNA-binding indicating that a reduced state in the proteins is necessary for optimal DNA binding (Serpa *et al*, 2007; Tavares *et al*, 2014).

In subsequent experiments, Li found that SARD1 can be S-nitrosylated *in vitro* using the biotin-switch assay in a NO-concentration dependent fashion. Furthermore, he generated four SARD1 mutants with an individual Cys to serine (Ser) substitution (C211S, C311S, C333S and C438S) and identified C438 as the target for S-nitrosylation.

The data generated by Yuan Li (Li, 2015) indicated that Cys-438 of SARD1 is the target for S-nitrosylation and that this post-translational modification reduces its DNA-binding efficiency. To further investigate the relevance of S-nitrosylation of SARD1 in the modulation of SARD1 DNA-binding activity, we performed a quantitative DNA-binding assay and calculated the binding affinity of wild-type SARD1 and SARD1 with a Cys-438 to Ser-438 mutation to the *ICS1* promoter. We hypothesised that a Cys to Ser substitution at amino acid residue 438 would render SARD1 less sensitive to modulation by NO.

Results

SARD1 DNA-binding to the *ICS1*$_{25bp}$ promoter sequence

We performed EMSA using recombinant SARD1 and SARD1C438S after S-nitrosylation. Previously, we used a 181 bp *ICS1* promoter fragment reported by Zhang (2010). A more recent publication showed that SARD1 could bind to a 56 bp fragment of the *ICS1* promoter containing the binding motif GAAATTT and drive the expression of *Luciferase* in a promoter activity assay in *Arabidopsis* protoplasts (Sun *et al*, 2015). Using a smaller DNA probe can offer advantages by reducing background noise and unspecific binding in an EMSA (Hellman & Fried, 2007). Therefore, we prepared a 25 bp *ICS1* promoter fragment flanking the specific DNA wild-type (WT) binding motif and a mutant 25 bp version where the GAAATTT motif was mutated to GAAGGGT, as described by Sun *et al* (2015).

We first labelled the *ICS1*$_{25bp\ WT}$ and *ICS1*$_{25bp\ MT}$ probes 5'-ends with a radioactive phosphorus isotope (γ-32P) and expressed recombinant MBP-SARD1 and MBP-SARD1C438S fusion proteins and purified them by affinity chromatography (Fig 4.1A). We measured the protein concentrations by the Bradford assay. Subsequently, we titred increasing protein concentrations in EMSA using the radiolabelled *ICS1* probes. No shift was observed for the free probe lanes and a strong band indicating DNA-protein binding was observed for both SARD1 and SARD1C438S when incubated with the WT *ICS1* probe but not for the mutant version. This experiment confirmed that the recombinant proteins could bind to the 25 bp *ICS1* probe *in vitro* and show specificity for the shorter probe (Fig 4.1B).

Interestingly, we could detect DNA-binding with lower SARD1C438S concentration relative to that of SARD1 (Fig 4.1B). Therefore, we optimised the protein concentration calculations by confirming Bradford data through running an SDS-PAGE of the purified fractions together with a BSA standard followed by analysis of the bands intensities using ImageJ and selecting fractions with equal intensity of the fusion protein to guarantee equal protein loading.

Effect of S-nitrosylation of SARD1 in DNA-binding activity

We then proceed to evaluate the effect of S-nitrosylation on DNA binding. To do this, we performed EMSA after incubating equimolar concentrations of the recombinant SARD1 and SARD1C438S protein samples with increasing concentrations of GSNO, a natural NO donor, ranging from 0.1 to 5 mM before undertaking the DNA-binding

reaction. We could observe reduced binding in wild-type SARD1 in a GSNO concentration-dependent effect between 0.5 – 5 mM which could be reversed by the addition of DTT (Fig 4.2A and 4.2B), consistent with the effect reported for Myb protein before (Serpa *et al*, 2007; Tavares *et al*, 2014). Conversely, we noted less DNA-binding inhibition in the mutant SARD1C438S by S-nitrosylation (Fig 4.2A and 4.2B), supporting our hypothesis of a regulatory effect of S-nitrosylation of Cys-438 on SARD1 binding to the *ICS1* promoter.

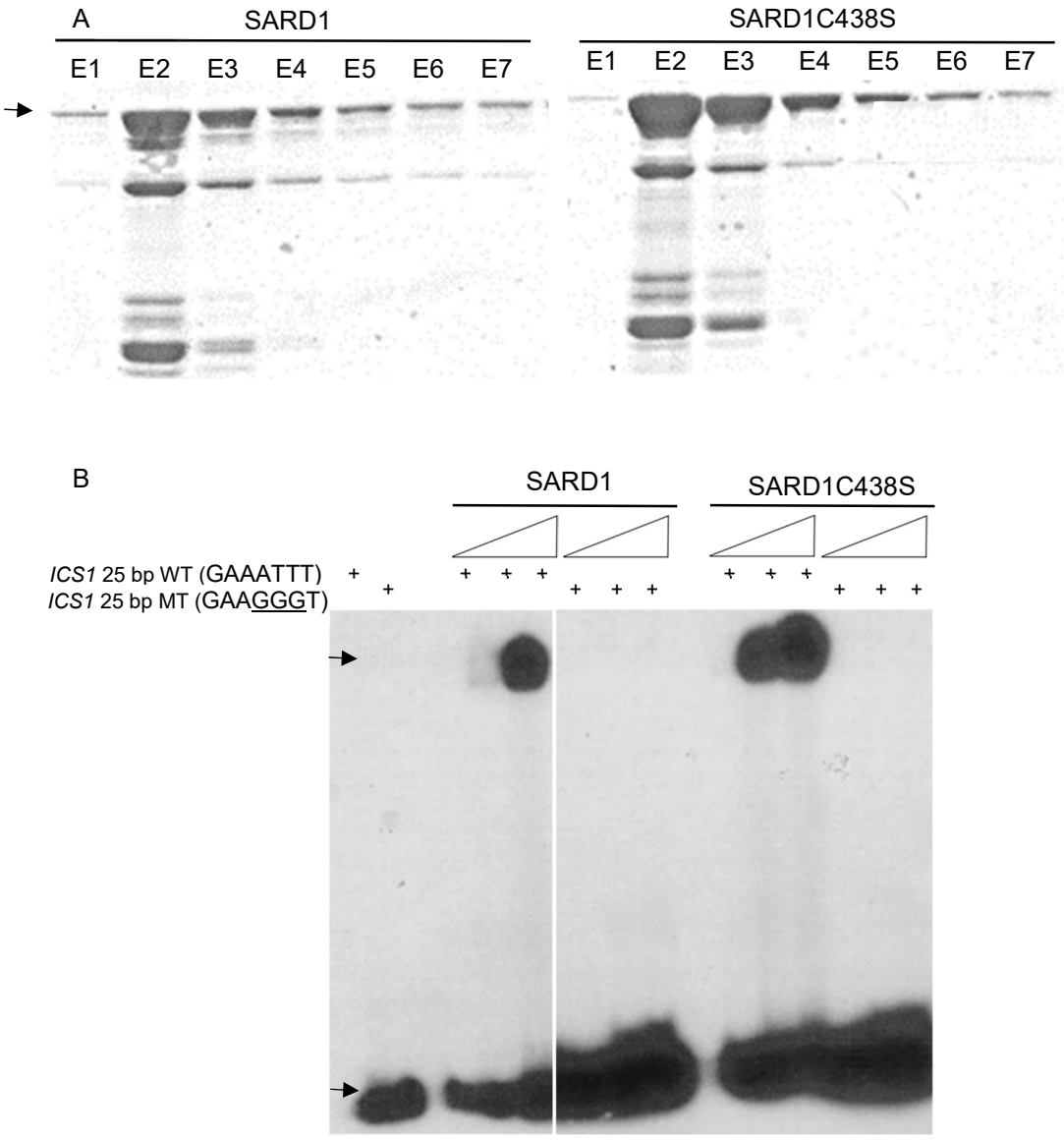

Figure 4.1. SARD1 and SARD1C438S DNA binding assay. A) Coomasie staining after SDS-PAGE of affinity chromatography purified recombinant MBP-SARD1 and MBP-SARD1C438S. The upper arrow indicated the expected size of the MBP-SARD1 fusion protein (93 KDa). B) Electromobility shift assay using a 25 bp *ICS1* promoter fragment containing the specific binding motif GAAATTT and the mutated GAAGGGT version. EMSA performed in a 6% poly-acrylamide TGE native resolving gel pH8.3 and 4% stacking gel. The upper and bottom arrows represent the DNA-protein shift and free probe, respectively. The gel was cropped for presentation purposes.

Equilibrium dissociation constant (K_D) of SARD1 and SARD1C438S

We proceed to calculate the equilibrium dissociation constant (K_D) of wild-type MBP-SARD1 and MBP-SARD1C438S. This parameter represents the binding affinity of a protein for its DNA substrate, defined by the protein concentration at which fifty per cent of the DNA is found as a DNA-protein complex. A lower K_D value indicates a higher affinity of the protein for its substrate (Heffler *et al*, 2012).

To calculate K_D, we titrated increasing concentrations of both recombinant proteins in non-radioactive EMSA using a constant concentration of the *ICS1* 25 bp promoter probe labelled with a near-infrared fluorophore. After the binding reactions and non-denaturing PAGE, the gels were scanned using a LI-COR Odyssey system at 700 nm wavelength. We subsequently calculated the DNA-protein and free-DNA fluorescence intensities using the software ImageJ. To remove background noise, we subtracted the baseline signal from blank regions of the gel from the DNA band intensities. We calculated the fraction of DNA bound using the expression: bound/[bound + unbound] and plotted the fraction bound with respect to the SARD1 concentration. We then fitted the data in a non-linear regression to the equation: Fraction Bound= B_{Max}([SARD1]/(K_D+[SARD1])) using MATLAB to calculate K_D and B_{Max} values, as described by Heffler *et al*, (2012). We observed similar K_D values for both proteins, being 219.5 nM and 247.3 nM for SARD1 WT and SARD1C438S, respectively. This experiment suggests that the mutation of Cys438 does not affect the DNA binding (Fig 4.3A and B).

Effect of S-nitrosylation on SARD1 K_D

Subsequently, we calculated K_D after S-nitrosylation of the protein samples with 1mM GSNO for 20 minutes, considering that from previous experiments we observed a reduction in DNA binding using this NO-donor concentration.

Interestingly, we observed a two-fold increase in SARD1 K_D after S-nitrosylation, rising from 219.5 nM to 494.2 nM concerning the control assay (Fig 4.3A). However, SARD1C438S K_D was not strongly affected by S-nitrosylation (Fig 4.3C), showing K_D values of 240.5 nM for the untreated sample and 276.8 nM after S-nitrosylation (Fig 4.3C), suggesting that NO can regulate the affinity of SARD1 to the *ICS1* promoter by S-nitrosylation of Cys-438 *in vitro*. Furthermore, the observation that SARD1 DNA-binding activity is reduced upon treatment with GSNO but not wholly abolished could

represent a NO-mediated regulatory mechanism for SARD1 bioactivity sensing the redox cellular state.

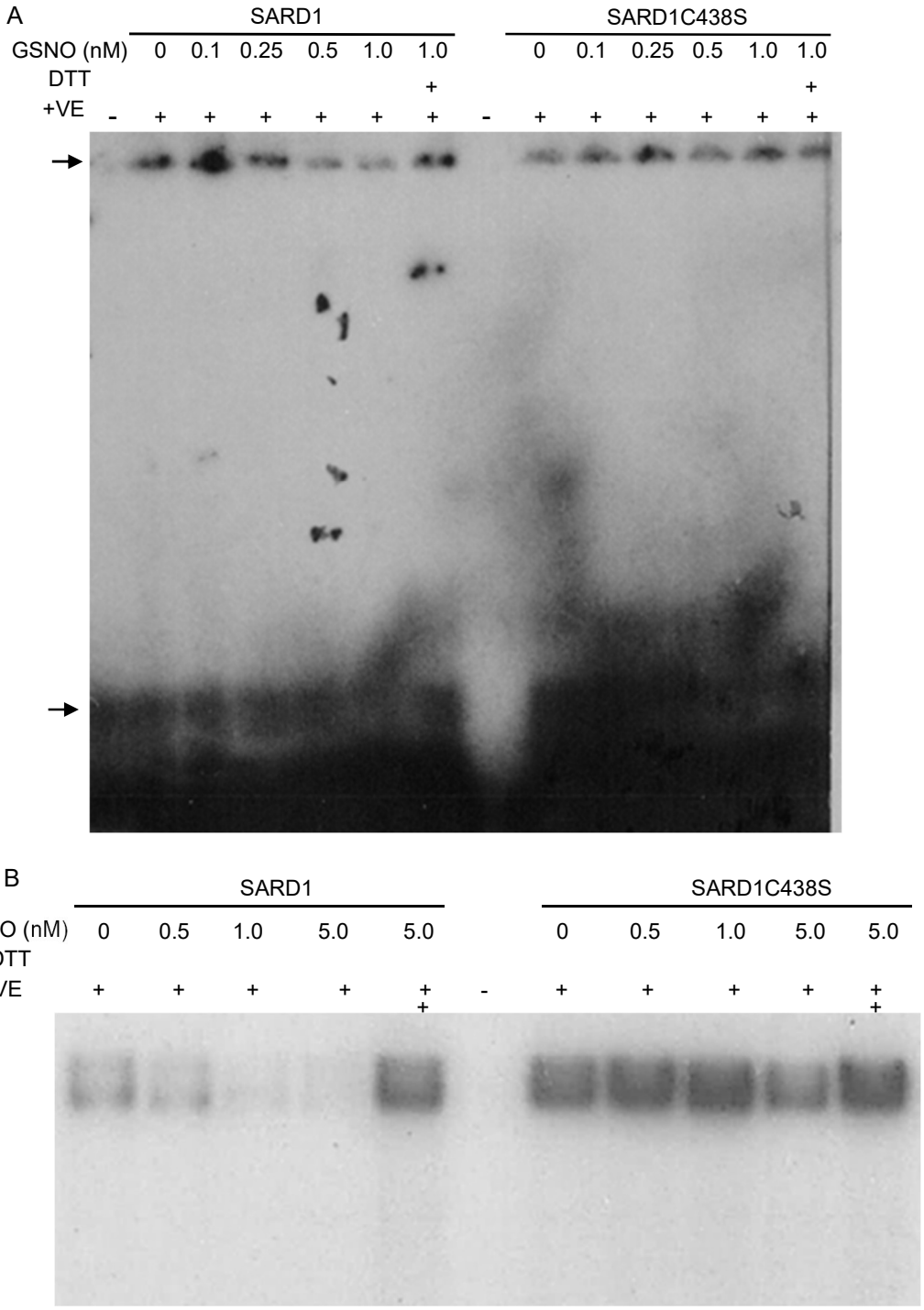

Figure 4.2. Concentration dependant effect of S-nitrosylation on DNA-binding of SARD1. A and B) Radioactive EMSA after S-nitrosylation of recombinant MBP-SARD1 and MBP-SARD1C438S. Protein samples were incubated with increasing GSNO concentrations covering a range from A) 0.1, 0.25, 0.5 and 1mM and B) 0.5, 1.0 and 5.0 mM with or without the addition of DTT. +VE indicated protein loading. The DNA-protein shift and free-*ICS1* probe is indicated by the upper and bottom arrows.

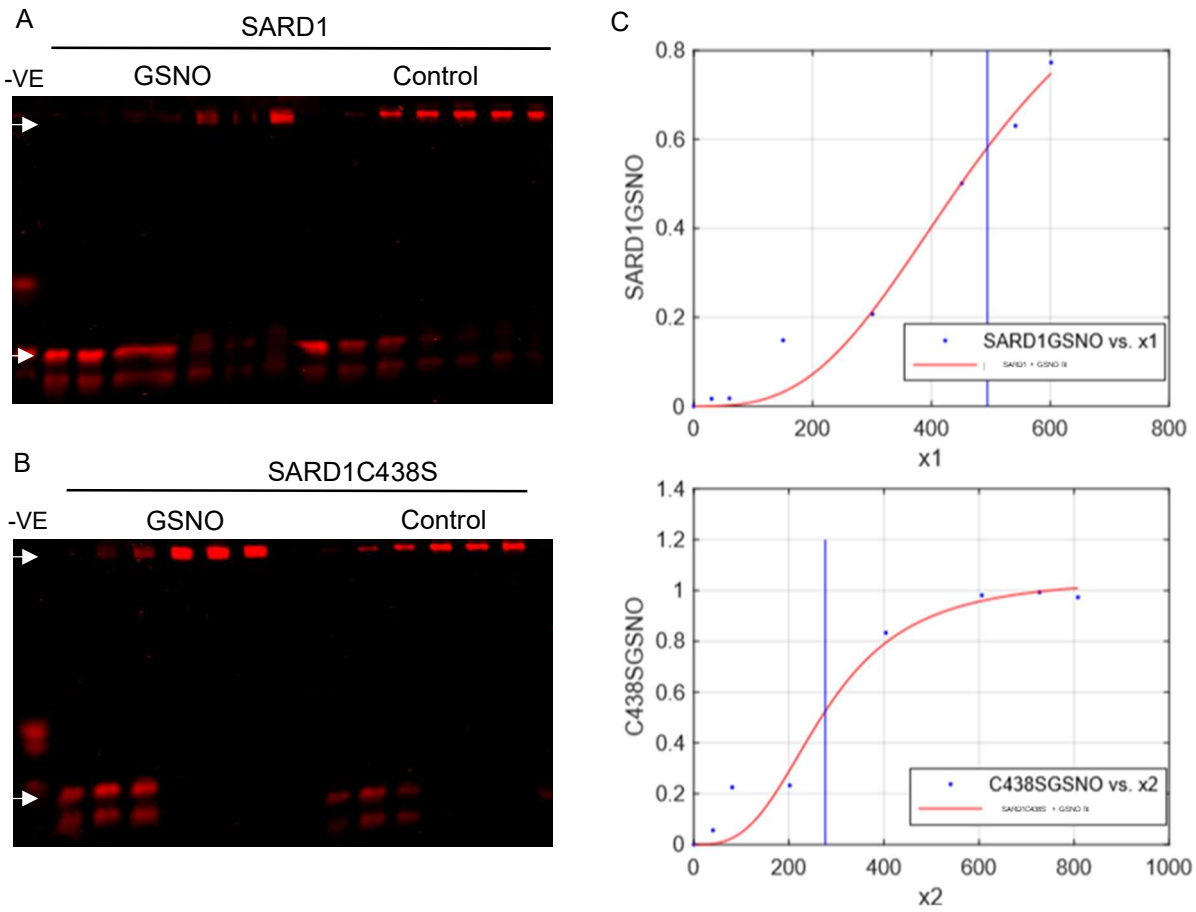

Figure 4.3. Binding affinity of SARD1 and SARD1C438S to the *ICS1* promoter. Titration of recombinant SARD1 proteins in non-radioactive EMSA after S-nitrosylation with 1 mM GSNO and control treatment. A) SARD1 and B) SARD1C438S. Upper and bottom arrows indicate protein-DNA shift and free probe, respectively. Protein concentrations range from 30 to 600 nmol. C) Plot shows the fraction of DNA bound as SARD1 and SARD1C438S are titrated. The binding intensities were calculated using ImageJ. The values of KD and BMAX were calculated in MATLAB using the general equation (x)=(a*x^3)/(k^3+x^3). Coefficient with 95% confidence bounds: The KD and BMAX values are: SARD1 control and GSNO (141.3 and 494.2 nM, 0.82 and 1.16) and for SARD1C438S control (240.5, 276.8 nM, 0.99 and 0.98).

Discussion

SARD1 and CBP60g play a critical role in modulating *ICS1* expression (Zhang *et al*, 2010). Also, they were proposed as master regulators of plant immunity on the grounds of their ability to bind to the promoter region of different immune-related genes, including both positive and negative regulators (Sun et al, 2015). The fact that the effector protein VdSCP41 from *Verticillium dahliae* targets SARD1 and GBP60g to promote virulence by inhibiting their ability to drive *ICS1* expression via direct interaction with their c-terminal domain highlights their relevance in immunity (Qin *et*

al, 2018). However, our current understanding of how are SARD1 and CBP60g are regulated to activate the transcription machinery is limited. Also, the observed transcriptional repression on *ICS1* expression in *ICS1::GUS par2-1* plants, together with the previous finding from our lab regarding the repression of SARD1 binding to the *ICS1* promoter by S-nitrosylation at Cys-438, suggests the possibility of a NO-mediated regulatory mechanism of SARD1 bioactivity.

Effect of S-nitrosylation on DNA-binding

Here, we confirmed that S-nitrosylation of Cys-438 reduced the ability of SARD1 to bind to the *ICS1* promoter in a NO-donor concentration-dependent effect. We performed radioactive EMSA after incubating SARD1 and SARD1C438S samples with different concentrations of GSNO, ranging from 0.1 to 5 mM. Consistent with the NO-donor concentration used in different reported S-nitrosylation *in vitro* studies (Hussain *et al*, 2016; Jaffrey & Snyder, 2001). We observed compromised DNA binding in the WT protein, which was reversible by reduction with 5 mM DTT. Conversely, SARD1C438S binding was not strongly affected by incubation with the NO-donor, which indicated that S-nitrosylation at cysteine 438 could be responsible for the decrease in affinity and that a reduced state of the protein is necessary for DNA-binding.

A similar effect was reported for the plant proteins MYB-2 and MYB-30, where S-nitrosylation of Cys49 and Cys53 inhibited DNA-binding (Serpa *et al*, 2007; Tavares *et al*, 2014). In follow up experiments, different Myb30 Cys to Alanine (Ala) mutants (C49A and C53A) were used to calculate K_D values to evaluate if the formation of disulphide bonds was critical for Myb30 DNA-binding activity and if S-nitrosylation of these residues could mediate changes in the secondary structure to explain the inhibitory effect on DNA-binding. The authors observed similar K_D values for all proteins: Myb30, Myb30C49A and Myb30C53A, indicating that the formation of disulphide bonds between Cys-49 and Cys-53 was not critical for DNA binding of MYB-30 and supporting the idea that a reduced state in the protein was necessary for binding (Tavares & Terenzi, 2016). However, the authors did not measure changes in K_D after S-nitrosylation.

K_D of plant TFs

We quantified the extent of S-nitrosylation on SARD1 DNA-binding by calculating the dissociation constant for both proteins before and after S-nitrosylation. We obtained

a K_D value of 219.5 nM for WT SARD1 and 240 nM for SARD1C438S, indicating that the mutation of this amino-acid has a minimum effect on DNA-binding and that C438 is not involved in the formation of a disulphide bond necessary for DNA-binding (Tavares *et al*, 2014). The reported K_D for plant TFs varies from pM to µM concentrations (Gusewski *et al*, 2018), ranging from 15 to 500 nM for MYB proteins (Tavares & Terenzi, 2016), 2 µM for DOF zinc fingers (ZF) (Moghaddas Sani *et al*, 2018), and 13 to 500 nM for SEP3 proteins (Gusewski *et al*, 2018). The calculated values for SARD1 and SARD1C438S fall within the stated range. However, the value is relatively high compared to other TF families.

Notably, ZF-TF show the lowest K_D from the available reported data. The effect of S-nitrosylation on ZF-TF DNA-binding has been reported for mammals (Hongo *et al*, 2005), yeast (Kröncke *et al*, 1994) and plants (Cui *et al*, 2018). It is proposed that S-nitrosylation disrupts the zinc core leading to significant conformational changes and reduction in DNA-binding activity (Kröncke *et al*, 1994). We observed a significant reduction in DNA-binding after S-nitrosylation of Cys438. Therefore, we propose that S-nitrosylation promotes a significant structural change that can modulate SARD1 bioactivity.

To evaluate if the calculated K_D for SARD1 using recombinant MBP-SARD1 is physiologically relevant it will be necessary to measure SARD1 concentrations *in vivo.* Urquiza-Garcia and Millar (2018) published a method to measure protein levels *in vivo* using the reporter protein Nano luciferase (NanoLUC). The method relies on generating transgenic *Arabidopsis* lines with a translational NanoLUC protein-of-interest fusion and measuring the bioluminescence *in vivo* or from protein extracts. The readings can be extrapolated into a NanoLUC standard curve to estimate the fusion protein present in the sample at specific times (Urquiza-García & Millar, 2018). To investigate *in vivo* concentration of SARD1 we will need to generate *SARD1::SARD1-NanoLUC* reporter lines and characterise the relative and total bioluminescence under basal conditions and upon activation of immune responses.

Effect of S-nitrosylation on SARD1 K_D

We observed a K_D of 494.2 nM in SARD1 after S-nitrosylation, which represents a 2.25 folds increase with respect to the untreated protein but only a 0.15-fold increase for SARD1C438S. The reduction in affinity by S-nitrosylation of wild type SARD1 could be due to conformational changes in the secondary protein structure upon the formation of the S-nitrosothiol group at Cys438. However, we did not observe a

significant reduction in affinity of the C438S mutant, supporting the role of Cys438 as the target for S-nitrosylation (Tavares & Terenzi, 2016).

Interestingly, this Cys residue is located close to the C-terminal end and outside the DNA-binding domain of SARD1. Qin *et al*, (2018) reported that the effector protein VdSCP41 from the fungal pathogen *V. dahliae* targets a conserved region of CBP60g ranging from amino acids 211 to 440 at the C-terminal chain of the DNA-binding domain, which harbours a proposed transcription activation domain. The binding of the effector protein to this conserved region of CBP60g and SARD1 compromises the expression of *ICS1,* potentially affecting SARD1 three-dimensional structure or preventing the interaction with cofactors (Qin *et al*, 2018). Notably, Cys438 locates within the region reported to be targeted by VdSCP41, close to the activation domain. S-nitrosylation of this residue may affect the activation domain via structural changes or reducing interactions with coactivators and comprise an additional regulation step to activate the transcription machinery.

K_D dynamic interplay of SARD1 model

Interestingly, even though SARD1 DNA-binding is reduced upon S-nitrosylation, the protein can still bind to its target DNA but at a lower rate. SARD1 and CBP60g have overlapping functions in plant immunity. CBP60g is thought to be involved in early stages of immunity and SARD1 is thought to participate at later stages (Wang *et al*, 2011a). Currently, the molecular mechanism regulating the interplay and appropriate timing to drive *ICS1* expression by these two transcription factors is not clear. It may be possible that modulation in affinity mediated by the level of S-nitrosylation according to the cellular REDOX state during the immune response can help fine-tune the dynamics between SARD1 and CBP60g, resulting in a dynamic interplay of increased and decreased affinities for the *ICS1* promoter at different stages of the immune response. To evaluate this hypothesis, it is necessary to generate *Arabidopsis* SARD1 and SARD1C438S reporter lines with Human influenza hemagglutinin (HA) tag to confirm *in vivo* S-nitrosylation of SARD1 and Chromatin Immunoprecipitation (ChIP) and investigate the changes in bioactivity in response to S-nitrosylation.

Chapter 5 Biological relevance of Cys-438 of SARD1

Introduction

Plant immunity

The plant's immune system is organised in different layers of defence. As an initial step, plants posess physical barrier to prevent the entrance of pathogen into the cells. Above this layer, plants evolve pathogen recognition receptors (PRR) which recognise conserved pathogen-associated molecular patterns (PAMPs) and induce an immune response upon activation, termed PAMP-triggered immunity (PTI). Some pathogens have evolved specialised virulence proteins (effectors) aimed to highjack PTI, resulting in effector-triggered susceptibility (ETS). As an escalated level of defence, plant developed functional cytoplasmic receptors termed R-proteins that recognise pathogen effector and induce effector-triggered immunity (ETI), characterised by a fast and robust immune response and localised cell-death (hypersensitive response) at the infection site. Above these layers of defence, plants evolved the systemic acquired resistance (SAR), in which plants prime their immune mechanisms in uninfected leaves after primary infection in order to respond quickly and efficiently against secondary infections (Dodds & Rathjen, 2010; Spoel & Dong, 2012; Walters, 2015).

Salicylic acid (SA) is a plant hormone that plays a critical role in the establishment of immune responses against biotrophic pathogens and a key player for the development of SAR (Loake & Grant, 2007; Vlot *et al*, 2009; Fu & Dong, 2013). In a reverse genetic screening testing *Arabidopsis thaliana* T-DNA insertion lines for compromised development of SAR, Zhang et al, (2010) identified a mutant significantly compromised in SAR, defined as *SAR-deficient 1 (SARD1)*.

SARD1

The T-DNA insertion was mapped to the transcription factor (TF) SARD1. Further structural analysis demonstrated that SARD1 belongs to a family of plant-specific TFs and plays a pivotal role in the regulation of salicylic acid biosynthesis through direct regulation of the *Isochorismate Synthase1 (ICS1)* gene (Zhang *et al*, 2010). The relevance of SARD1 and its homologue CBP60g in immunity has been demonstrated by the fact that the *sard1 cbp60g* double mutant is severely impaired in SA

biosynthesis and accumulation, and exhibits compromised basal and SAR, demonstrated by enhanced susceptibility to *Pseudomonas syringae* pv maculicula ES4326 infection (Zhang *et al*, 2010).

SARD1 and CBP60g

SARD1 shares 33% similarity with CBP60g at the amino acid level. These proteins contain a novel DNA-binding domain and share the binding motif GAAATT. Both proteins have been shown to have nuclear localisation and binding to the *ICS1* promoter upon pathogen infection *in vivo* (Zhang *et al*, 2010). SARD1 and CBP60g play partially redundant roles in mediating immunity. CBP60g can bind calmodulin and sense changes in calcium concentrations, and it is suggested to play a role during the early stages of the immune response, while SARD1 is proposed to participate at later stages (Wang *et al*, 2011a). Both SARD1 and CBP60g are rapidly induced upon treatment with salicylic acid, and they participate in the regulation of different nodes of plant immunity, including positive and negative regulation (Sun *et al*, 2015). Also, it was reported that the vascular pathogen *Verticillium dahliae* targets a conserved region toward the C-terminal of SARD1 and CBP60g to promote infection in roots (Qin *et al*, 2018).

Regulation of SARD1

Upon pathogen infection, SA accumulation mediates transcriptional reprogramming to activate the expression of defence genes. Recent studies described the role of NPR1, NPR3 and NPR4 as SA receptors, with NPR1 acting as a transcriptional activator and NPR3/NPR4 as transcriptional repressors. The transcriptional regulation of these proteins is dependent on the interaction with the TFs TGA2, TGA5 and TGA6 (Ding *et al*, 2018). Under basal conditions and low SA concentrations, NPR3/4 repress the expression of SA-dependent genes. At high SA concentrations, NPR1/3/4 bind SA with high affinity and activate or de-repress the expression of immune-related genes, respectively. Interestingly, NPR4 was found to repress the expression of *SARD1* and *WRKY70* via direct interaction with TGA elements in their promoters during low SA levels, but it was not found to regulate *CBP60g* (Ding *et al*, 2018).

Additionally, the TF TGA1 and TGA4 regulate SA and Pipecolic acid (Pip) synthesis by controlling *SARD1* and *CBP60g* expression. The *tga1* and *tga4* plants showed higher susceptibility to pathogen infection, compromised PTI and SAR linked with impaired SARD1/CBP60g expression and reduced SA and Pip biosynthesis (Sun *et*

al, 2018). SA and Pip mediate one branch for the activation of SAR (Gao *et al*, 2015; Shine *et al*, 2018). Notably, the transcription factor CCA1-Hiking Expedition (CHE) was reported to regulate the circadian oscillation of SA levels and the activation of SAR. The *che* plants showed compromised SAR and exhibited impaired *SARD1/CBP60g* expression levels. However, no CHE *cis*-binding elements are found within *SARD1/CBP60g* promoters, suggesting an indirect mechanism to regulate these proteins (Zheng *et al*, 2015).

The accumulating evidence indicates a complex network fine-tuning SA biosynthesis and accumulation to guarantee a rapid activation of defences and prevent spurious activation. Notably, SARD1 and CBP60g play a critical role in this tight regulation (Zhang *et al*, 2010; Wang *et al*, 2011a; Sun *et al*, 2015, 2018; Ding *et al*, 2018; Qin *et al*, 2018). However, the molecular mechanisms that regulate SARD1 bioactivity are not fully understood.

The evidence that under a high S-nitrosylation background SA biosynthesis is reduced (Feechan *et al*, 2005), together with our observations of transcriptional repression of the *ICS1* promoter by S-nitrosylation and the reduction in DNA-binding affinity to the *ICS1* promoter upon S-nitrosylation of SARD1 at Cys-438 in our *in vitro* study suggests an important regulatory mechanism of SARD1 bioactivity by S-nitrosylation, possibly contributing to integrate REDOX mediated posttranslational modification into the regulatory network of SA biosynthesis.

Here, we report the generation of *Arabidopsis thaliana* reporter lines to investigate the biological relevance of the S-nitrosylation of SARD1.

Results

Generation of transgenic *Arabidopsis thaliana* plants

To evaluate the biological relevance of S-nitrosylation of cysteine-438 of SARD1 we generated *Arabidopsis thaliana* transgenic plants expressing a fusion of SARD1 protein with a C-terminal Human influenza hemagglutinin (HA) or Nanoluciferase (nLUC) tag under the control of the native *SARD1* promoter and terminator using the same genomic region previously described by Zhang *et al* (2010). We designed primers to amplify the *SARD1* genomic region (Fig 5.1A) and flank the promoter + *5'UTR*, the *SARD1* coding sequence (without stop codon) and the *3'UTR* + terminator region with Bpi I restriction site and four base pair overhang for DNA assembly using the MoClo toolkit. The *SARD1* genomic region was domesticated removing internal Bsa I and Bpi I restriction sites according to established protocols (Engler *et al*, 2009). We simultaneously prepared a mutant version of SARD1 with a cysteine to serine substitution at position 438.

After confirmation of correct amplification, we used the MoClo protocol to assemble standard parts and confirm sequence integrity by Sanger sequencing. We then assembled independent transcriptional units containing *SARD1::SARD1-HA* or *SARD1::SARD1-nLuc* for both *SARD1* and *SARD1C438*. The constructions were tested in a transient expression assay in *Nicotiana benthamiana* (not shown) and were subsequently transformed into the *sard1* genetic background by floral dipping using the *Agrobacterium* strain GV3101. T1 transformant plants were identified for BASTA resistance and selected to obtain T3 homozygous plants.

Complementation of the *sard1* phenotype

The *sard1* knock out plants exhibits loss of basal and systemic resistance against different pathogens, including *Hyaloperonospora arabidopsidis* Noco 2 (*H.a.*Noco2) and *P.s.* pv maculicula ES4326 (*P.s.m* ES4326) (Zhang *et al*, 2010). Therefore, we evaluated the bioactivity of the fusion protein scoring for restored resistance to *Psm* infection and complementation of the *sard1* phenotype. To evaluate this, we infiltrated three-week-old plants with *P.s.m.* ES4326 $O.D._{600}$ =0.0002 and monitored the bacterial growth three days after infection. As expected, *sard1* plants showed compromised basal resistance to the bacterial pathogen indicated by a bacterial titre of nearly 2 logarithmic scales higher than wild type (WT) plants. We did not find significant differences between the HA and nLUC lines with respect to the control,

indicating that the *SARD1::SARD1* transgene is bioactive and complemented the *sard1* phenotype (Fig 5.1B).

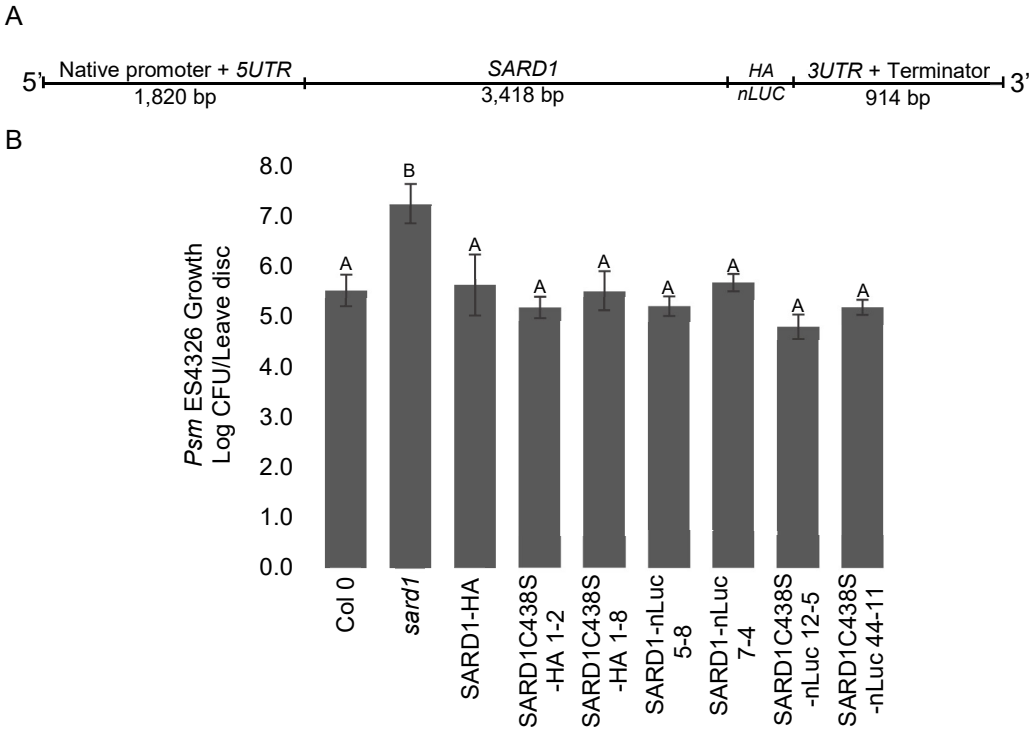

Figure 5.1. Complementation of *sard1* plants. A) Schematic representation of DNA constructions. The genomic region of *SARD1* was amplified covering 1,820 bp of the promoter + 5UTR and 914 bp of the 3UTR + terminator as described by Zhang *et al,* (2010). The stop codon was removed for C-terminal fusion with HA-tag and nLUC-tag. Independent constructions were prepared for SARD1 and SARD1C438S with each tag. B) Pathogen growth assay 72 hours after infiltration with *Psm* ES4326 $O.D._{600}$ =0.0002. The values presented are the mean value of 6 biological replicates per genotype and 6 technical repetitions. Error bars represent the standard error. One way ANOVA followed by Tukey's Multicomparison of means ($p<0.05$), different letters indicate statistically significant differences.

Expression of SARD1-HA

To further evaluate the significance of cysteine 438 we proceed to evaluated if SARD1 could be S-nitrosylated *in vivo*. We anticipated that the Cys to Ser substitution of Cys438 should result in less or no detectable S-nitrosylation in SARD1C438S. We first evaluated the protein expression levels in the HA lines in response to exogenous SA application by extracting total protein from plants twelve hours after foliar treatment with SA. After western blot using α-HA antibodies, we were able to detect a protein of 58 kDa, consistent with the expected molecular weight of the fusion protein. Also, the

band was not detectable in the Col-0 and *sard1* controls, confirming the identity of the SARD1-HA protein. Notably, we could observe a faint band in the un-induced SARD1-HA lane and a significant increase in the intensity of the band after induction with SA. Conversely, the SARD1C438S line analysed showed a band in the absence of SA and a minimal increase after induction (Fig 5.2A). We then tested more SARD1C438S-HA lines at different time points after SA treatment and observed a consistent SARD1C438S-HA band before SA induction in several lines. However, the intensity of the band increased significantly after SA (Fig 5.2B), consistent with previous reports showing increased SARD1 transcription from 3 hours after induction with *P.s.m*. ES4326 and significant transcript accumulation after 12 hrs (Li, 2015; Sun *et al*, 2018). The presence of a band without induction in the different *SARD1C438S* lines tested may be related with constitutive *SARD1C438S* expression due to the integration location of the transgene in the genome or by the possibility of negative feedback amplification mechanism on *SARD1* expression/accumulation mediated by S-nitrosylation.

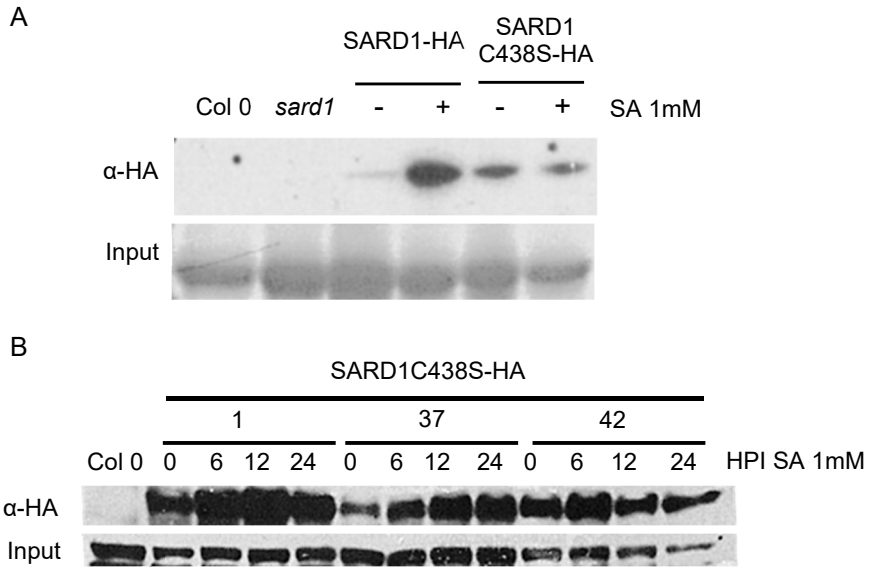

Figure 5.2. Characterisation of *SARD1::SARD1HA* lines. Western blot to detect SARD1-HA protein. Total protein was extracted in HEN buffer (250mM HEPES pH7.2, EDTA 1mM, 0.1mM Neucoproine) + 1mM PMSF + 0.5% Triton X100 and spun at 14,000G for 15 min. 20µL per sample were used for western blot analysis with primary mouse α-HA (1:3,000) and secondary α-mouse-HRP conjugated (1:3,000) antibodies. The nitrocellulose membrane was incubated with SuperSignal West Pico chemiluminescent substrate prior to exposure of X-ray films. A) Total protein extract from Col-0, *sard1,* SARD1::SARD1-HA and SARD1::SARD1C438S-HA 12 hours after induction with SA (1mM SA in 10mM Sodium phosphate buffer pH 7.2 + Triton X-100 0.01%). B) Total protein extract from SARD1::SARD1 C438S-HA lines (1, 37 and 42) at 0, 6, 12 and 24 hours post induction with SA.

In vivo S-nitrosylation of SARD1

After confirmation of expression and detection of the SARD1-HA and SARD1C438S-HA fusion proteins, we performed biotin switch from leaf extracts to evaluate if SARD1 could be S-nitrosylated *in vivo*. To do this, we first induced *SARD1* expression with exogenous SA treatment. After 12 hours post SA we infiltrated some leaves with 1 mM GSNO in $MgCl_2$ as positive control according to reported protocols (Albertos *et al*, 2015; Feng *et al*, 2013). After one hour incubation with GSNO, we harvested the leaves and ground them in liquid nitrogen. We performed the biotin switch assay from the leaf protein extract (Jaffrey & Snyder, 2001). The protocol was performed in the dark with the occasional use of indirect light. Notably, we could only observe a band on the SARD1-HA test samples without GSNO infiltration and not in the positive control (GSNO infiltrated) or any SARD1C438S samples (Fig 5.3A). The input control indicates that all the samples contain HA-tagged protein before pull-down of the biotinylated proteins. However, it is possible that the biotinylated proteins did not bind to the streptavidin beads probably due to incorrect biotin labelling. To confirm and expand these results we performed the biotin switch assay using total protein extract from SA-induced plants incubated with GSNO as positive and GSNO plus Dithiothreitol (DTT) as a negative control. We observed a strong S-nitrosylation band for the SARD1-HA line when incubated GSNO, and a reduction in the signal with the addition of DTT. The SARD1C438S-HA extract only produced a faint band on the sample treated with GSNO, and no signal was detected after reduction of the sample with DTT (Fig 5.3B). This result indicates that SARD1 can be S-nitrosylated from a total protein. However, the band observed on the SARD1C438S sample could indicate a secondary S-nitrosylation target, suggesting that SARD1 is S-nitrosylated preferentially at Cys438.

SARD1 temporal profile

To further investigate the biological relevance of Cys438 of SARD1 we prepared transgenic lines expressing a SARD1-nLUC fusion protein. nLUC is a small enzyme with an emerging potential for bioluminescent assays *in vivo* covering a wide range of application, from receptor-ligand binding to transcriptional regulation (Zhang *et al*, 2013b; Basu *et al*, 2017; Urquiza-García & Millar, 2018). In our study, the SARD1-nLUC fusion allows us to monitor the *de novo* synthesis of SARD1 to elucidate the molecular dynamics and temporal profile of SARD1.

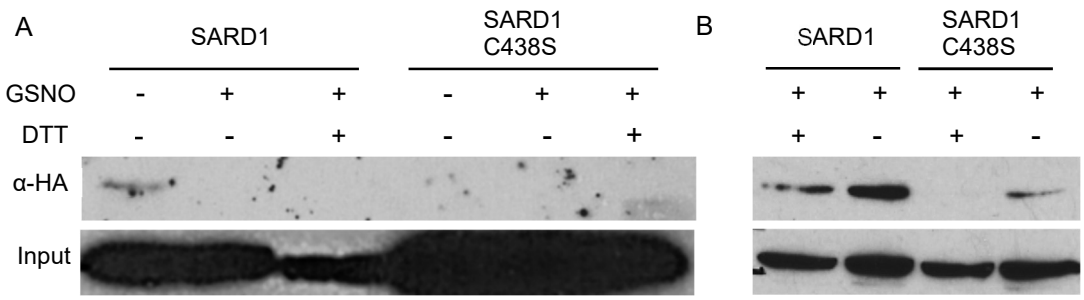

Figure 5.3. In vivo S-nitrosylation of SARD1. Biotin switch assay from leaf extract. A) SARD1-HA and SARD1C438S infiltrated with 1mM GSNO in 10mM $MgCl_2$ 12 hours after induction with 1mM SA. After 1-hour incubation with GSNO, the samples were collected in the dark and frozen. DTT was added to the negative control. Protein extracted from GSNO untreated samples were homogenized in buffer containing 25mM NEM and blocked directly. B) Biotin Switch after incubating the total protein extract with GSNO with or without DTT.

We first characterise the SARD1-nLuc lines to select plants with similar expression levels. We induce the expression of the fusion protein with SA 1 mM for 12 hours and subsequently harvested three leaf discs from independent leaves per plant and four plants per genotype. The discs were placed at the bottom of the well from a black 96-wells plate and covered with 100 µL of a 1:50 furimazine in distilled water + 0.01% Triton X-100 solution. The bioluminescence was read in a Tecan luminometer (Fig 5.4A). We observed a base bioluminescence level for the untreated plants and a significant increase in response to SA treatment. We selected lines that exhibited similar luciferase activity and used them in an *in vivo* bioluminescence essay to evaluate changes in SARD1 dynamics in a time-course.

To do this, we germinated SARD1-nLuc and SARD1C438S-nLuc seeds in a black 96-well plate containing 100µL MS media per well under long-day conditions. Subsequently, we sprayed the one-week-old seedlings with SA plus furimazine solution and monitored the emittance of light each hour for an additional week. We noticed an increase in bioluminescence within 3 to 6 hours after SA treatment (Fig 5.4C), consistent with what we observed for the HA lines (Fig 5.2B). Also, we noticed stronger bioluminescence in response to SA in the SARD1C438S lines compared to that of the wild-type SARD1 line. The luminescence dropped to a baseline level within 20 hours after SA induction.

We observed the same dynamic after a second SA-induction, characterised by the stronger signal for the SARD1 mutant lines and a drop to the baseline level within 20 hours after SA. We noticed that after the third induction with SA, the initial SARD1C438S-nLuc accumulation was reduced compared to the previous treatments, while the SARD1-nLuc wild type line retained the same amplitude.

Interestingly, the expression level of SARD1-nLuc did not drop to the baseline and followed a prolonged oscillatory pattern (Fig 5.4C), which we speculated could be related to the activation of SAR and the critical regulatory role of SARD1 in this process (Zhang *et al*, 2010). The observation that the SARD1C438S lines did not show this oscillatory pattern could suggests a potential role for S-nitrosylation of SARD1 in the establishment of SAR.

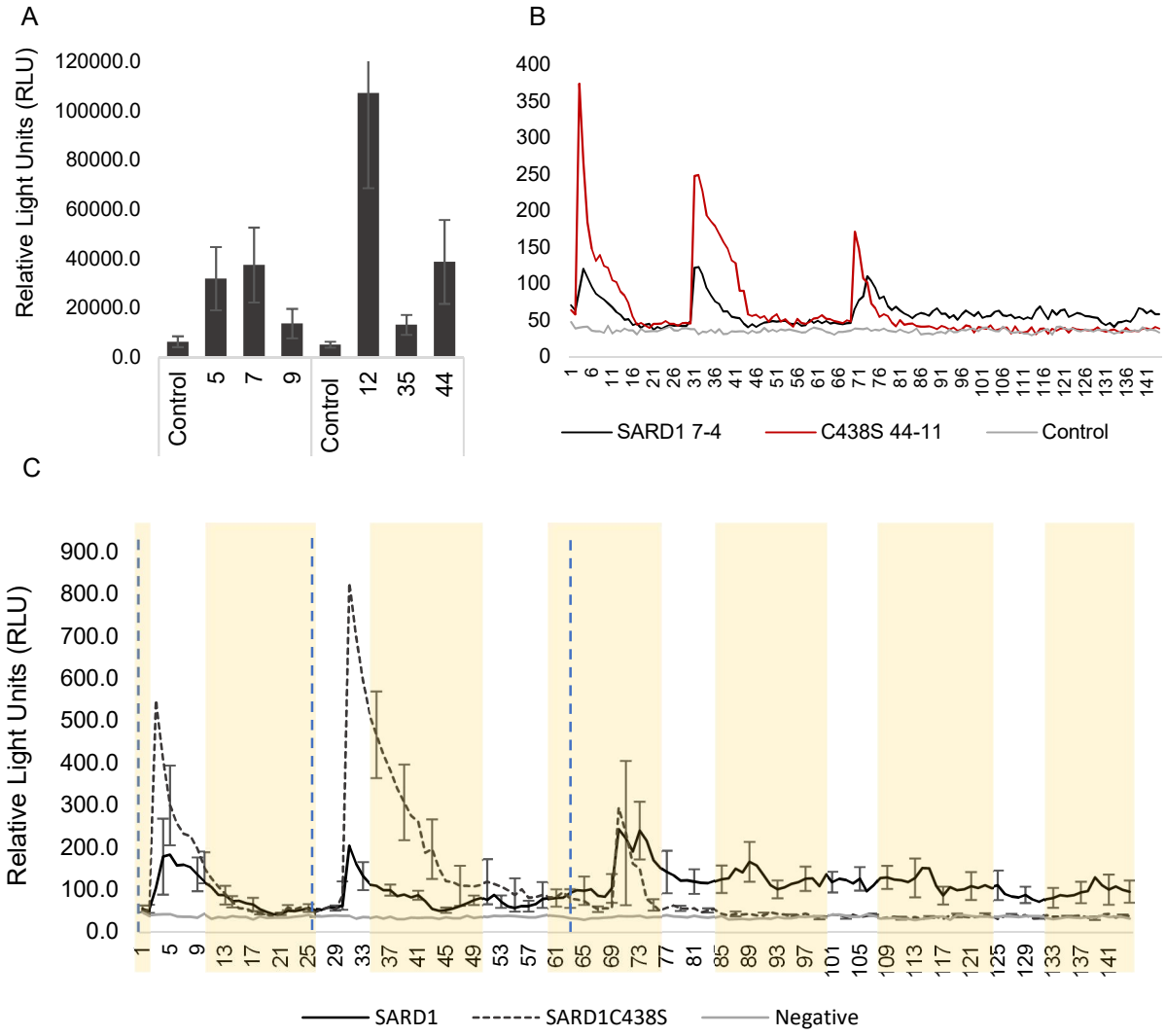

Figure 4. Characterisation of *SARD1::SARD1-nLuc* lines. Quantitative analysis of bioluminescence after SA induction. The substrate (furimazine) was diluted 1:50 in distilled water with 0.01% Triton X-100. A) Mean luminescence value of leaf discs collected from T3 *SARD1::SARD1-nLuc* plants 12 hours after induction with SA 1 mM. Three leaf discs collected per plant and four plants analysed per treatment. Error bars represent the standard error. B and C) In vivo bioluminescence assay. *SARD1::SARD1-nLuc* seeds were germinated in a 96-wells plate. The seven days old seedlings were sprayed with a 1 mM SA + 1:50 furimazine solution. Luminescence measurements were collected every hour for 1 week. B) Individual comparison of lines SARD1-nLuc 7 and C438S-nLuc 44. C) Mean value of three SARD1-nLuc and three SARD1C438S-nLuc lines with 12 seedlings per line. Error bars represent the standard error. The yellow shadow indicates light period, the blue dotted line represents SA induction.

Role of C439 in systemic acquired resistance

To assess the possible involvement of C438 in SAR establishment, we monitored bacterial growth in the SARD1 transgenic lines in a SAR assay. We first induced SAR by infiltrating a bottom leaf of three-week-old plants with a high dose (O.D.600 =0.025) of *P.s.m* ES4326 carrying the avirulent gene *avrB*. Three days after the primary infection, we inoculated three different leaves per plant with virulent *P.s.m*. ES4326 O.D.600 = 0.0002 of both SAR-induced and control plants to compare local and systemic immunity. We monitored the bacterial growth at 0, 24 and 72 hours post infection. As expected, the *sard1* plants showed the highest bacterial load at 24 and 72 HPI for both local and systemic immunity (Fig 5.5A).

In local immunity, we observed similar bacterial growth in Col 0 and the SARD1 HA lines at 24 and 72 HPI, confirming that the *SARD1::SARD1-HA* transgene complements the *sard1* phenotype. No significant difference was found at any time point indicating that S-nitrosylation of C438 does not have a significant impact in local immunity.

Interestingly, we observed in the distal leaves of the SAR-induced plants a higher bacterial load in the SARD1C438S-HA plants with respect to that of the SARD1-HA line at 24 HPI. We noticed this same effect in additional SARD1C438S lines tested. However, no statistically significant difference was found between the HA lines and the Col 0 control at this time point. At 72 HPI all lines showed comparable bacterial level with no significant difference found between any of the genotypes tested. The higher susceptibility at 24 HPI in the SARD1C438S-HA with respect to the SARD1-HA plants during SAR possibly suggests the requirement of S-nitrosylation of SARD1 for the proper establishment of the systemic response. Further experiments are required using a bigger sample size to confirm this possibility.

Discussion

In vivo S-nitrosylation of SARD1

We generated *SARD1* and *SARDC438S* transgenic *Arabidopsis* plants expressing SARD1 as C-terminal HA and nLUC fusion to evaluate if SARD1 can be S-nitrosylated *in vivo* and evaluate what is the biological relevance of this modification. We confirmed that the transgenic SARD1 proteins are bioactive by complementing the *sard1*

phenotype which exhibit compromised basal immunity and systemic acquired resistance (Zhang *et al*, 2010; Wang *et al*, 2011a).

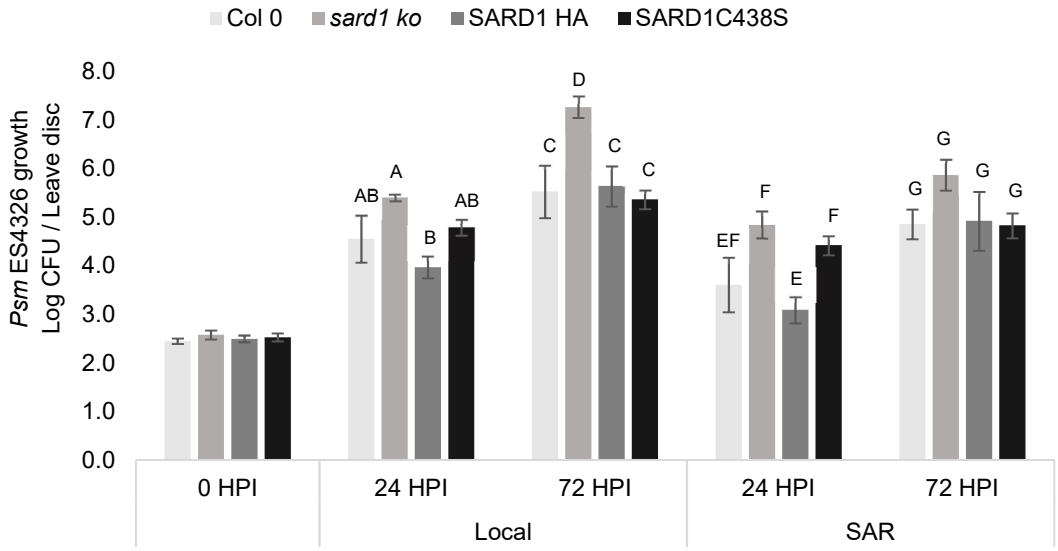

Figure 5.5. Systemic Acquired Resistance assay *SARD1::SARD1HA* lines. Pathogen growth assay 0, 24 and 72 hours after infiltration with *Psm* ES4326 $O.D._{600}$ =0.0002. Local infection or SAR. The virulent pathogen was infiltrated 3 days after induction of systemic acquired resistance with *Psm* ES4326 (*avrB)* $O.D._{600}$ = 0.025. Two leaf discs collected from independent leaves and ground together per sample. Error bars represent the standard error for 6 biological replicates and 6 technical replicates. The statistical difference within groups was analysed with one-way ANOVA followed by Tukey HSD test to identify pairs of treatments that are significantly different with each other, indicated by different letters within groups.

We showed that SARD1 can be S-nitrosylated *in vivo* and from plant extracts preferentially at Cys438. Interestingly, when we promoted S-nitrosylation by infiltration of GSNO according to previous reports (Albertos *et al*, 2015; Feng *et al*, 2013) we could only observe S-nitrosylation of SARD1 for the WT sample without GSNO infiltration and no signal was detected for any SARD1C438S sample. We expected to detect S-nitrosylation in the WT SARD1 after GSNO treatment. A possible explanation relates to the activation of de-nitrosylation mechanisms by GSNO infiltration and endogenous SA application. Quick transcriptional reprogramming occurs in response to NO-donor infiltration (Polverari *et al*, 2003; Begara-Morales *et al*, 2014; Hussain *et al*, 2016; Sharma *et al*, 2016) involving a high number of upregulated genes associated with REDOX counter-responses, including Thioredoxin-h5 (TRXh5), which was increased by over 30-fold shortly after NO-donor infiltration (Hussain *et al*, 2016). TRXh5 mediates selective denitrosylation of S-nitrosylated proteins both in

vitro and in vivo. *Arabidopsis* protoplast treated with CysNO (2mM) exhibited rapid TRXh5 accumulation and significant de-nitrosylation activity within 20 minutes after Cys-NO treatment, resulting in SNO level comparable to the negative control without ascorbate (Kneeshaw et al, 2014). It is possible that GSNO infiltration promoted upregulation of de-nitrosylation mechanisms resulting in the identification of nitrosylated protein only in the SARD1-HA sample without GSNO treatment.

Self-regulation of SARD1

The SARD1-nLUC line allow us to investigate if cysteine 438 mediates changes in the dynamics and timing of *SARD1* expression. The SARD1-nLUC lines does not show constitutive bioluminescence, therefore our approach of supplying the plants with SA and furimazine mix allowed us to observe the de novo synthesis of SARD1 in response to SA. Notably, all the Nano luciferase lines analysed showed induction by SA with a peak in luminescence within 4 to 6 hours after SA, consistent to the SARD1 transcript levels reported by Wang *et al*, (2011) in response to flg22. We also observed that C438S mutants produced a higher luminescence peak compared to that of the SARD1 WT lines in response to SA. Also, we observed higher accumulation of SARD1C438S-HA protein in different lines analysed. S-nitrosylation commonly mediates negative regulation of protein function, including the DNA-binding of the TF DNA-binding of MYB-2, MYB-30 and SRG1 (Serpa *et al*, 2007; Tavares *et al*, 2014; Cui *et al*, 2018).

SARD1 regulates gene expression preferentially through the GAAATTT motif, which is absent in the *SARD1* promoter. However, the related sequence G(A/T)AATT(T/G) was enriched within the promoter of genes identified as SARD1 target in a chromatin immunoprecipitation sequencing (ChIP seq) study (Sun *et al*, 2015). We analysed the *SARD1* promoter using the Plant Promoter Analysis Navigator 2.0 (PlantPAN 2.0, Chow *et al*, 2016) and identified two GAAATTG motifs within 700 to 800 bp from the start site which suggests *SARD1* could be self-regulated. We could not access the reported ChIP-seq data (Sun *et al*, 2015) to confirm if *SARD1* promoter was enriched within the SARD1 sample. However, the higher induction of *SARD1* expression in *SARD1C438S* lines together with the presence of alternative *cis*-elements in *SARD1* promoter suggest the involvement of S-nitrosylation in a negative self-amplification mechanism or promoting protein stability. To evaluate this hypothesis it is possible to perform a *trans*-activation assay in *Arabidopsis* protoplast overexpressing *SARD1* and *SARD1C438S* using a *SARD1::LUC* construction in response to SA and GSNO

treatments. Additionally, it is possible to evaluate the binding of SARD1 to its own promoter using ChIP with the SARD1-HA lines.

Role of Cys438 in SAR

We observed a persistent expression pattern of SARD1-nLUC after consecutive induction with SA, which we speculated could be related to the establishment of SAR. Interestingly, this pattern could not be observed in the SARD1C438S-nLUC line, which could suggest a role for S-nitrosylation mediating this process. However, the SAR assay did not show significant difference in susceptibility to *Psm* infection in the SARD1C438S lines with respect to the WT.

During SAR, plants prime defences in order to respond faster in case of secondary infections. The systemic response encompass the systemic accumulation of SA following the translocation of a chemical signal from the primary infection site towards systemic leaves (Fu & Dong, 2013; Shine *et al*, 2018). It is known that NO plays a central role for proper SAR establishment (Wang *et al*, 2014a). However, the molecular mechanisms behind the role of NO in SAR are not known. It is necessary to re-evaluate if S-nitrosylation of SARD1 has an effect on SAR. It will be interesting to compare gene expression in the SARD1 and SARD1C438S line during SAR and increase the sample size in the SAR assay.

Additionally, it is critical to evaluate if the oscillation observed in the SARD1-nLUC line follows a circadian rhythm during SAR to link S-nitrosylation of SARD1 with this process. Different immune associated genes are known to be under regulation by the circadian clock, which allows plants to synchronise immune responses according to pathogenic signals (Wang *et al*, 2011b; Zheng *et al*, 2015; Karapetyan & Dong, 2018).

The TF Circadian Clock Hiking Expedition (CHE/TCP21) is a known component of the circadian clock (Pruneda-Paz *et al*, 2009) and is known to regulate the circadian expression of *ICS1* and SA accumulation during SAR. *Arabidopsis* plants deficient in *che* display compromised SAR and showed reduced expression of *SARD1* and *CBP60g* (Zheng *et al*, 2015). However, no CHE *cis*-binding elements are located within the *SARD1* and *CBP60g* promoters, suggesting that CHE indirectly regulates *SARD1/CBP60g* during SAR.

Our analysis of the *SARD1* and *CHE* promoter using the PlantPAN 2.0 tool (Chow *et al*, 2016) showed that both promoters contain binding sites for the TF circadian-clock associated 1 (CCA1). Moreover, the *SARD1* and *CHE* promoters were identified as a

potential targets of CCA1 in the data from the ChIP-Seq study by Nagel *et al*, (2015). CCA1 is a central regulator of circadian immunity. Affections on *CCA1* expression result in higher susceptibility to *Pseudomonas* infection (Zhang *et al*, 2013a). TOC1 is known to repress CCA1 expression. However, TOC1 does not contain a DNA-binding domain. Therefore, TOC1 interacts with the N-terminal domain of CHE, which recruits TOC1 to the *CCA1* promoter (Pruneda-Paz *et al*, 2009).

The *CHE* promoter contains two alternative SARD1 *cis*-elements GTAATTT, together with *cis*-elements for CCA1, TGA2/6, WRKY TFs, EIN3/EIL1, ANAC TFs and Myb2, which are also involved in the regulation of *ICS1* expression. Notably, SARD1 has not been associated with the clock and the *SARD1* transcripts could not be detected in the transcriptomic analysis of circadian genes undertaken by Covington *et al*, (2008), probably because *SARD1* is only expressed in response to specific stimuli and not under basal conditions (Zhang *et al*, 2010). However, proteins that do not follow a circadian rhythm can also regulate clock components (Spoel & van Ooijen, 2013).

We observed a potential SARD1 accumulation peak during the day, consistent with the timing of CHE accumulation. Also, both proteins display nuclear localization (Pruneda-Paz *et al*, 2009, Zhang *et al*, 2010), indicating spatiotemporal coincidence. SARD1 contains a SAM-like domain in its sequence, which is usually involved in protein-protein interactions (Denay *et al*, 2017). It will be interesting to investigate if SARD1 and CHE can physically interact with each other and if this interaction affects TOC1-CHE mediated regulation of CCA1 during SAR and if this interplay could be mediated by S-nitrosylation of SARD1.

Similarly, it will be relevant to explore if S-nitrosylation of SARD1 can regulate the expression of other SAR regulators. For instance, the pathogen-induced expression of *Agd2-like Defense Response Protein 1 (ALD1)* and *SARD4,* involved in the biosynthesis of pipecolic acid (Pip) is suppressed in *sard1* plants. Pip is proposed to be a central intermediary and movable signal for SAR establishment (Navarova *et al*, 2012; Bernsdorff *et al*, 2016) and the *ALD1* and *SARD4* promoters have been identified as SARD1 targets (Sun *et al*, 2015).

The fact that specific NO concentrations are necessary for optimal SAR establishment could suggest a role for S-nitrosylation in this process. However further research is needed to determine if S-nitrosylation of Cys-438 of SARD1 is relevant in this process. If this is confirmed, it could contribute to integrate S-nitrosylation SAR establishment.

Chapter 6 Purification of recombinant SARD1

Introduction

DNA binding domain of SARD1

SARD1 and CBP60g are plant-specific transcription factors containing a novel DNA-binding domain (DBD) and play a vital role in modulating plant immunity. Since their first report nearly 10 years ago (Wang *et al.*, 2009; Zhang *et al.*, 2010) significant research has demonstrated their importance in salicylic acid biosynthesis and immunity (Kong *et al*, 2016; Truman *et al*, 2013; Truman & Glazebrook, 2012; Sun *et al*, 2015; Qin *et al*, 2018; Wang *et al*, 2009a; Zhang *et al*, 2010). However, the crystal structure of this novel family of transcription factors and this DBD remains elusive.

Protein crystallography

Obtaining protein crystals allow the identification of the three-dimensional conformation of the protein and provide significant information about the physiological processes these proteins are involved. Protein function is fundamentally tied to their three-dimensional conformation and understanding the interactions taking place at the molecular level can help to elucidate enzymatic reactions, recognition of substrates and interactions with other proteins and macromolecules (Zhang *et al*, 2007).

For instance, the obtention of the crystal structure of the MYC transcription factor and JAZ proteins allowed us to understand the molecular dynamics involved in the repression of the transcription factor MYC3 by JAZ proteins in the absence of jasmonate. In the presence of jasmonate, JAZ proteins function as a co-receptor for jasmonate and forms a complex with COI1, this interaction promotes a significant conformation change of MYC3 which mediate ubiquitination and subsequent JAZ proteins' proteasome-mediated degradation, resulting in the release of MYC3 to activate defence genes against herbivorous and microbial pathogens (Zhang *et al*, 2015).

An essential requirement for crystallography studies of a protein involves the production of high-purity and high concentrations of the target protein samples in conditions that do not perturb its natural state and allow the formation of supersaturated solutions (McPherson & Gavira, 2014).

The expression of recombinant protein in *E. coli* is a well-established platform for *in vitro* biochemical assays and structural biology studies. In general terms, the process is straightforward, involving cloning of the gene of interest in an expression plasmid and the subsequent transformation of an *E. coli* expression strain (Rosano & Ceccarelli, 2014). However, the expression of the protein can be affected by toxicity to the host, formation of inclusion bodies or misfolding affecting solubility and function. Different strategies to optimise protein production are available (Chen, 2012; Rosano & Ceccarelli, 2014). However, the success of the recombinant protein expression depends on the intrinsic properties of each protein and require a systematic optimisation process.

Recombinant full-length SARD1 and truncated versions of SARD1 have been successfully expressed before. However, they have been expressed as fusion proteins using GST or MBP tags, which are a known strategy to increase protein solubility and are efficient for in vitro biochemical and DNA-binding studies (Zhang *et al*, 2010; Wang *et al*, 2011a; Li, 2015). Nevertheless, crystallography studies require removal of the solubility tag to obtain the desired resolution.

Here we report the systematic optimisation process for recombinant expression of untagged SARD1 and a purification strategy with the aim to solve the three-dimensional structure of SARD1.

Results

Expression of MBP-FXA-SARD1 for tag removal

The crystallisation of proteins relies on the obtaining a highly-pure supersaturated solution of the protein of interest in conditions that do not alter its native conformation and functionality (McPherson & Gavira, 2014).

To obtain SARD1 in the required concentration and purity for crystallography studies we first expressed recombinant SARD1 with an N-terminal MBP-tag flanked by the recognition site of the Factor XA protease for tag cleavage. Previous experiments in the lab have shown that the N-terminal MBP tag provides good solubility to the fusion protein and it does not affect its DNA-binding ability. We first amplified *SARD1* sequence from Col 0 cDNA adding restriction sites for cloning into the pMAL C5X vector. The pMAL C5X SARD1 vector was introduced into the expression *E. coli* strain BL21(DE3) (NEB 2527). The fusion protein was expressed overnight at room temperature after induction with IPTG 0.5 mM. The cells were harvested and lysed by sonication, and the MBP-FXA-SARD1 fusion protein was purified by affinity chromatography. We subsequently incubate the protein with the Factor XA protease to remove the solubility tag. However, our attempts to remove the MBP-tag by protease cleavage were unsuccessful due to unspecific cleavage within the SARD1 protein. The efficiency and cleavage of Factor XA can be affected by the accessibility of the cleavage site, the degree of protein aggregation and the digestion conditions including protease concentrations, temperature and buffer composition. We followed an optimisation protocol for tag-cleavage but observed consistent unspecific cleavage on SARD1.

Expression of untagged SARD1 and SARD1-His

Previously, full-length and truncated SARD1 has been successfully expressed as an N-terminal GST-fusion protein. Also, fragments of SARD1 (aa 1-214, aa149-270 and aa 215-451) were expressed as His-tag protein and used in EMSA (Zhang *et al*, 2010) but no full-length SARD1 had been expressed with a histidine tag. To circumvent the unspecific cleavage of SARD1, we decided to express SARD1 without a tag and designed a strategy to purify the protein by ion-exchange chromatography and screen its DNA-binding activity to the *ICS1* promoter.

We first cloned the full-sequence of SARD1 with or without the stop codon into a modified pET28 vector compatible with Goldendale assembly to generate the

expression plasmids pET28$_{CD}$-SARD1-NT (NT, untagged) and pET28$_{CD}$-SARD1-His. The plasmids were introduced into *E. coli* BL21(DE3) (NEB 2527).

We then performed a small-scale expression assay to test expression conditions varying expression temperature, time and IPTG concentrations. To do this, we grew an overnight culture and used it to inoculate 50 ml of LB media. The culture was grown at 37ºC until it reached an optical density at 600 nm of 0.7. The culture was induced with 0.5 mM IPTG and separated into 5 ml fractions in 50 ml falcon tubes. The tubes were incubated at different temperatures and for different times. The cells were collected by centrifugation and resuspended in lysis buffer based on 20mM Tris pH 7.5. The cell suspension was sonicated and centrifuged at 20,000 G for 15 min to separate the soluble and insoluble fractions. The insoluble protein pellet was dissolved in 8M urea, and the protein fractions were loaded in SDS-PAGE and visualised by Coomassie staining.

Notably, a band corresponding to the expected recombinant protein size could be found only in the insoluble fraction despite the optimisation of the expression conditions (Fig 6.1A). The abundance of insoluble SARD1 could be related to partially folded protein and the formation of inclusion bodies. We hypothesised that SARD1, as a REDOX sensitive protein, could require oxidising expression conditions for proper protein folding or the formation of disulphide bonds to stabilise the protein structure.

The expression strain BL21(DE3) is not suitable for the formation of disulphide bonds in the cytoplasmic region, so we switched to the *E. coli* BL21 Shuffle T7 express strain (NEB C3029J) which has been engineered to promote disulphide bonds formation in the cytoplasm. This strain carries deletions on the *glutaredoxin reductase* and *thioredoxin reductase (Δgor ΔtrxB)* genes in addition to the constitutive cytoplasmic expression of the periplasmic disulphide bond isomerase DsbC to aid protein folding (Lobstein *et al*, 2012).

After introducing the SARD1 plasmids into the Shuffle strain, we tested expression conditions as previously described. We could observe a stronger band in the soluble fraction for SARD1 (NT) concerning the empty vector, although a significant proportion of the protein was still visible in the insoluble fraction (Fig 6.1B).

Solubility optimisation

Different strategies to increase protein solubility have been reported (Wang *et al*, 2014b; Santos *et al*, 2012; Rosano & Ceccarelli, 2014; Chen, 2012) including switching expression strains, co-expression of chaperones and foldases, reducing protein expression rate, modification to culture conditions, protein refolding/solubilisation of inclusion bodies, and the use of additives in lysis buffer (Leibly *et al*, 2012). We took a systematic approach combining these strategies to increase the solubility of SARD1.

SARD1 has an estimated isoelectric point (IP) of 7.161 which is very close to neutral. Therefore we increased the pH in the lysis buffer to 1.5 points above the IP to guarantee the protein will show a net negative charge.

To further increase the solubility of SARD1 we tested independent modifications to the expression media, as shown in table 6.1. We grew the culture until it reached an OD_{600} of 0.75 and induced the culture with 0.5 mM IPTG and simultaneously supplement independent cultures with glucose (1%), sucrose (1%), glycerol (1%) and EtOH (3%). We could observe an increase in the intensity of the SARD1 band after expressing the protein in the presence of glucose, sucrose and glycerol in the Shuffle (Fig 1D) but not in the BL21(DE3) strain (Fig 1C). Conversely, a considerable fraction of insoluble protein was also present under these treatments.

Subsequently, we tried two different approaches to increase SARD1 solubility. The first approach consisted in modifying the lysis buffer including components to stabilise protein structure as described by Leibly *et al*, (2012) in which they screened the effect of 144 additives to solubilise 44 insoluble proteins. They found that the addition of 750 mM trehalose in the lysis buffer had a positive effect on the solubilization of 21 out of 44 insoluble proteins and was suitable for large-scale purification. We tested the trehalose enriched lysis buffer and observed an increase in the solubility of SARD1 in both SARD1(NT) and SARD1-His (Fig 6.2A). To guarantee that the solubilised protein was functional, we used the trehalose soluble fraction in EMSA to evaluate the ability of the protein to bind to the *ICS1* promoter. However, these fractions did not produce any visible shift, indicating the protein was not able to bind to the *ICS1* promoter, possibly due to the interference of the buffer components with the binding buffer (Fig 6.2C).

The second approach we followed consisted in promoting the formation of non-classical inclusion bodies and subsequently solubilising the protein under mild-solubilising conditions described by Jevševar (2005). Non-classical inclusion bodies refer to the aggregation of properly-folded and functional protein (Jevševar *et al*, 2005). We induced the formation of non-classical inclusion bodies by expressing the protein in LB media + 1% sucrose and 0.5 mM IPTG at 16 ºC for 16 hours.

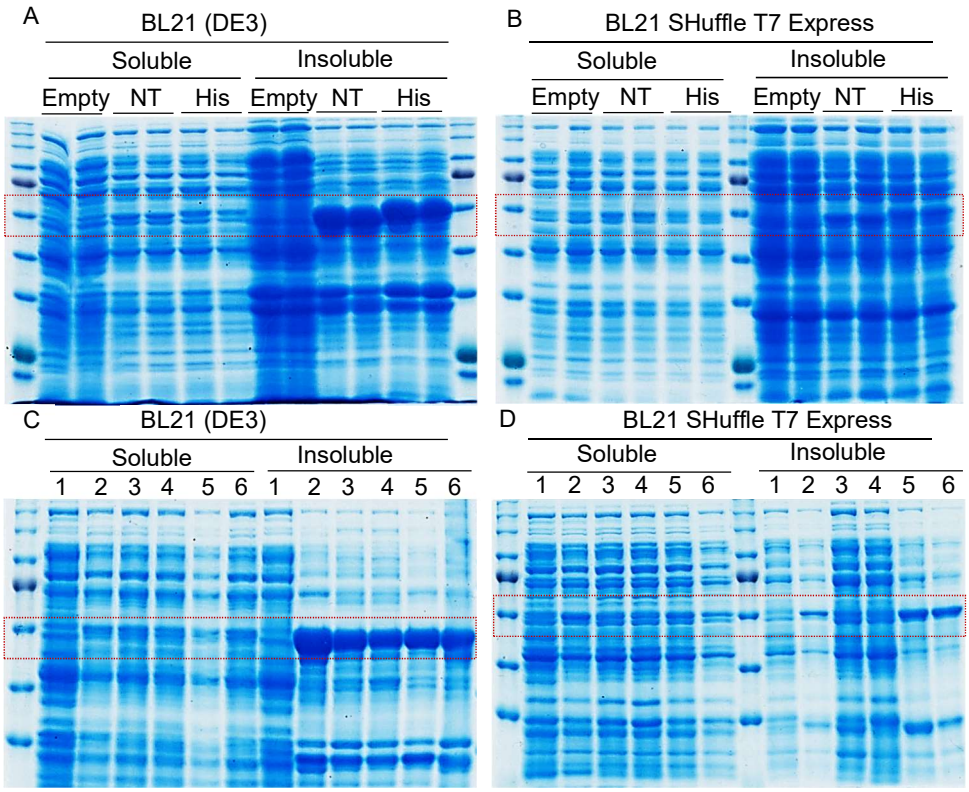

Figure 6.1. Optimisation of recombinant SARD1 expression. SDS-PAGE gels after Coomassie staining. 12% acrylamide gel. The recombinant protein was expressed in 5 ml cultures in 50ml Falcon tubes. The E. coli expressions strain were grown at 28°*C* until reaching $O.D._{600}$ = 0.7. The protein expression was induced with 0.5 mM IPTG for 16 hours at 16°C. The cells were collected by centrifugation at 4,000 RPM for 15 min. The pellet was lysed by sonication and the soluble fraction recovered after centrifugation at 20,000 G for 15 min. The insoluble pellet was resuspended in 8M Urea. A and B) Expression test of untagged SARD1 and SARD1His tag. Empty = pET28CD, NT = SARD1 no Tag, His = SARD1His. A) BL21 T7 express, B) BL21 Shuffle t7 express. C and D) Modifications to culture media. 1) Control empty $pET28_{CD}$, 2) Control SARD1 (NT), 3)1% Glucose, 4)1% sucrose, 5)1% glycerol and 6) 3% ethanol. C) BL21 (DE3), D) BL21 Shuffle t7 express.

Table 1. Modification to culture media

Additive	Mechanism	Reference
1% Glucose	Repress lac promoter to avoid unspecific expression without induction by IPTG	(Rosano & Ceccarelli, 2014)
1% Sucrose	Increase osmotic pressure to promote the formation of osmoprotectant inside the cell and increase protein stability and native conformation	(Reyes *et al*, 2017)
1% Glycerol	Alternative carbon source. Induce alkalisation by acetate production	(Wang *et al*, 2014b)
3% Ethanol	Modification to membrane fluidity and increase DNA-synthesis rate	(Chhetri *et al*, 2015)

After harvesting the cells, the pellet was resuspended in lysis buffer with pH 8.5. After centrifugation, the soluble fraction was recovered, and the non-classical inclusion bodies pellet washed twice with sterile water.

We subsequently tested five mild-solubilising agents, including 5% N-propanol, 2M urea, 0.5% Triton X-100 and 5% DMSO. The washed insoluble protein pellet was resuspended in 20 mM Tris buffer pH 8.5 supplemented with the mild-solubilising agent. We noticed a significant recovery of SARD1 using this approach (Fig 2B). Following, we evaluated the ability of the solubilised SARD1 protein fractions to bind to the *ICS1* promoter in EMSA. Notably, the addition of Triton X-100 had the most significant effect on DNA-binding for both SARD1(NT) and SARD1-His, producing a shift only in the SARD1 fractions and not in the empty $pET28_{CD}$ control, suggesting the recovery of soluble and functional SARD1 (Fig 6.2C). Interestingly, when we test the previously recovered soluble fractions we found a considerable proportion of SARD1, indicating that expressing the protein at low rate (low IPTG and 16 ºC) in LB media supplemented with 2% sucrose using the BL21 Shuffle strain and using a lysis buffer with a pH 1.5 points above the IP can increase the solubility of the protein.

Ion exchange chromatography

Next, we proceed to purify the SARD1 protein by ion exchange chromatography (IEX). SARD1 has a calculated isoelectric point of 7.161; we previously adapted the lysis buffer to a pH of 1.5 units above the isoelectric point. Therefore the protein would be expected to have a net negative charge. A requirement for ion exchange chromatography and crystallography is to obtain the protein in a buffer with a minimal composition to avoid interference of the buffer components with the ion exchange

resin. We removed the salt from the lysis buffer and confirmed the solubility of the protein in the minimal lysis buffer consisting of only 20mM Tris pH 8.5 compatible with IEX. We express one litre of culture using the conditions defined before. The cells were harvested by centrifugation, and the pellet was lysed in 10 ml of lysis buffer, followed by centrifugation at 30,000 G for 20 min, and the lysate was filtered using a 0.22 µm syringe filter.

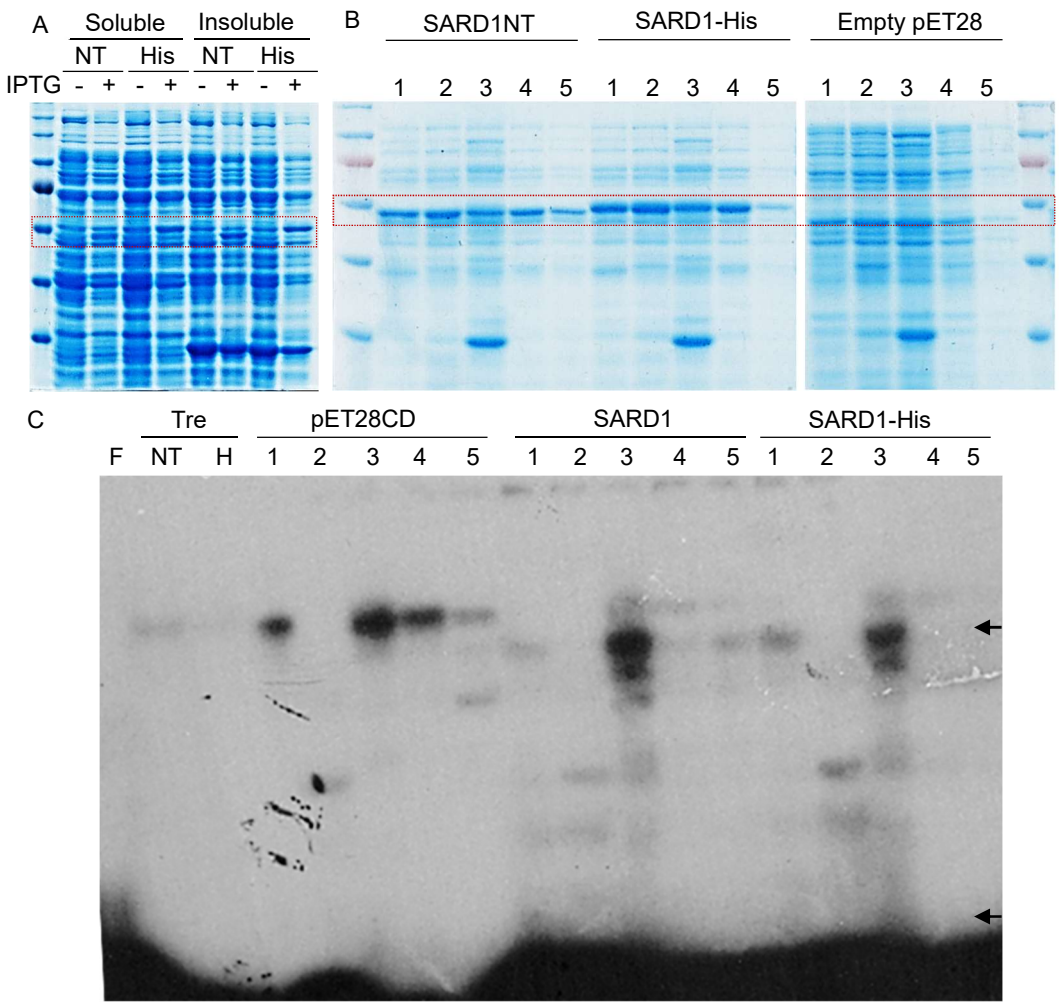

Figure 6.2. Solubilisation of SARD1. SDS-PAGE gels after Coomassie staining. A) Lysis buffer adapted according to the solubilisation protocol by Leibly *et al,* (2012) Standard buffer (25mM HEPES pH 7.4, 500mM NaCl, 10% glycerol, 0.025% Na Azide, 0.5% CHAPS, 10 mM $MgCl_2$, 0.1% lysozyme, 750mM trehalose, 1mM PMSF). NT= SARD1NT, His=SARD1-His, + and – indicate induction with IPTG. The red dotted box indicates the region of interest. B) Mild solubilisation of non-classical inclusion bodies. After removal of soluble protein, the insoluble pellet was washed with sterile water and resuspended overnight in 20mM Tris pH 8.5 + 1) 5% N-propanol, 2) 2M Urea, 3) 0.5% Triton X-100, 4) 5% DMSO and 5) Control 20mM Tris pH 8.5. C) Electro mobility Shift Assay to test DNA-binding of the solubilised SARD to a fragment of the *ICS1* promoter. F) free probe, Tre indicates trehalose solubilisation. 1 to 5) Solubilised reactions according to B. Upper arrow indicated SARD1 binding, differential shift concerning the empty vector control. Bottom arrow indicates free probe.

We used a 5ml HiTrap Q HP column (GE Healthcare) for anion exchange chromatography. The column was equilibrated with degassed lysis buffer. After binding the protein to the column, we performed the elution using a stepwise ionic strength gradient, covering an initial 20% salt gradient step followed by 5% increasing steps. We recovered 5ml fractions from the protein peaks in the chromatogram (Fig 6.3A). The fractions containing protein were loaded on SDS-PAGE followed by Coomassie staining. We identified bands corresponding to the expected size of SARD1 eluting before reaching the 20% salt gradient and within the 25 to 45% interval (Fig 6.3B). We had noticed before the existence of a native *E. coli* protein with a very similar size to that of the SARD1 size. Therefore we proceed to screen the fractions in EMSA.

To confirm the identity of the protein. We used the fractions showing a band within the SARD1 size range in non-radioactive EMSA to test for specific binding to the *ICS1* promoter. We could observe a shift indicating binding to the *ICS1* probe in the samples that eluted before the 20% salt gradient (Fig 6.3C), indicating a weak interaction of SARD1 to the resin. We have observed before a high molecular weight unspecific binding of the native *E. coli* proteins to the *ICS1* probe in previous EMSA. Therefore we included an empty $pET28_{CD}$ BL21 T7 express SHuffle lysate as a negative control. Notably, the shift related to SARD1 was visible only in the positive crude extract control ($pET28_{CD}$ SARD1NT BL21 T7 express Shuffle) and in the purified fractions that eluted within 20% of the salt gradient but not in the negative control or other protein fractions, confirming the identity of SARD1.

On a subsequent IEX purification, we further characterised the optimal ionic gradient for the release of SARD1 from the column by repeating the analysis with stepwise ionic strength gradient in 5% intervals covering the range from 0 to 20% salt concentration, followed by analysis of the fractions by SDS PAGE and EMSA. We found a band corresponding to the expected size eluting from the column within the 5 to 10% salt interval, which can bind to the *ICS1* promoter in EMSA (Fig 6.4). The fraction obtained from IEX showed a well-defined band of the expected size, consistent with the empty and SARD1 crude extract controls. The samples also contained additional unspecific bands, so we proceed to polish the purification by gel filtration.

Size exclusion chromatography

To fine-tune the purification and remove the rest of the unspecific bands from the SARD1 sample, we combined the fractions containing the band of interest and that showed positive binding in EMSA and concentrated them using a Vivaspin column with a molecular cut-off of 30 kDa to a final volume of 2.2 ml. We proceed to load the sample into a Sephacryl S400 column (GE Healthcare) for gel filtration. We equilibrated the column with lysis buffer and loaded 2ml of the concentrated protein fraction. We recovered 4 ml fractions from the protein peaks in the chromatogram (Fig 6.5A). The fractions were analysed on SDS-PAGE. We could observe a protein band of the size we expected, together with additional unspecific bands on the SDS-Page gel (Fig 6.5B). Notably, the chromatogram showed three protein peaks, but the proteins were only detected in the first fractions collected. The S400 column has a resolution between 20 to 8000 kDa which should allow the separation of SARD1 from the other proteins.

To increase the resolution of the gel filtration, we expressed more protein and repeated the purification strategy using a Sephacryl S200 column, which has a resolution between 5 to 250 KDa. Similarly, we noticed a single protein peak in the chromatogram, and we observed unspecific bands in the purified samples (Fig 6.5C) after the SDS-PAGE analysis, suggesting possible protein aggregation during the purification steps resulting in a high-weight protein complex eluting faster from the column. To evaluate this, we loaded the concentrated protein fractions on a native PAGE. After Coomassie staining, we could observe a well-defined band above the 100 KDa protein marker, which indicates the formation of a protein complex. Here we showed that untagged SARD1 could be expressed *in vitro* after optimisation of the expression conditions and designed a strategy to purify the protein purified by ion exchange and size exclusion chromatography while preserving its biological activity. However, further fine-tuning using reducing conditions to eliminate unspecific protein interactions is needed before scaling-up the production for protein crystallography assays.

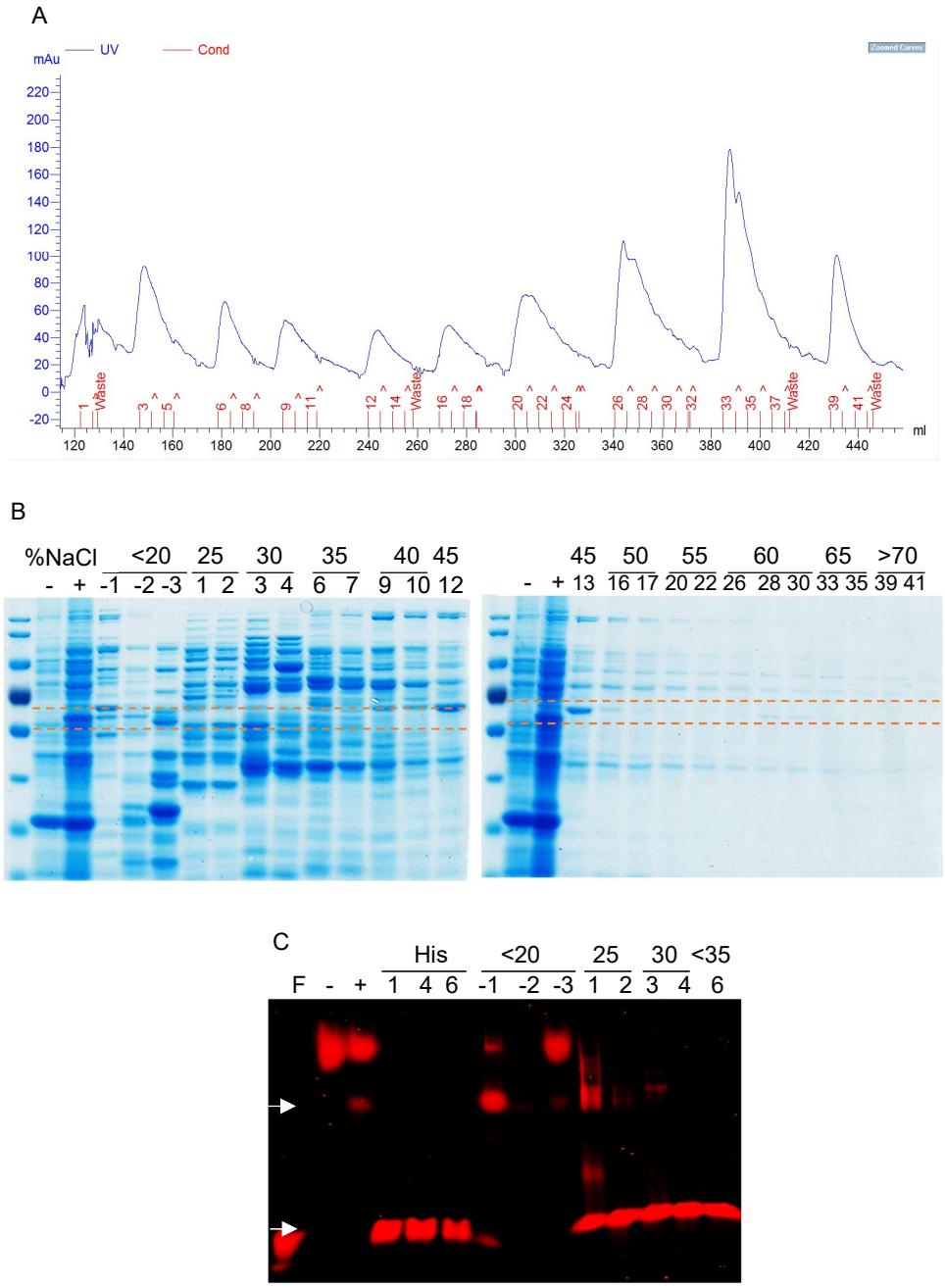

Figure 6.3. Ion exchange chromatography (IEX). Ion exchange chromatography to purify un tagged SARD1. The recombinant protein was expressed in a 250 ml culture. After harvesting the cells, the pellet was lysed in 20mM Tris pH 8.7 containing 1mg/ml lysozyme, 1mM PMSF. After clarification at 30,000G, the soluble fraction was filtered through a 0.22 µm syringe filter. The protein of interest was separated using a 5 ml Hi-Trap Q HP column in an Äkta Prime following an elution with stepwise ionic strength gradients method. A) Chromatogram of ion exchange. 5 ml fractions were collected for each protein peak corresponding to a 5% increase in the ionic strength gradient. B) SDS-PAGE after Coomassie staining of the iEX fractions. The dotted line indicates the region of interest for the expected SARD1 size. C) DNA-binding to a fragment of the *ICS1* promoter in Non-radioactive EMSA. The upper arrow indicates the expected binding for SARD1. The bottom arrow shows the free *ICS1* probe.

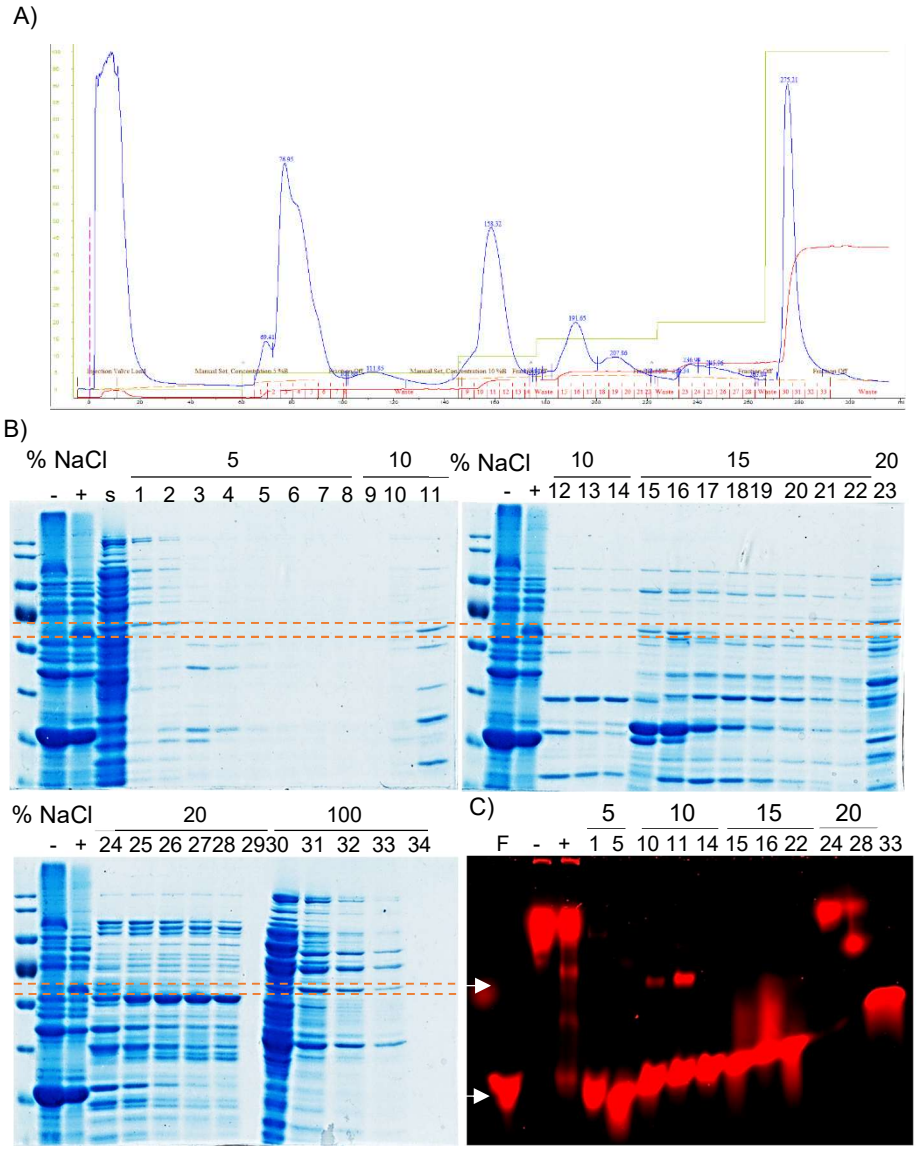

Figure 6.4. Fine-tuning Ion exchange chromatography. IEX chromatography to analyse elution of proteins within the 0 to 20% NaCl concentration. Chromatogram of ion exchange. 5 ml fractions were collected for each protein peak corresponding to a 5% increase in the ionic strength gradient. B) SDS-PAGE after Coomassie staining of the iEX fractions. The dotted line indicates the region of interest for the expected SARD1 size. C) DNA-binding to a fragment of the *ICS1* promoter in Non-radioactive EMSA. The upper arrow indicates the expected binding for SARD1. The bottom arrow shows the free *ICS1* probe.

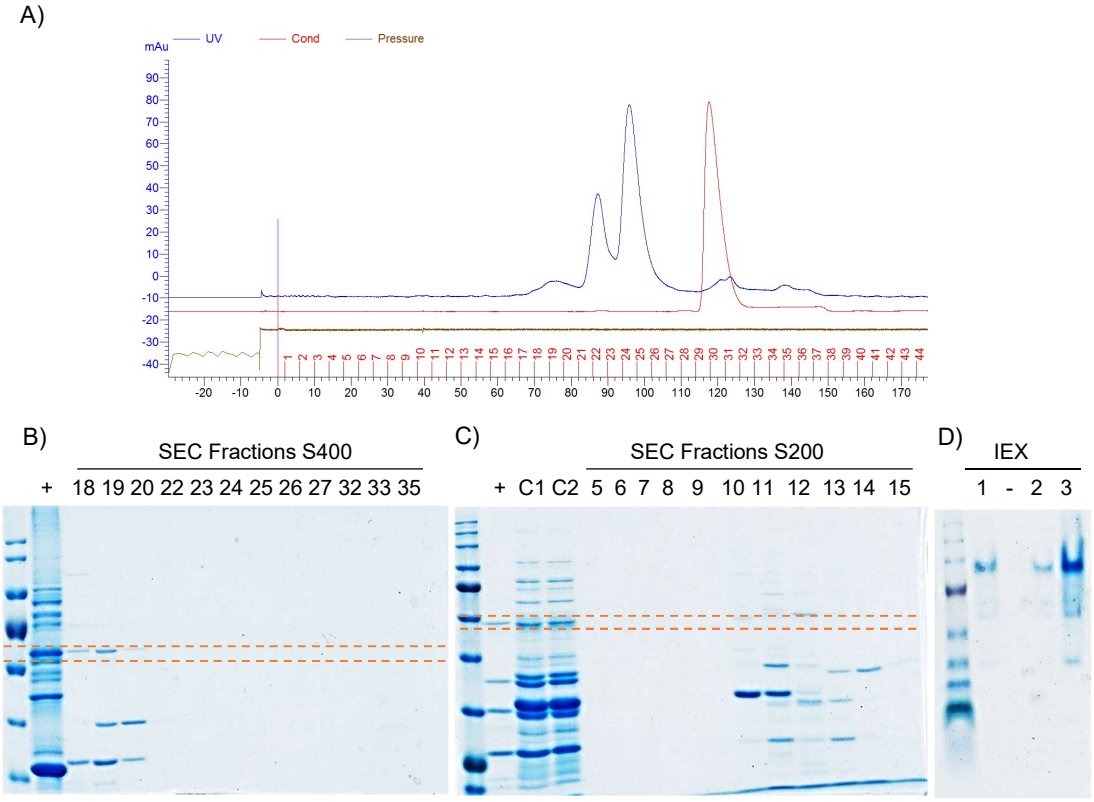

Figure 5. Size Exclusion Chromatography. The fractions obtained from IEX showing a band of the expected size and positive DNA-binding to the *ICS1* promoter were pooled and concentrated in a Vivaspin column (molecular cut-off of 30 KDa) to a final volume of 2.2ml. After column equilibration, 2 ml of concentrated protein sample were loaded for SEC at a flow rate of 0.5ml*min^{-1}. A) Chromatogram of SEC with Sephacryl S-400 column. B and C) SDS-PAGE gel after Coomassie staining of SEC using a Sephacryl column B)S-400 and C)S-200. D) Native gel after Coomassie staining of IEX fractions before SEC.

Predicted model of SARD1

To further understand the structure of SARD1, we used the Protein Homology/analogY Recognition Engine V 2.0 (Phyre2, Kelly et al, (2015), www.sbg.bio.ic.ac.uk and www.predictprotein.org) to build a predictive model of SARD1. The predicted model only showed a partial structure for 51 amino acids (aa 259 to 310) with high similarity to a SAM-like domain. Additionally, the software predicted a highly disordered region towards the C-terminal end of SARD1, which suggests considerable flexibility in this region of the protein (Fig 6.6A). We subsequently used the Swiss Model homology-modelling server to build a three-

dimensional model of SARD1. Interestingly, the result only showed a small fragment of the protein, covering from amino acids 250 to 310, composed of a five alpha-helix conformation (Fig 6.6B), consistent with the classical SAM domain structure (Camille Sayou *et al*, 2016; Denay *et al*, 2017).

Interestingly, the proteins used as templates to build the model are involved in DNA-repair, transcription elongation and the alpha subunit of RNA polymerase. The characteristics inferred from the partial model suggest SARD1 is a highly dynamic protein with a relevant biological function. Solving the crystal structure will allow us to understand the biological role of SARD1.

Discussion

Solubility of SARD1

SARD1 and CBP60g are members of a plant-specific family of transcription factors containing a novel structure of a DNA-binding domain. They play a pivotal role in plant immunity. However, nearly one decade after their discovery the three-dimensional structure of this family of TF remains elusive. Although full-length SARD1 has been successfully expressed as a fusion protein with GST and MBP tags, only truncated versions have been reported with a histidine tag (Wang *et al*, 2009a; Zhang *et al*, 2010; Wang *et al*, 2011a; Li, 2015). One possibility for this is the low solubility exhibited by SARD1 when expressed *in vitro*, requiring the fusion with bigger tags to increase solubility. Here we report the expression of full-length SARD1 and a purification strategy by anion exchange chromatography and gel filtration suitable to scale-up and subsequent fine-tuning to express functional SARD1 for crystallography studies.

We hypothesised that the formation of inclusion bodies when expressing SARD1 without a tag or with a histidine tag could be due to protein misfolding, potentially related to the requirement of oxidising conditions to preserve the tridimensional protein structure. Therefore, the rationale in the strategy to express SARD1 focused on generating specific expression condition to promote proper protein folding in an oxidising cytoplasmic environment to allow the formation of possible disulphide bonds.

A)

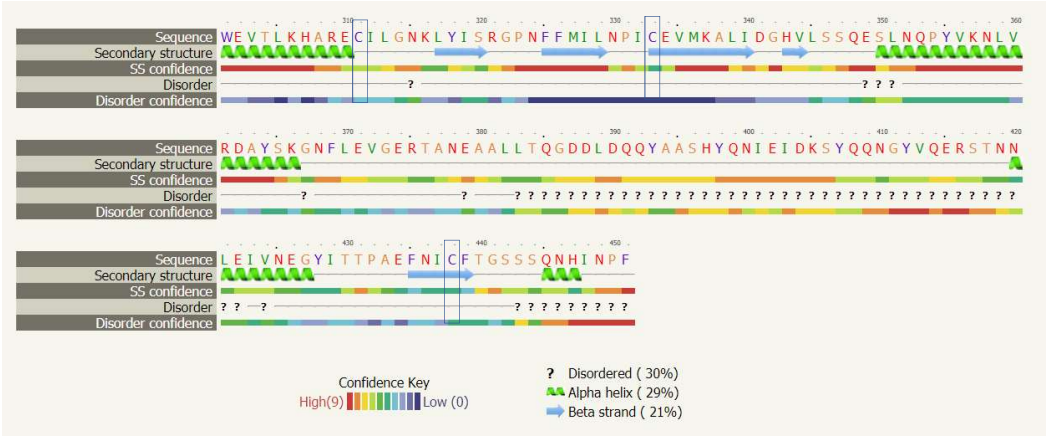

B)

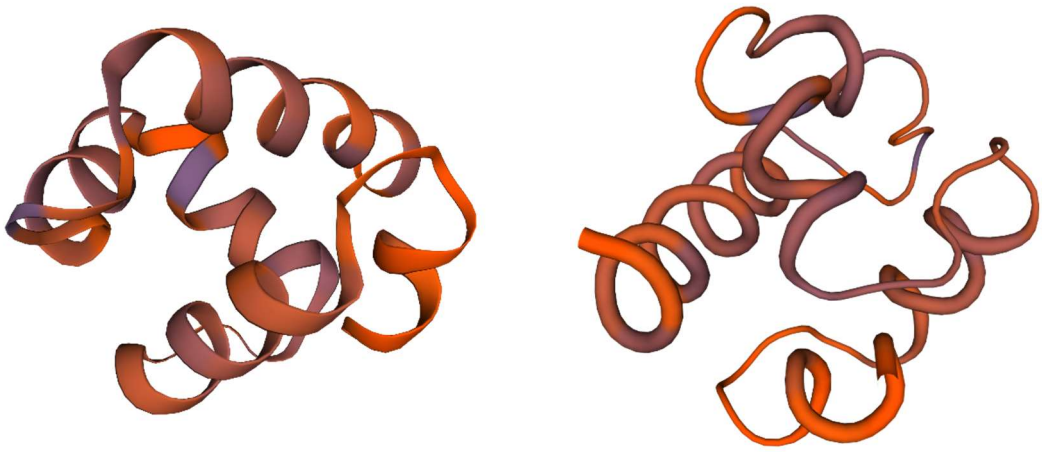

Figure 6.6. Predicted model of SARD1. A) Result of disorder prediction using the software Phyre[2] (Protein Homology/analogy Recognition Engine 2.0) http://www.sbg.bio.ic.ac.uk/~phyre2 from the Structural Bioinformatics Group in Imperial College London. B) Cartoon from the partial model obtained from the SWISS-MODEL Homology Modelling server, showing the five alpha-helix structure comprising amino acids 250 to 310.

Recombinant SARD1 expression

The SARD1 expression strategy combines well-documented strategies for protein expression (Chen, 2012; Rosano & Ceccarelli, 2014). It comprises the use of an engineered *E. coli* expression strain with oxidising cytoplasmic conditions and the cytoplasmic coexpression of a periplasmic disulphide bond isomerase DsbC (Lobstein et al, 2012). Also, the addition of sucrose to induce the formation of intracellular osmoprotectants to aid in proper protein folding (Reyes et al, 2017). Finally, the use of low IPTG concentration and low expression temperature to reduce

the protein expression rate (Rosano & Ceccarelli, 2014), high pH in the lysis buffer and the use of additives to solubilise proteins (Leibly et al, 2012). The fact that SARD1 formed a protein complex under native PAGE conditions, similar with previous observations in the lab and in previous reports (Zhang *et al*, 2010), together with the elution of a high molecular weight protein complex from the size exclusion column could indicate oligomerisation of SARD1 or protein aggregation.

SAM-like domain of SARD1

Furthermore, a predicted model using SARD1 amino acid sequence and analysis of order and flexibility within the sequence supports the hypothesis of a dynamic C-terminal region on SARD1 and potential homodimerisation. The predicted model of SARD1 showed a domain with 93% similarity to a SAM-like domain. The sterile α-motif (SAM) represents a protein module, around 70 to 80 amino acids in length, generally composed of a five α-helix array, associated with protein-protein interactions and the formation of dimers, oligomers and polymers. Structural studies suggest the SAM domain is involved in the regulation of a diverse array of functional protein including transcription factors, enzymes and receptors (Denay *et al*, 2017)

In *Saccharomyces cerevisiae*, the SAM-domain of the Serine/Threonine-protein kinases (STE) 11 and STE 50 mediates a reversible homo/heterodimerization which modulates efficient signal transduction in MAPK cascades (Bhattacharjya *et al*, 2005).

Additionally, functional characterisation of the SAM-like domain of the *Arabidopsis* transcription factor TFCP2L1, which participates in the establishment and maintenance of pluripotency in embryonic stem cells, showed that TFCP2L1 undergoes hexamerization through the C-terminal SAM-like domain and that this conformation promotes DNA-binding through the CP2-like domain at the N-terminal of TFCP2L1 (Kim *et al*, 2016). Similarly, the Tankyrase 1 (TNKS1) and TNKS2 proteins, members of the poly(ADP-ribose) polymerase enzymes participate in the regulation of a plethora of cellular processes, including signalling. These TNKS proteins were found to oligomerise via SAM-like domain interactions, which could represent an inhibitory mechanism for substrate binding (DaRosa *et al*, 2016).

In *Arabidopsis*, the structural analysis of the transcription factor LEAFY, a master regulator of flower development, showed the presence of a 50 residues SAM domain located at the N-terminal end of the TF. The SAM domain mediates LEAFY oligomerisation which allows the TF to bind to low-affinity DNA regions, including

closed chromatin regions (Camille Sayou *et al*, 2016). An additional eleven SAM-containing *Arabidopsis* proteins have been annotated, involved in diverse processes (Denay *et al*, 2017). The SAM-like domain is present in essential biologically active proteins, suggesting a regulatory role for oligomerisation in the bioactivity of these proteins conserved in different organisms. The SAM-like domain in SARD1 could indicate a similar mechanism regulating its bioactivity. However, the role of the SAM-like domain of SARD1 and its biological implications potentially promoting SARD1 oligomerisation remains to be investigated.

C-terminal of SARD1

Interestingly, the predicted model of SARD1 also showed disordered regions along the C-terminal domain of the protein and specifically flanking cysteine 438. The disordered regions refer to fragments of proteins that do not have a stable, permanent secondary structure in solution but assume a specific structure in a precise functional state (Zhang *et al*, 2007). Additionally, proteins containing intrinsically disorder regions and hybrid ordered/disordered regions are recognised as dynamic functional proteins or protein domains that fulfil essential biological functions (Lieutaud *et al*, 2016). The disordered regions are likely to be located in loops and turns rather than in stable α-helix and β-sheets conformations (Zhang *et al*, 2007), suggesting flexibility in the C-terminal of SARD1, potentially allowing the formation of disulphide bonds with other cysteines. However, our observation that SARD1C438S from the in vitro DNA-binding assay that SARD1 and SARD1C438S show similar K_D suggests Cys 438 is not directly involved in the formation of a disulphide bond, or that this bond is not a requirement for DNA-binding.

Moreover, protein regions with a predicted ~50% disorder probability can exist as semi-disorder regions (interplay order/disorder) and have been shown to participate in protein aggregation, protein-protein interactions and folding (Lieutaud *et al*, 2016). Notably, around 70% of semi-disorder sequences are predicted to be involved in post-translational modifications, and specifically, amino acids located within five residues away from semi-disorder regions are 20% more likely to be modified by post-translational modification (Zhang *et al*, 2007).

According to the predicted model and estimation of disorder of SARD1, Cys 438 which was identified by Li (2015) as the target for S-nitrosylation is located five amino acids away from a disordered region, supporting the hypothesis of an essential regulatory mechanism at the C-terminal of SARD1, potentially mediated by S-nitrosylation.

The fact that SARD1 showed to be insoluble in *E. coli* BL21 (DE3) indicates the requirement of an oxidant cellular environment for proper folding, possibly aided by the formation of disulphide bonds or different interaction to promote protein stability and supported by the predicted disorder and flexibility at the C-terminal domain of SARD1, containing cysteines 311, 333 and 438. The prediction of a SAM-like domain opens the possibility of SARD1 oligomerisation, potentially contributing to regulate SARD1 bioactivity. However, to confirm this possibility, it is necessary to solve the SARD1 crystal structure. The next steps in the purification process include IEX and SEC in a reducing buffer to eliminate unspecific protein interaction and monomerisation of SARD1 to increase the resolution of gel filtration, followed by scaling-up and structural analysis. Alternatively, the gel filtration could be optimised to promote SARD1 oligomerisation and reduce the resolution of the resin to promote the elution of the SARD1 oligomer faster that other smaller proteins. Understanding the structure of SARD1 alone, as a DNA-protein complex and after S-nitrosylation will shed some light on the molecular regulatory interactions coordinating the activation of plant immunity.

Chapter 7 Forward genetic screening of mutagenized *PR1::LUC par2-1* lines

Introduction

Arabidopsis thaliana genome annotation

Arabidopsis thaliana is the most studied model organism in plant science due to its fast generation time and relatively small diploid genome. Besides, the whole genome has been fully sequenced, and significant progress has been made in gene annotation (Arabidopsis Initiative, 2000). The availability of transcriptomic sequencing techniques and databases set the ground for understanding the function of all types of transcripts, expanding over mRNA, non-coding RNA and small RNA, allowing a comprehensive annotation of the *Arabidopsis* genome. A recent effort to update and maintain the accuracy of the annotation used 113 datasets from RNA-seq libraries and constructed 48,359 transcripts models of protein-coding genes. The analysis resulted in the Araport11 annotation update, consisting in 37,686 genes, out of which 27,655 are protein-coding, 5,178 non-coding, 956 pseudogenes, and 3,901 transposable element-related loci (Cheng *et al*, 2017). Although many genes have been associated with a particular function, the function of a significant proportion of genes remains unknown.

Genetic screenings

A common strategy for the functional characterisation of genes is the design of forward and reverse genetic screenings (Page & Grossniklaus, 2002). The approach is to generate a mutant population with altered phenotypes and physiological responses. Different mutagenesis methods have been described, including chemical, irradiation and insertional methods. The alkylating agent ethylmethane sulphonate (EMS) induce chemical modification of nucleotides resulting in mispairing and base substitutions randomly distributed throughout the genome. Commonly, EMS induces C-to-T mutations resulting in C/G to A/T substitution, which can introduce a stop codon within the coding sequence or the replacement of crucial amino acids, allowing the identification of gain- or loss-of-function mutants (Kim, YongSig, Karen, Schumaker, Zhu, 2006).

Forward genetic screening allows the direct study of specific biological processes. The screen relies on determining a genetic background that allows the identification

of a phenotype of interest through a smooth and tight screening procedure. Next, random mutations are artificially induced by chemical or physical means and the plants are screened for a particular phenotype. Subsequently, the underlying mutation responsible for the phenotype is mapped to a specific location in the genome (Page & Grossniklaus, 2002). To further dissect a biological process, a second screen can be done to identify second-site-mutations that can suppress or enhance the primary phenotype. Typically, suppressor mutations uncover alternative pathways or interacting proteins that became activated by the second mutation (Page & Grossniklaus, 2002).

PR1::LUC line

To investigate the molecular components of the defence signalling network, Murray *et al*, (2002) generated a transgenic *Arabidopsis* line expressing *luciferase* under the control of the *PR1* promoter. The *PR1::LUC* transgenic line was mutagenized with EMS and screened for mutations that caused miss-expression of the *PR1* gene, leading to the identification of the *constitutive induction of resistance(cir)* mutants *cir1, cir2,* and *cir3* which exhibit constitutive and broad-spectrum resistance against at least one of the virulent pathogens *Pseudomonas syringae* pv. Tomato, *Hyaloperonospora parasitica* NOCO2 and the necrotrophic pathogen *Botrytis cinerea.* Interestingly, each of the *cir* alleles displayed different defence mechanisms (Murray *et al*, 2002, 2005). In a different experiment, Grant *et al*, (2003) used an activation tagging approach with the *PR1::LUC* reporter line and identified the gene *Activated Disease Resistance 1 (ADR1)* which encodes an NBS-LRR disease resistance protein. The *ADR1* mutant showed elevated SA and ROS levels and expression of defence related genes. The *PR1::LUC* line was shown to accurately reports the engagement of SA-mediated immunity

S-nitrosylation is known to play a central role in the regulation of plant immunity and other physiological processes. In *Arabidopsis,* a loss-of-function mutation of the *S-nitrosoglutathione* (*GSNO) reductase 1 (GSNOR1)* gene resulted in high cellular S-nitrosylation, severe developmental impairments and reduced basal, non-host and *R*-mediated immunity, together with compromised salicylic acid biosynthesis and signalling (Feechan *et al*, 2005). Currently, the only known mechanisms in plants that directly control GSNO turnover involves the activities of the enzymes GSNOR1 and Thioredoxins (Kneeshaw *et al*, 2014).

We speculated that the expression of *PR1::LUC* would be reduced and delayed in a *gsnor1* background as a result of compromised SA-signalling by the high S-nitrosylation level (Feechan *et al*, 2005). Therefore, we designed a forward mutant screening using the line *PR1::LUC* in the *gsnor1* background of *par2-1* to search for second site modifiers that can suppress the *par2-1* phenotype and restore *PR1* expression under high S-nitrosylation and potentially, uncover additional molecular components involved in alternative GSNO turnover pathway.

Results

Characterisation of *PR1::LUC* transgene

To screen for second site mutations that can suppress/enhance the overall accumulation of GSNO in the *gsnor1* background, we designed a forward mutant screening based on transgenic *Arabidopsis thaliana* plants carrying a chimeric *PR1::LUC* transgene previously generated in the lab (Murray *et al*, 2002). This reporter line was shown to act as a robust reporter of the engagement of the endogenous *PR1* gene and the establishment of defence mechanisms (Murray *et al*, 2002; Grant *et al*, 2003; Murray *et al*, 2005).

We first characterised the expression level of *PR1::LUC* in response to exogenous SA in the *PR1::LUC* plants to confirm that the temporal expression of *PR1* and *LUC* was consistent with the reported *PR1* expression profile in response to *Pst* DC3000 (*avrB*) infection (Murray *et al*, 2002).

To do this, *PR1::LUC* Col 0 seeds were germinated on MS plates. The one-week-old seedlings were sprayed with salicylic acid 1 mM and were subsequently sprayed with a 5 mM luciferin solution and captured the resulting bioluminescence using an ultra-low-light EM-CCD (Electron Multiplier Charged Coupled Device) camera system. The pictures were collected at different time-points following SA induction. We observed low bioluminescence without SA induction and an increase in luminescence following SA application, with a significant increase from 12 hours and a peak in luminescence at 48 hours post-SA. Notably, our observation is consistent with the temporal profile of *PR1* expression reported by Murray *et al,* (2005), where they noticed *PR1* transcript accumulation within six to twelve hours after infection with avirulent *Pst* and a peak of expression after 24 hours (Fig 7.1A).

Characterisation of *PR1::LUC par2-1* plants

We proceed to cross the *PR1::LUC* transgene into the *gsnor1* background of *par2-1.* After crossing the lines, we selected F2 plants carrying the *PR1::LUC* transgene by screening seedlings for kanamycin resistance and then selecting adult plants displaying the *par2-1* phenotype. We then selected F3 double homozygous and characterise the bioluminescence in both lines after induction with SA 1 mM. To quantify the effect of S-nitrosylation on *PR1* expression, we did a time course assay using a Berthold luminometer which provides higher resolution compared to the EM-CCD system. We germinated *PR1::LUC* Col 0 and *par2-1* seeds in a 96-well black

plate containing 100 µL of MS media per well. The one-week-old seedlings were sprayed with luciferin solution and the resulting luminescence was recorded in the luminometer every hour for several hours to check for background luminescence.

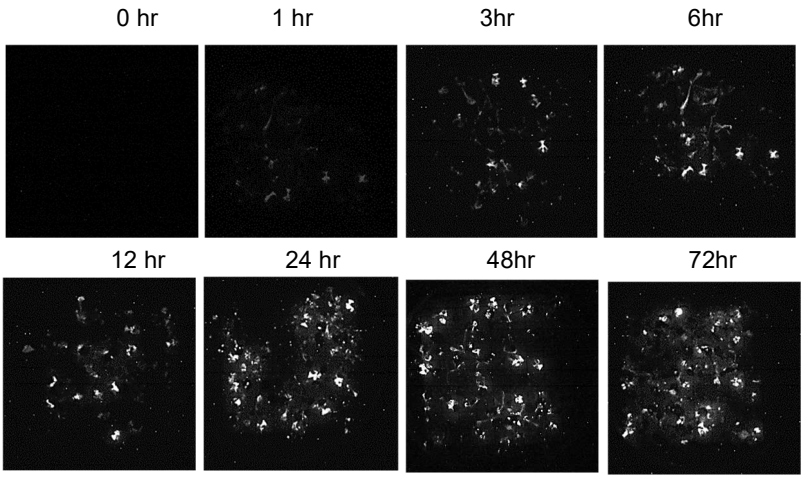

Figure 7.1. Expression pattern of *PR1::LUC* Colombia 0. Ultra-low light imaging of *PR1::LUC* Colombia 0 plants after exogenous SA application. The images were collected using a Hamamatsu EM-CCD C9100 camera. Pictures taken with 10 seconds exposure-time +217 gain calibration. The background noise was subtracted from the images.

After defining the background luminescence level, we induced *PR1* expression by spraying the plants with SA 1 mM and collect luminescence readings every hour for three additional days. We could observe strong bioluminescence in the *PR1::LUC* Col 0 from nine hours after SA. Interestingly, the *PR1::LUC par2-1* line showed reduced and delayed *luciferase* expression with respect to the expression in the Col-0 background. The *PR1::LUC par2-1* line showed a maximum bioluminescence level around forty hours after SA. The most striking difference between the Col 0 and *par2-1* lines occur within 12 hours after *PR1* induction with SA, when *PR1* expression increases significantly in the Col 0 background (Fig 7.2A). Therefore, this time point was suggested as a potential screening parameter.

To confirm the suitability of this time-point for the luciferase screening, we germinated seeds on MS plates and sprayed the *PR1::LUC* Col 0 and *par2-1* plants with SA and captured the bioluminescence in the EM-CCD system. As expected, the wild type (WT) line showed strong luminescence at 12 and 24 hours after SA, while significantly lower luminescence was detected in the *par2-1* plants at these time-points (Fig 7.2B).

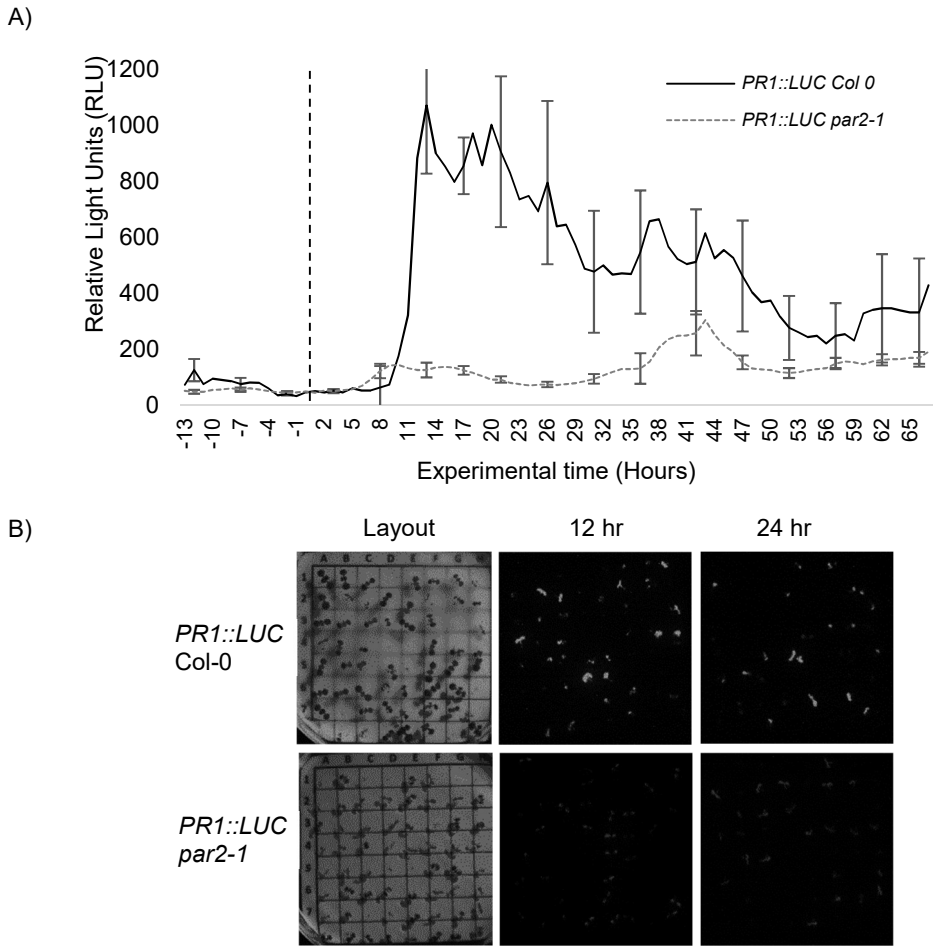

Figure 7.2. *PR1::LUC* expression in *par 2-1* background. Bioluminescence measurements of *PR1::LUC* plants in Col-0 and *par2-1* backgrounds. A) Relative light measurements of *PR1::LUC* seedlings after induction with SA 1mM. The plot represents the mean relative light units (RLU) value for Col-0 and *par2-1* lines following SA application, indicated by the dotted line in the plot. Reading collected in a Berthold luminometer. Error bars represent the standard error for approximately 30 plants per genotype. B) Ultra-low light imaging of *PR1::LUC* plants twelve and twenty-four hours after SA. Images captured with 10 seconds exposition time and +217 gain calibration.

EMS mutagenesis

To identify second site modifiers that can suppress the *par2-1* phenotype, we sought mutations that could reduce the delay in LUC expression in response to SA or mutations that result in constitutive *PR1* expression in the high S-nitrosylation background. We mutagenized a batch of *PR1::LUC par2-1* seeds (.75 g ~ 35,000 seeds) with 0.4% EMS solution for 16 hr at room temperature. The mutagenized M0 seeds were split into ~100 seeds/pool and let the plants to set seeds in a glass house. We could observe discolouration and irregular phenotypes in some pools suggesting efficient mutagenesis. We could observe a homogenous *par2-1* phenotype among all

pools. We were not able to identify any dominant suppressor mutation on M1 plants that could restore the WT phenotype.

First round screening

For the first round of screening to select for suppressor mutants of the *par2-1* phenotype approximately 5,000 of the resulting M2 plants were screened via luciferase imaging. The first stage aimed to identify mutants expressing *PR1* in response to SA. To do this, we sprayed the seedlings first with SA 1mM. Twelve hours later, we sprayed the plants with luciferin and incubated them for five minutes in the dark before collecting images using the EM-CCD camera. The M2 pools were imaged under low-light conditions and plants exhibiting strong luciferase activity were transferred to soil and let to set seeds. Also, we selected plants that showed long roots and displayed physical characteristics similar to WT at the seedling stage, regardless of their luciferase expression profile.

Subsequently, we scored the M2 plants for visible WT phenotype at the bolting stage, considering that the *gsnor1* phenotype encompasses distinctive physical characteristics such as loss of apical dominance, a high number of lateral shoots, stunted growth and short roots (Feechan *et al*, 2005). This specific phenotype facilitated the screening for plants that exhibit WT morphology.

We scored the phenotype of the selected M2 plants at different physiological stages and classified the pools according to their luciferase activity and their morphological characteristics. We genotyped the M2 plants using primers targeting the G-to-A *par2-1* mutation to confirm the presence of the *par2-1* allele.

From the original 47 pools, the plants from eight pools failed to produce seeds, either because they did not survive after the screening or infertility. Notably, a considerable number of plants selected for high luciferase activity showed significantly stunted growth and infertility, probably related to constitutive activation of defence mechanisms.

Second round screening

To differentiate between mutants expressing inducible *PR1* in response to SA treatment form those plants expressing constitutive *PR1* expression we prepared M3 seeds in MS plates and perform a two-phase sequential screen. First, the one-week-old seedlings were sprayed with a mix of SA and luciferin and were scanned after 5 minutes incubation in the dark to select plants showing constitutive *PR1* expression.

Subsequently, the plates were rescreened 12 hours later to select SA-inducible mutants. The plants exhibiting strong luciferase activity at 0 and 12 hour post SA were transferred to soil. We identified plants from four different pools that exhibit strong luciferase activity in response to SA and four pools with strong constitutive *LUC* expression (Fig 7.3). Interestingly, all these plants display a *par2-1* phenotype. The selected plants were let to set seeds, and we confirmed the luciferase phenotype in M4 plants.

Further characterisation of the selected candidate mutants is required to shorten the number of mutants and proceed to identify the underlying mutation responsible for the observed phenotypes.

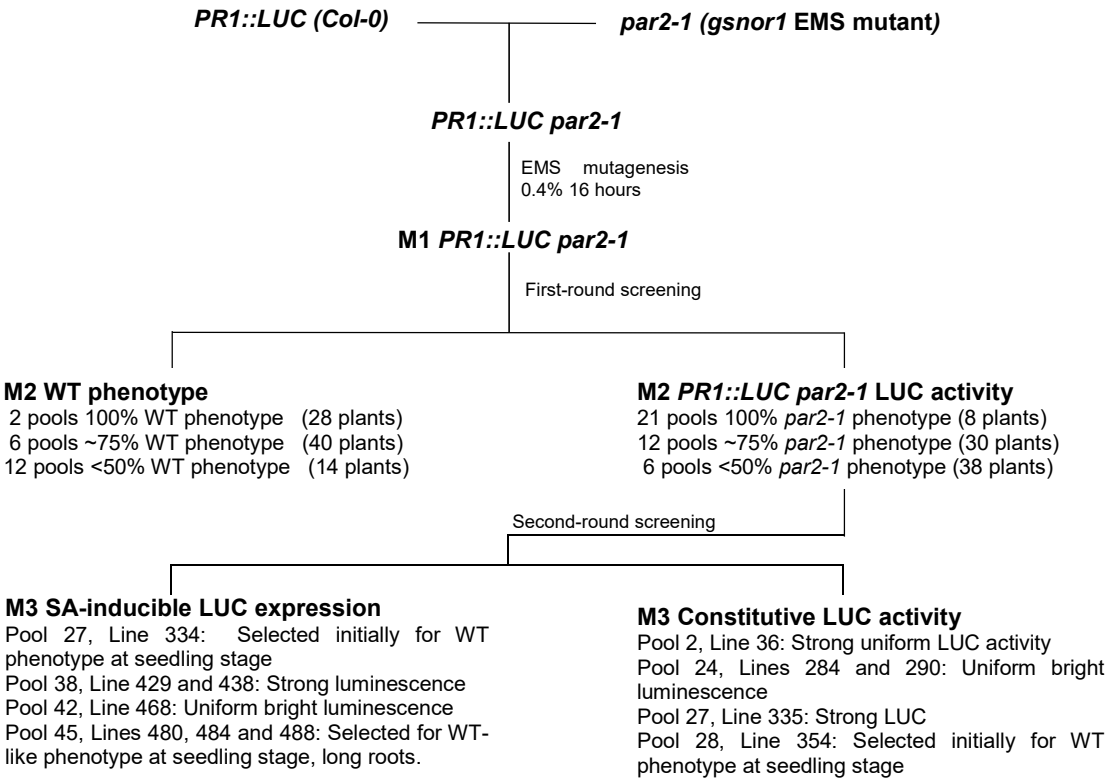

Figure 7.3. Schematic representation of first and second round of screening. First round aimed to select mutants exhibiting strong luciferase activity twelve hours after induction with SA 1 mM. Second round screen designed to discriminate between constitutive and SA-inducible *luciferase* expression.

Discussion

Here we report the basis for a *PR1::LUC par2-1* second-site suppressor mutant screening. We first characterised the expression pattern of luciferase under the control of the *PR1* promoter in a high S-nitrosylation background and observed reduced and delayed *PR1* expression with respect to WT plants, which was more evident at 12-hour post SA induction. It is well documented that the expression of SA-dependent genes is reduced and delayed in *gsnor1-3* plants which contain high cellular S-nitrosylation concentration (Feechan *et al*, 2005). Additionally, nitric oxide (NO) has been shown to be required for proper activation of SAR (Wang *et al*, 2014a) and that a partial reduction in GSNOR1 activity promotes the expression of *PR1* in response to SA induction (Espunya *et al*, 2012). We hypothesise that a mutation that can upregulate GSNO turnover and decrease global S-nitrosylation level to the extent that favours immunity could correlate with restored timing of *PR1* expression in response to SA.

A previous *atgsnor1-3* suppressor mutant screening conducted in the lab led to the identification of two alleles of the gene *CAT3,* termed *spl7* and *spl8,* which could partially revert the *gsnor1-3* phenotype (Brezezek, 2013). Further characterisation of the role of *cat3* suggested that GSNO may be decomposed by reacting with the hydroxyl radical (OH^-) in the absence of *CAT3,* thus reducing GSNO concentration (Chang, 2017). Notably, *PR1* expression was delayed in the *spl7* and *spl8* mutants compared to Col-0 plants, but it was faster than in *gsnor1-3*, correlated with the partial suppression of the *atgsnor1-3* phenotype (Brezezek, 2013), supporting the suitability of our screening methodology.

Phenotype of *gsnor1* suppressor EMS mutants

We have currently identified two main types of mutant phenotypes; 1) plants with inducible luciferase expression in response to SA and 2) plant constitutive Luc activity. We speculate that inducible *PR1* mutants could contain mutations involved with NO and GSNO turnover, potentially reducing cellular SNO-level, allowing SA-signalling. Similarly, we hypothesize that the mutants exhibiting constitutive *PR1* expression could carry mutations that reactivate SA-signalling under low SA concentrations or in a SA-independent *PR1* expression pathway.

NO and GSNO turnover

We expect to identify genes involved in GSNO turnover. GSNO is formed by the reaction on NO with the thiol group of glutathione (GSH). Therefore an indirect mechanism to regulate GSNO formation may involve the upregulation of genes involved in NO metabolism. For instance, oxyphytoglobins catalyse the oxygenation of NO into nitrate (NO_3^-). Additionally, NO can react with superoxide (O_2^-) to form peroxynitrite ($ONOO^-$), which is further detoxified by the activity of thioredoxins (TRXs) (Igamberdiev *et al*, 2016). Additionally, GSNO can be depleted by reacting with OH^- derived from H_2O_2 metabolism (Chang, 2018).

In mammals, Calcium (Ca^{2+})-dependent NO-release mechanism was observed in pancreatic cells. It was found that Ca^{2+} promotes the NO release from intracellular SNO groups, contributing to mediate NO responses (Chvanov *et al*, 2006). Also, the REDOX state of copper (Cu^+) can promote the formation or scavenging of SNO *in vitro* (Stubauer *et al*, 1999). It will be interesting to search for mutations that can promote the accumulation or reactive intermediaries that can prevent NO and GSNO formation or depletion.

Also, an important characteristic of GSNO is its ability to trans-nitrosylate other proteins. A direct mechanism for denitrosylation of proteins involves the activity of TRXs. For instance, TRH-*h5* (TRX*h5*) has selective protein-SNO activity and was shown to restore immunity in *nox1* plants accumulating high NO levels (Kneeshaw *et al*, 2014; Karapetyan & Dong, 2018). TRXs are highly conserved across the plant kingdom. The *Arabidopsis* genome contains 46 TRXs and TRX-like genes with a big proportion of them with no biochemical data available (Meyer *et al*, 2005). It is possible that this screen would discover a gain-of-function mutation of a TRX family member which can ameliorate the *gsnor1* phenotype.

SA-signalling

A relevant characteristic of *gsnor1* plants is the reduced SA-biosynthesis and accumulation in response to pathogen infection (Feechan *et al*, 2005). SA accumulation is a central step for the downstream expression of defence genes (Loake & Grant, 2007; Dempsey & Klessig, 2017). The protein non-expresser of PR genes 1 (NPR1) plays a critical role in SA-signalling. It is proposed to locate in the cytoplasm in an oligomer state stabilised by S-nitrosylation and requires SA-mediated conformational changes for nuclear translocation (Tada *et al*, 2008). However, NPR1

has been reported to translocate into the nucleus independent of SA during Endoplasmic Reticulum (ER) stress where it interacts with bZIP transcription factors (TF) (Lai *et al*, 2018). Furthermore, NPR1 activity driving *PR1* expression depends on SA-binding as plants expressing NPR1R432Q, impaired in SA-binding, shows expression of SA-dependant genes to a similar level than *npr1* plants (Ding *et al*, 2018). Additionally, *PR1* was significantly expressed in plants defective in SA biosynthesis after infection with avirulent *Pseudomonas* as a result of sustained activation of mitogen-activated protein kinases (MAPK) MAPK3 and MAPK6 (Tsuda *et al*, 2013). Taken together, the evidence suggest the existence of compensatory mechanisms to add robustness and specificity to the immune response. Our screening can facilitate the identification of additional components of the immune signalling network.

Future work

We have currently identified four *PR1*-inducible mutants and four constitutive-*PR1* mutants. It is important to confirm that the phenotype observed is not the result of a revertant mutation that reactivates GSNOR1 activity. The *par2-1* plants carry a G-to-A mutation in exon six which converts a highly conserved glycine (Gly) into aspartic acid (Asp) at position 236. This mutation was found to significantly affect GSNOR1 stability (Chen *et al*, 2009b). The WT codon GGC was changed to GAC in the *par2-1* allele. EMS induce G-to-A substitutions, it is unlikely that a GAA or AAC mutation that would convert Asp into glutamic acid (Glu) or asparagine (Asp) would restore protein stability and activity given the physicochemical differences between them; Gly is a nonpolar, Asp and Glu are acidic electrically charged and Asp is a polar amino acid (Gromiha *et al*, 1999).

Biochemical characterisation

The main objective of our mutant screening is to identify genes that can reduce the total S-nitrosylation level. A critical experiment to perform is to evaluate the total S-nitrosylation level in the mutant candidates. This experiment can be performed from total protein and subsequent biotin switch. If the mutation upregulates GSNO turnover or activates a denitrosylation mechanism we would expect a reduction in total S-nitrosylation in the mutants compared to the parental *PR1::LUC par2-1* lines.

Additionally, the base of our screening relies on the restoration of *PR1* expression under the high S-nitrosylation background. Therefore, it is essential to confirm that

the observed *LUC* expression accurately reports the endogenous *PR1* expression in the mutant plants. We speculate that a mutation that reduces general S-nitrosylation level could restore SA-biosynthesis and SA-signalling. It will be interesting to measure the total and free SA-level. The identification of a mutant candidate that shows reduced total protein S-nitrosylation together with increased SA biosynthesis and restored *PR1* expression could represent an interesting candidate for further characterisation.

Genetic characterisation of mutants

We have confirmed the inducible and constitutive phenotype in M2 and M3 generations, which suggests the mutation is heritable. We started generating an *Arabidopsis* ecotype *Landsberg erecta* (Ler) *PR1::LUC par2-1* introgression line to generate a mapping population. After crossing the mutant candidates into the *Ler* ecotype, we will be able to assess if the mutation is dominant or recessive on the F1 population (Li-Jia & Genji, 2006). We plan to use the F2 mapping population to perform rough mapping of the mutation using 22 molecular markers which will allow us to map the mutation to a specific genomic location (Lukowitz *et al*, 2002; Brezezek, 2013). Additionally, new protocols are available to identify the causal mutation using next-generation sequencing (Schneeberger, 2014; Uchida *et al*, 2011; Austin *et al*, 2011) which can accelerate the identification of the specific mutation. After linking the mutation to a specific gene, it will be interesting to characterise the function of this gene in GSNO metabolisms by undertaking biochemical and genetic analysis.

We have developed a forward mutant screening to search for second-site suppressors that can reduce the increased cellular S-nitrosylation in *gsnor1* background. We have identified eight candidate mutants that show inducible *PR1* expression or constitutive *PR1* expression which could contain mutations that upregulate GSNO/NO turnover, activate denitrosylation mechanisms or activate components of the defence network independent of SA. Further characterisation of the mutant candidates is required to identify the underlying mutation and link the gene with a function.

Chapter 8 General Discussion

S-nitrosylation in plant immunity

Plants have evolved different ways to perceive environmental and biological stimuli, interpret these signals and efficiently modify their metabolism accordingly. Salicylic acid (SA) is a critical hormone that mediates different aspects of plants development and the activation of defence responses against biotrophic pathogens (Dempsey & Klessig, 2017). In plants, the major proportion of SA in response to pathogens is produced via the activity of the enzyme Isochorismate Synthase 1 (ICS1) (Wildermuth *et al*, 2001).

It is well accepted that the concentration and localisation of reactive and nitrosative species (ROS and NOS) play an essential role in mediating protein modifications with the outcome of triggering signal cascades (Mittler, 2017; Wrzaczek *et al*, 2013). Nitric oxide (NO) stands as a central signalling molecule. NO transfer its bioactivity via S-nitrosylation (Lamotte *et al*, 2015; Yu *et al*, 2014). The cellular levels of S-nitrosylation are partially regulated by the activity of the enzyme S-nitrosoglutathione (GSNO) Reductase 1 (GSNOR1) (Feechan *et al*, 2005). *Arabidopsis thaliana* plants impaired in GSNOR1 activity and show a dramatic increase in total cellular S-nitrosylation, together with compromised SA biosynthesis and signalling, which affects different modes of plant immunity (Feechan *et al*, 2005). Recent studies show the effect of S-nitrosylation on SA-signalling (Tada *et al*, 2008; Cui *et al*, 2018). However, the molecular mechanisms by which S-nitrosylation regulates SA biosynthesis are not known.

Transcriptional repression of *ICS1* by S-nitrosylation

To investigate if *ICS1* could be subjected to transcriptional or posttranscriptional regulation by S-nitrosylation, we prepared the reported line *ICS1::GUS* and crossed it into the *gsnor1* genetic background (*ICS1::GUS par2-1*). Our data support the hypothesis of transcriptional repression of *ICS1* mediated by S-nitrosylation.

NO is a well-established global regulator of gene expression during plant immunity (Bellin *et al*, 2012) and exert quick transcriptional reprogramming (Polverari *et al*, 2003; Begara-Morales *et al*, 2014; Hussain *et al*, 2016; Sharma *et al*, 2016). However, how this molecule controls the transcriptional dynamics in the nucleus remains elusive. It was recently shown that the DNA-binding of the zinc-finger transcription

factor (ZF-TF) SRG1 is abolished by S-nitrosylation of Cys87. Additionally, the DNA-binding of the TFs MYB2 and MYB30 is blocked upon S-nitrosylation at Cys49 and 53, respectively (Serpa *et al*, 2007; Tavares *et al*, 2014). Contrary, it was reported that S-nitrosylation of Cys172/287 of TGA1 enhances the DNA-binding of the complex TGA1-NPR1 (Mengel *et al*, 2013; Lindermayr *et al*, 2010).

The observed effect on ICS1 expression could be the result of inhibition of the DNA-binding of the TFs that positively regulate ICS1 by S-nitrosylation. The main TFs driving *ICS1* expression are SARD1 and CBP60g. Both proteins contain Cys residues within their amino acid sequence, suggesting the possibility of S-nitrosylation. We showed that S-nitrosylation of Cys438 of SARD1 reduces its DNA-binding affinity to the *ICS1* promoter *in vitro* (Fig 8.1). Additionally, a central process in transcriptional regulation relies on the assembly of the transcriptional complex between RNA polymerase II, general TFs and the Mediator complex. The Mediator complex orchestrates transcriptional reprogramming against both biotrophic and necrotrophic pathogens and its proposed to facilitate the hormonal crosstalk (Caillaud *et al*, 2013; Kidd *et al*, 2009; Dhawan *et al*, 2009). Importantly, the mediator subunits Med14 and Med16 were found to play a pivotal role in the regulation of SA biosynthesis and signalling, respectively (Zhang *et al*, 2013c, 2012). Both proteins are rich in Cys residues, suggesting the possibility of transcriptional REDOX regulation by S-nitrosylation (Fig 8.1).

It is possible that in a high S-nitrosylation environment, SARD1 and possibly CBP60g will be S-nitrosylated, resulting in inhibition of their binding activity to the *ICS1* promoter. Additionally, the complex subunits Med14 and Med16 which are rich in cysteine residues could also be S-nitrosylated in this context, potentially affecting the assembly and interaction with *ICS1*-specific TFs (including SARD1 and CBP60g), thus contributing to explain the significant transcriptional repression observed in the *ICS1::GUS par2-1* lines (Fig 8.1).

To explore this possibility, it is necessary to investigate if SARD1 and MED14/16 can physically interact by performing *in vitro* protein-protein assays, such as yeast-two-hybrid assay. Moreover, it is possible to investigate if S-nitrosylation blocks this interaction. Confirming this hypothesis could represent a novel mechanism to integrate S-nitrosylation mediating the transcriptional reprogramming during SA-mediated immunity.

Additional mechanisms regulating transcription can be the upregulation of posttranscriptional mechanisms. A quick search on the *Arabidopsis* database for miRNA that matches the *ICS1* transcript identified six-candidate miRNAs. However, the line *ICS1::GUS* reporter line only allows us to evaluate transcriptional changes. It will be interesting to prepare an additional reporter line *ICS1::ICS1-GUS* or *ICS1::ICS1-nLUC* line to investigate if *ICS1* expression can also be regulated at the posttranscriptional level and if this process is modified by S-nitrosylation. The regulation of *ICS1* expression at both transcriptional and posttranscriptional level could contribute to understanding the mechanisms fine-tuning the temporal dynamics for SA accumulation during plant immunity.

Biological relevance of S-nitrosylation of Cys438 of SARD1

Our *in vitro* data suggests that the binding of SARD1 to the *ICS1* promoter is reduced upon S-nitrosylation of Cys438. We confirmed that SARD1 could be S-nitrosylated *in vivo* and investigated the biological relevance of this modification. We assumed that SARD1C438S would be insensitive to regulation by S-nitrosylation, showing a constant affinity for the *ICS1* promoter. We observed in the *SARD1::SARD1C438S-nLUC* stronger accumulation of SARD1 compared to SARD1-nLUC plants. Our analysis of the *SARD1* promoter showed the presence of two SARD1 *cis*-elements within the SARD1 promoter (Chow *et al*, 2016), suggesting a self-regulatory mechanism (Fig 8.2). It is possible that SARD1C438S remain bound to its own promoter resulting in an amplification effect.

In addition, we observed a persistent accumulation of SARD1-nLUC after sustained induction with SA. SARD1 play a critical role for the establishment of systemic acquired resistance (SAR) and SA-biosynthesis (Zhang *et al*, 2010). Interestingly, *Arabidopsis* plants deficient in the circadian regulator TF CHE showed impaired SAR (Zheng *et al*, 2015), similar to the observed phenotype in *sard1* plants (Zhang *et al*, 2010). The effect of CHE in SAR correlates with impaired *SARD1* expression in *che* plants. However, no CHE *cis*-regulatory elements are found within *SARD1* promoter, suggesting an indirect regulatory mechanism of CHE for *SARD1* expression (Zheng *et al*, 2015).

The apparent rhythm of *SARD1* expression could suggests the possibility of circadian regulation on SARD1 during SAR. Notably, the *SARD1* promoter contains CCA1 binding site and the *SARD1* promoter was identified as a potential CCA1 target in a genome-wide search for CCA1 targets study (Nagel *et al*, 2015). CCA1 is considered as an activator of immunity against bacteria and oomycetes and synchronises immune mechanisms at times with higher pathogenic activity (Wang *et al*, 2011b). Importantly, *CCA1* expression is negatively regulated by TOC1 via physical interaction with CHE (Pruneda-Paz *et al*, 2009). SA mediates REDOX changes that result expression of SA-dependent genes via NPR1 signalling (Tada *et al*, 2008). NPR1 follows a circadian rhythm regulated by CCA1 and act as a negative regulator of TOC1 to allow gating of immune responses (Zhou *et al*, 2015).

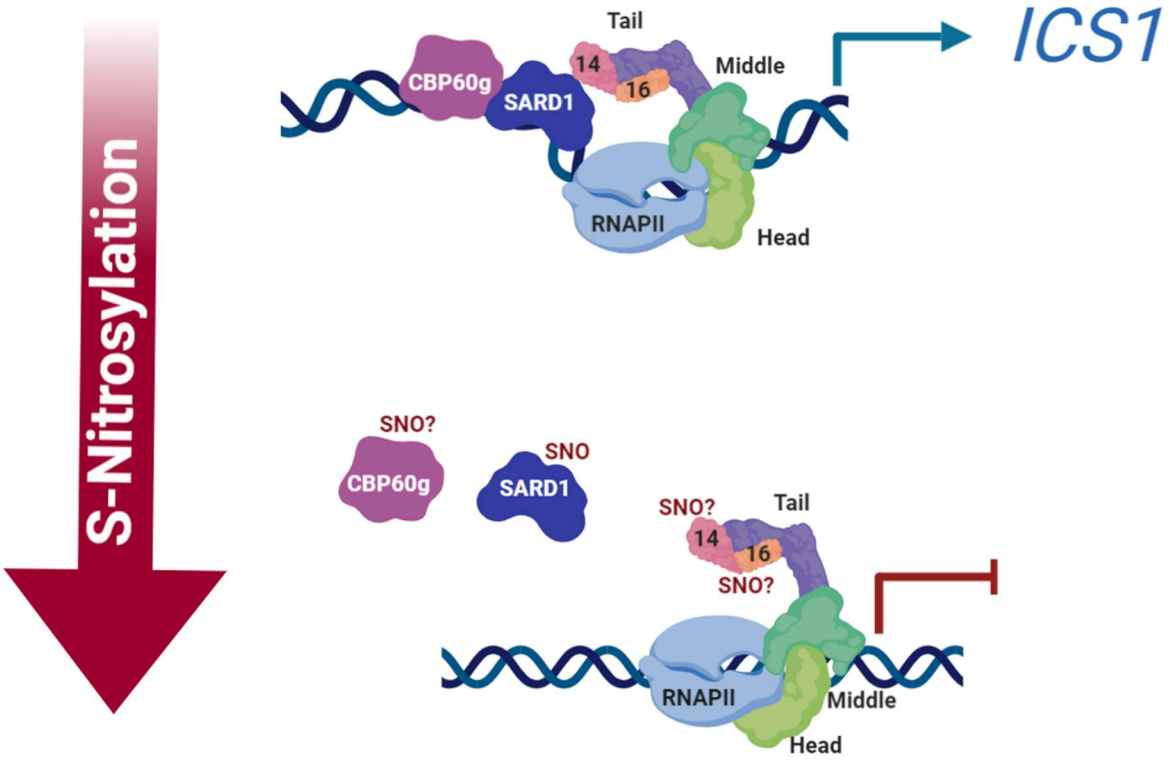

Figure 8.1. Schematic representation of transcriptional repression of *ICS1* expression by S-nitrosylation. Proposed mechanism by which S-nitrosylation may regulate *ICS1* expression under high cellular SNO concentrations. S-nitrosylation of the transcription factor SARD1 reduces its DNA-binding affinity, potentially having a similar effect on CBP60g. Additionally, it is possible that S-nitrosylation of the Mediator complex subunits Med14 and Med 16 regulates the interactions with *ICS1* specific TFs, including SARD1 and CBP60g resulting in transcriptional repression of *ICS1.*

A possible mechanism to explain the apparent rhythmic expression pattern observed in the SARD1-nLUC lines and not in SARD1C438S could result from a mechanism that requires S-nitrosylation of SARD1, possibly involving protein-protein interactions. It may be possible that after the release of SARD1 from its target promoters upon S-nitrosylation at Cys438 the concentration of unbound SARD1 will increase, allowing SARD1 to interact with other protein, including CHE and possibly compete with TOC1 for CHE interactions. In this scenario, the formation of SARD1-CHE complex would prevent the repression of *CCA1* by TOC1, allowing the expression of criticl immune genes, including *SARD1* and *NPR1,* amplifying the immune response. The release of SARD1 from its own promoter by S-nitrosylation of Cys438 could act as a negative feedback loop to switch the defence off. Less SARD1 concentration would favour CHE-TOC1 interaction to repress *CCA1* (Fig 8.2).

In this scenario, SARD1C438S would remain bound to its target promoters and would be unable to interact with CHE. Additionally, SARD1C438S constant DNA-binding could sequester its promoters preventing the interaction of additional TFs, thus affecting the timing and extent of the immune response. Furthermore, it has been shown that NO accumulation is a critical requirement for the optimal establishment of SAR and activation of immune responses (Wang *et al*, 2014a; Kachroo *et al*, 2016). Further research is needed to confirm the role of S-nitrosylation of SARD1. However, if the role is identified it could contribute to integrate nitric oxide signalling during SAR.

To validate our model, it is necessary to investigate if SARD1 and CHE can physically interact *in vitro* and *in vivo* and test if this interaction is regulated by S-nitrosylation. It will be interesting to cross the *SARD1::SARD1* lines into *che* and *cca1* background to evaluate if SARD1 rhythm is lost in the absence of CCA1 and CHE, together with the effect in SAR. Additionally, we started preparing *SARD1::SARD1* lines in the *par2-1* background to compare if S-nitrosylation regulates the specificity of SARD1 to its target promoters, which includes both positive and negative regulators of immunity (Sun *et al*, 2015).

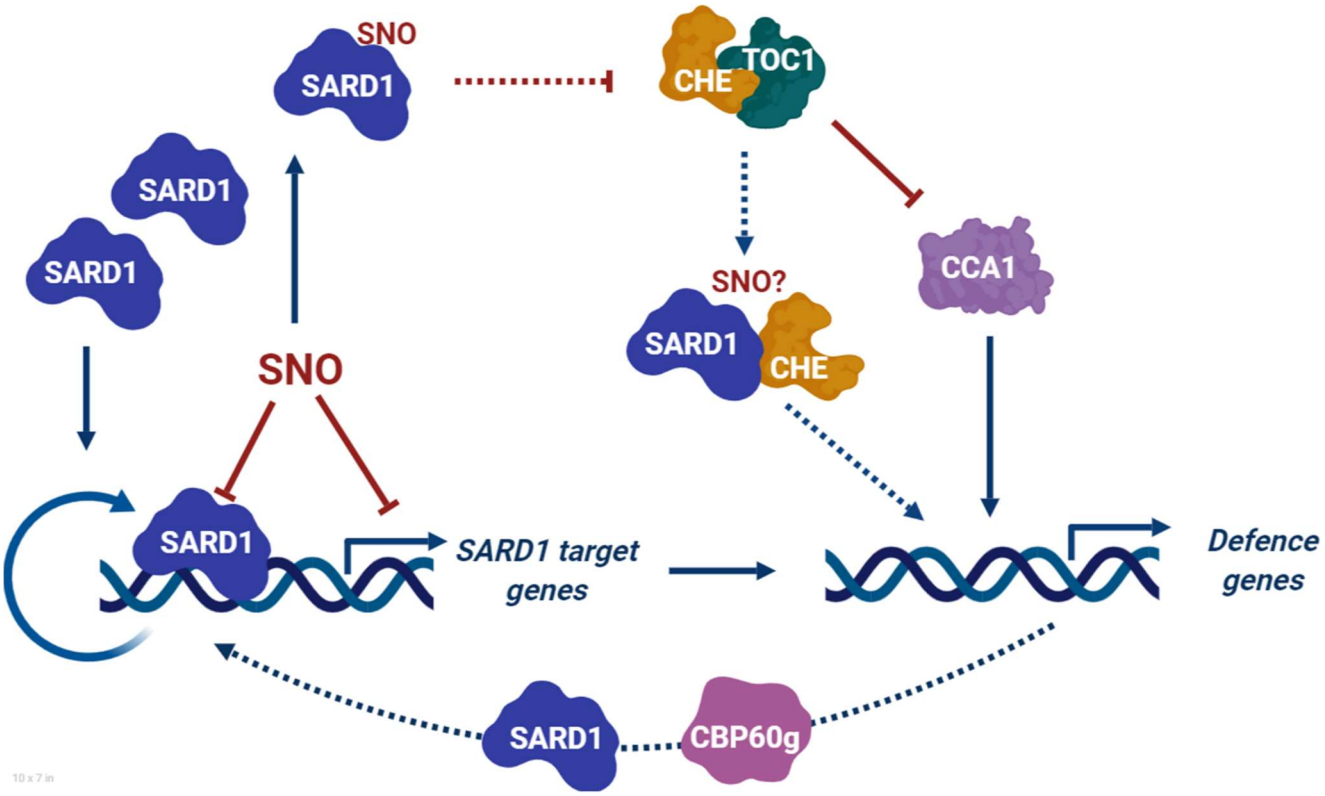

Figure 8.2. Proposed model for the role of S-nitrosylation of Cys438 in SAR. S-nitrosylation of Cys438 of SARD1 may regulate the DNA-binding affinity of SARD1 to its target genes. The presence of SARD1 binding motif within *SARD1* promoter suggests a self-regulatory mechanism for *SARD1* expression. CCA1 is proposed as a transcriptional activator of defence genes. CCA is negatively regulated by TOC1 mediated by the interaction with the N-terminal end of CHE. The S-nitrosylation-mediated release of SARD1 from its target promoters may facilitate protein-protein interactions between SARD1 and CHE, preventing the interaction between CHE and TOC1 and allowing the transcriptional activation of defence genes by CCA1, including *SARD1*. Dotted arrows represent potential mechanisms.

Novel regulators of S-nitrosylation and GSNO turnover

We designed a forward genetic screening to look for second-site modifiers that can suppress the *gsnor1* phenotype, potentially representing an alternative pathway for GSNO metabolism. The screening used the *Arabidopsis* line *PR1::LUC par2-1* in which the expression of *PR1* is reduced and delayed as a consequence of the high cellular S-nitrosylation. We have currently identified mutants that exhibit restored

expression of *PR1* in response to SA induction and mutants displaying constitutive expression of *PR1.* From the inducible lines, we expect to identify genes that can reduce the cellular S-nitrosylation level potentially by activating denitrosylation mechanisms, upregulating of GSNO turnover or promoting GSNO degradation. From the constitutive lines, we expect to identify regulators of *PR1* expression which act independently of SA.

Further characterisation of the candidate mutants is required to confirm that the underlying mutation reduces total S-nitrosylation. This can be performed by analysing total protein S-nitrosylation from plant extract. Additionally, it is necessary to evaluate if the reduction in cellular S-nitrosylation correlates with SA biosynthesis and the expression of SA-dependent genes.

The identification of new genes involved in GSNO turnover or denitrosylation mechanism can help us to understand S-nitrosylation better. S-nitrosylation plays a fundamental role in signalling and regulation of central processes. It has important implications in plant immunity (Karapetyan & Dong, 2018; Frederickson Matika & Loake, 2014; Yun *et al*, 2016). Understanding the molecular mechanisms behind S-nitrosylation, we will be able to engineer crops to be more resistant to disease and tolerant to abiotic stress (Hussain *et al*, 2019).

Furthermore, S-nitrosylation has been shown to regulate changes in transcriptional dynamics and regulate the function of transcription factors (Cui *et al*, 2018; Begara-Morales *et al*, 2014; Hussain *et al*, 2016; Tavares *et al*, 2014). It may be possible to exploit our knowledge on how posttranslational modifications regulate gene expression to generate synthetic TF to fine-tune gene expression in biological systems.

Additionally, S-nitrosylation is a critical factor if human disease. It has been implicated in pulmonary, cardiovascular, musculoskeletal, and neurological dysfunction. Also it correlates with different types of cancer (Foster *et al*, 2009). Targeting dysregulation of S-nitrosylation is emerging as a novel therapeutic target (Nakamura & Lipton, 2016). The identification of new mechanisms to regulate S-nitrosylation in plants could be transferred to animal system if these mechanisms are conserved. If it is conserved among species, it will be possible to use a pharmacological approach to use this mechanism for therapeutic applications. Further characterisation of the mutant candidates is necessary, but it can have important implications for both plant and health sciences.

Conclusion

The objective of the project was to investigate the molecular mechanisms by which S-nitrosylation regulates salicylic acid biosynthesis. Our findings suggest that *ICS1* is subjected to transcriptional regulation by S-nitrosylation of Cys438 of SARD1, which reduces its DNA-binding affinity for the *ICS1* promoter. Consistent with SARD1 role in SAR, we hypothesise that S-nitrosylation of Cys438 is necessary for the correct establishment of SAR, probably mediating interactions with other SAR regulators, such as CHE. However, *in vitro* and *in vivo* experiments are necessary to fully understand the mechanisms behind S-nitrosylation of SARD1 in SAR. In addition, it is necessary to solve the crystal structure of SARD1 to elucidate the molecular changes on SARD1 structure by S-nitrosylation. We developed a strategy to express recombinant SARD1 and purify it by ION exchange and gel filtration. Further optimizations is necessary to obtain the concentration and purity for crystallography studies. Moreover, we used a forward mutant screening to identify genes involved in GSNO turnover. We have identified interesting mutant candidates which can contain mutations that can probably regulate S-nitrosylation.

Our findings can contribute to integrate NO cues into SA biosynthesis and SAR and provide a basis to further understand S-nitrosylation regulation and the molecular mechanisms behind S-nitrosylation bioactivity.

Bibliography

Aarts N, Metz M, Holub E, Staskawicz BJ, Daniels MJ & Parker JE (1998) Different requirements for EDS1 and NDR1 by disease resistnace genes define at least two R gene-mediated signaling pathway in Arabidospsis.pdf. **95:** 10306–10311

Albertos P, Romero-Puertas MC, Tatematsu K, Mateos I, Sánchez-Vicente I, Nambara E & Lorenzo O (2015) S-nitrosylation triggers ABI5 degradation to promote seed germination and seedling growth. *Nat. Commun.* **6:** 1–10

Astier J, Gross I & Durner J (2017) Nitric oxide production in plants: an update. *J. Exp. Bot.***:** 1–11

Austin RS, Vidaurre D, Stamatiou G, Breit R, Provart NJ, Bonetta D, Zhang J, Fung P, Gong Y, Wang PW, McCourt P & Guttman DS (2011) Next-generation mapping of Arabidopsis genes. *Plant J.* **67:** 715–725

Basu S, Adams L, Guhathakurta S & Kim YS (2017) A novel tool for monitoring endogenous alpha-synuclein transcription by NanoLuciferase tag insertion at the 3′end using CRISPR-Cas9 genome editing technique. *Sci. Rep.* **8:** 1–11

Begara-Morales JC, Sánchez-Calvo B, Luque F, Leyva-Pérez MO, Leterrier M, Corpas FJ & Barroso JB (2014) Differential transcriptomic analysis by RNA-seq of GSNO-responsive genes between arabidopsis roots and leaves. *Plant Cell Physiol.* **55:** 1080–1095

Bellin D, Asai S, Delledonne M & Yoshioka H (2012) Nitric Oxide as a Mediator for Defense Responses. *Mol. Plant-Microbe Interact.* **26:** 271–277

Bernsdorff F, Döring A-C, Gruner K, Schuck S, Bräutigam A & Zeier J (2016) Pipecolic Acid Orchestrates Plant Systemic Acquired Resistance and Defense Priming via Salicylic Acid-Dependent and -Independent Pathways. *Plant Cell* **28:** 102–129

Bhattacharjya S, Xu P, Chakrapani M, Johnston L & Ni F (2005) Polymerization of the SAM domain of MAPKKK Ste11 from the budding yeast: implications for efficient signaling through the MAPK cascades. *Protein Sci.* **14:** 828–35 Available at: http://www.pubmedcentral.nih.gov/articlerender.fcgi?artid=2279271&tool=pmcentrez&rendertype=abstract

Brezezek K (2013) S-nitrosothiols and reactive oxygen species in plant disease resistance and development. **:** 1–207

Caillaud MC, Asai S, Rallapalli G, Piquerez S, Fabro G & Jones JDG (2013) A Downy Mildew Effector Attenuates Salicylic Acid-Triggered Immunity in Arabidopsis by Interacting with the Host Mediator Complex. *PLoS Biol.* **11:**

Camille Sayou, Nanao MH, Jamin M, Pose´ D, Thevenon E, Gregoire L, Tichtinsky G, Denay G, Ott F, Llobet MP, Schmid M, Dumas R & Parcy F (2016) A SAM oligomerization domain shapes the genomic binding landscape of the LEAFY transcription factor. *Nat. Commun.* **48:** 829–834

Cao H, Glazebrook J, Clarke JD, Volko S & Dong X (1997) The Arabidopsis NPR1 gene that controls systemic acquired resistance encodes a novel protein containing ankyrin repeats. *Cell* **88:** 57–63 Available at: http://dx.doi.org/10.1016/S0092-8674(00)81858-9

Chaki M, Shekariesfahlan A, Ageeva A, Mengel A, von Toerne C, Durner J &

Lindermayr C (2015) Identification of nuclear target proteins for S-nitrosylation in pathogen-treated Arabidopsis thaliana cell cultures. *Plant Sci.* **238:** 115–126

Chamizo-Ampudia A, Sanz-Luque E, Llamas A, Galvan A & Fernandez E (2017) Nitrate Reductase Regulates Plant Nitric Oxide Homeostasis. *Trends Plant Sci.* **22:** 163–174 Available at: http://dx.doi.org/10.1016/j.tplants.2016.12.001

Chamizo-Ampudia A, Sanz-Luque E, Llamas Á, Ocaña-Calahorro F, Mariscal V, Carreras A, Barroso JB, Galván A & Fernández E (2016) A dual system formed by the ARC and NR molybdoenzymes mediates nitrite-dependent NO production in Chlamydomonas. *Plant Cell Environ.* **39:** 2097–2107

Chang T-H (2018) Redox regulation of plant S-nitrosylation. *PhD thesis*

Chen H, Xue L, Chintamanani S, Germain H, Lin H, Cui H, Cai R, Zuo J, Tang X, Li X, Guo H & Zhou J-M (2009a) ETHYLENE INSENSITIVE3 and ETHYLENE INSENSITIVE3-LIKE1 Repress SALICYLIC ACID INDUCTION DEFICIENT2 Expression to Negatively Regulate Plant Innate Immunity in Arabidopsis. *Plant Cell Online* **21:** 2527–2540

Chen R (2012) Bacterial expression systems for recombinant protein production: E. coli and beyond. *Biotechnol. Adv.* **30:** 1102–7

Chen R, Sun S, Wang C, Li Y, Liang Y, An F, Li C, Dong H, Yang X, Zhang J & Zuo J (2009b) The Arabidopsis PARAQUAT RESISTANT2 gene encodes an S-nitrosoglutathione reductase that is a key regulator of cell death. *Cell Res.* **19:** 1377–1387

Cheng CY, Krishnakumar V, Chan AP, Thibaud-Nissen F, Schobel S & Town CD (2017) Araport11: a complete reannotation of the Arabidopsis thaliana reference genome. *Plant J.* **89:** 789–804

Chhetri G, Kalita P & Tripathi T (2015) An efficient protocol to enhance recombinant protein expression using ethanol in Escherichia coli. *MethodsX* **2:** 385–391

Chow CN, Zheng HQ, Wu NY, Chien CH, Huang H Da, Lee TY, Chiang-Hsieh YF, Hou PF, Yang TY & Chang WC (2016) PlantPAN 2.0: An update of Plant Promoter Analysis Navigator for reconstructing transcriptional regulatory networks in plants. *Nucleic Acids Res.* **44:** D1154–D1164

Chvanov M, Gerasimenko O V., Petersen OH & Tepikin A V. (2006) Calcium-dependent release of NO from intracellular S-nitrosothiols. *EMBO J.* **25:** 3024–3032

Covington MF, Maloof JN, Straume M, Kay SA & Harmer SL (2008) Global transcriptome analysis reveals circadian regulation of key pathways in plant growth and development. *Genome Biol.* **9:**

Cui B, Pan Q, Clarke D, Villarreal MO, Umbreen S, Yuan B, Shan W, Jiang J & Loake GJ (2018) S-nitrosylation of the zinc finger protein SRG1 regulates plant immunity. *Nat. Commun.* **9:** 1–12

Cui H, Gobbato E, Kracher B, Qiu J, Bautor J & Parker JE (2017) A core function of EDS1 with PAD4 is to protect the salicylic acid defense sector in Arabidopsis immunity. *New Phytol.* **213:** 1802–1817

DaRosa PA, Ovchinnikov S, Xu W & Klevit RE (2016) Structural insights into SAM domain-mediated tankyrase oligomerization. *Protein Sci.* **25:** 1744–1752

Delaney TP, Uknes S, Vernooij B, Friedrich L, Weymann K, Negrotto D, Gaffney T, Gut-rella M, Kessmann H, Ward E & Ryalst J (1994) a Central Role of Salicylic Acid in Plant Disease Resistance : Delaney. **266:** 1247–1250

Dempsey DA & Klessig DF (2017) How does the multifaceted plant hormone salicylic acid combat disease in plants and are similar mechanisms utilized in humans? *BMC Biol.* **15:** 1–11

Dempsey DA, Vlot a C, Wildermuth MC & Klessig DF (2011) Salicylic Acid biosynthesis and metabolism. *Arabidopsis Book* **9:** e0156

Denay G, Vachon G, Dumas R, Zubieta C & Parcy F (2017) Plant SAM-Domain Proteins Start to Reveal Their Roles. *Trends Plant Sci.* **22:** 718–725 Available at: http://dx.doi.org/10.1016/j.tplants.2017.06.006

Dhawan R, Luo H, Foerster AM, AbuQamar S, Du H-N, Briggs SD, Scheid OM & Mengiste T (2009) HISTONE MONOUBIQUITINATION1 Interacts with a Subunit of the Mediator Complex and Regulates Defense against Necrotrophic Fungal Pathogens in Arabidopsis. *Plant Cell Online* **21:** 1000–1019

Ding Y, Sun T, Ao K, Peng Y, Zhang Y, Li X & Zhang Y (2018) Opposite Roles of Salicylic Acid Receptors NPR1 and NPR3/NPR4 in Transcriptional Regulation of Plant Immunity. *Cell* **173:** 1454-1467.e10 Available at: https://doi.org/10.1016/j.cell.2018.03.044

Dodds PN & Rathjen JP (2010) Plant immunity: towards an integrated view of plant-pathogen interactions. *Nat. Rev. Genet.* **11:** 539–48

Engler C, Gruetzner R, Kandzia R & Marillonnet S (2009) Golden gate shuffling: A one-pot DNA shuffling method based on type ils restriction enzymes. *PLoS One* **4:**

Engler C, Youles M, Gruetzner R, Ehnert TM, Werner S, Jones JDG, Patron NJ & Marillonnet S (2014) A Golden Gate modular cloning toolbox for plants. *ACS Synth. Biol.* **3:** 839–843

Espunya MC, De Michele R, Gómez-Cadenas A & Martínez MC (2012) S-Nitrosoglutathione is a component of wound-and salicylic acid-induced systemic responses in Arabidopsis thaliana. *J. Exp. Bot.* **63:** 3219–3227

Feechan A, Kwon E, Yun B-W, Wang Y, Pallas JA & Loake GJ (2005) A central role for S-nitrosothiols in plant disease resistance. *Proc. Natl. Acad. Sci.* **102:** 8054–8059

Feng J, Chen L & Zuo J (2019) Protein S -Nitrosylation in Plants: Current Progresses and Challenges . *J. Integr. Plant Biol.* **XXXX:**

Feng J, Wang C, Chen Q, Chen H, Ren B, Li X & Zuo J (2013) S-nitrosylation of phosphotransfer proteins represses cytokinin signaling. *Nat. Commun.* **4:** 1529

Feys BJ (2005) Arabidopsis SENESCENCE-ASSOCIATED GENE101 Stabilizes and Signals within an ENHANCED DISEASE SUSCEPTIBILITY1 Complex in Plant Innate Immunity. *Plant Cell Online* **17:** 2601–2613

Feys BJ, Moisan LJ, Newman MA & Parker JE (2001) Direct interaction between the Arabidopsis disease resistance signaling proteins, EDS1 and PAD4. *EMBO J.* **20:** 5400–5411

Flores T, Todd CD, Tovar-Mendez A, Dhanoa PK, Correa-Aragunde N, Hoyos ME, Brownfield DM, Mullen RT, Lamattina L & Polacco JC (2008) Arginase-Negative Mutants of Arabidopsis Exhibit Increased Nitric Oxide Signaling in Root Development. *Plant Physiol.* **147:** 1936–1946

Foresi N, Mayta ML, Lodeyro AF, Scuffi D, Correa-Aragunde N, García-Mata C, Casalongué C, Carrillo N & Lamattina L (2015) Expression of the tetrahydrofolate-dependent nitric oxide synthase from the green alga Ostreococcus tauri increases tolerance to abiotic stresses and influences stomatal development in Arabidopsis. *Plant J.* **82:** 806–821

Foster MW, Hess DT & Stamler JS (2009) Protein S-nitrosylation in health and disease: a current perspective. *Trends Mol. Med.* **15:** 391–404

Foyer CH & Noctor G (2015) Defining robust redox signalling within the context of the plant cell. *Plant, Cell Environ.* **38:** 239–239

Frederickson Matika DE & Loake GJ (2014) Redox Regulation in Plant Immune Function. *Antioxid. Redox Signal.* **00:** 1–17

Frungillo L, Skelly MJ, Loake GJ, Spoel SH & Salgado I (2014) S-nitrosothiols regulate nitric oxide production and storage in plants through the nitrogen assimilation pathway. *Nat. Commun.* **5:** 1–10

Fu ZQ & Dong X (2013) Systemic acquired resistance: turning local infection into global defense. *Annu. Rev. Plant Biol.* **64:** 839–63

Gao Q-M, Zhu S, Kachroo P & Kachroo A (2015) Signal regulators of systemic acquired resistance. *Front. Plant Sci.* **06:** 1–12

Gao X, Chen X, Lin W, Chen S, Lu D, Niu Y, Li L, Cheng C, McCormack M, Sheen J, Shan L & He P (2013) Bifurcation of Arabidopsis NLR immune signaling via Ca^{2+}-dependent protein kinases. *PLoS Pathog.* **9:** e1003127

Gelvin SB (2003) Agrobacterium-Mediated Plant Transformation: the Biology behind the “Gene-Jockeying” Tool. *Microbiol. Mol. Biol. Rev.* **67:** 16–37

Grant JJ, Chini A, Basu D & Loake GJ (2003) of the Arabidopsis NBS-LRR gene , ADR1 , Conveys Resistance to Virulent Pathogens. **16:** 669–680

Gromiha MM, Oobatake M, Kono H, Uedaira H & Sarai A (1999) Relationship between amino acid properties and protein stability: Buried mutations. *J. Protein Chem.* **18:** 565–578

Guo F.Q., M. O & N.M. C (2003) Identification of a Plant Nitric Oxide Synthase Gene Involved in Hormonal Signaling. *Science (80-.).* **302:** 100–103

Gupta KJ & Igamberdiev AU (2011) The anoxic plant mitochondrion as a nitrite: NO reductase. *Mitochondrion* **11:** 537–543 Available at: http://dx.doi.org/10.1016/j.mito.2011.03.005

Gupta KJ & Kaiser WM (2010) Production and scavenging of nitric oxide by barley root mitochondria. *Plant Cell Physiol.* **51:** 576–584

Gupta KJ, Stoimenova M & Kaiser WM (2005) In higher plants, only root mitochondria, but not leaf mitochondria reduce nitrite to NO, in vitro and in situ. *J. Exp. Bot.* **56:** 2601–2609

Gusewski S, Melzer R, Rümpler F, Gafert C & Theißen G (2018) The floral homeotic protein SEPALLATA3 recognizes target DNA sequences by shape readout involving a conserved arginine residue in the MADS-domain. *Plant J.* **95:** 341–357

Hancock JT (2019) Considerations of the importance of redox state on reactive nitrogen species action. *J. Exp. Bot.*

Hancock JT, Craig TJ & Whiteman M (2018) Competition of Reactive Signals and Thiol Modifications of Proteins. *J. Cell Signal.* **02:** 24–26

Hancock JT & Whiteman M (2016) Alone NO Longer Elsevier Ltd

Heffler MA, Walters RD & Kugel JF (2012) Using electrophoretic mobility shift assays to measure equilibrium dissociation constants: GAL4-p53 binding DNA as a model system. *Biochem. Mol. Biol. Educ.* **40:** 383–387

Hellman LM & Fried MG (2007) Electrophoretic mobility shift assay (EMSA) for detecting protein-nucleic acid interactions. *Nat. Protoc.* **2:** 1849–1861

Hong RL, Hamaguchi L, Busch MA & Weigel D (2003) Regulatory Elements of the Floral Homeotic Gene. *Plant Cell* **15:** 1296–1309 Available at: http://www.ncbi.nlm.nih.gov/pubmed/12782724%0Ahttp://www.pubmedcentral.nih.gov/articlerender.fcgi?artid=PMC156367

Hongo F, Garban H, Huerta-Yepez S, Vega M, Jazirehi AR, Mizutani Y, Miki T & Bonavida B (2005) Inhibition of the transcription factor Yin Yang 1 activity by S-nitrosation. *Biochem. Biophys. Res. Commun.* **336:** 692–701

Hunter LJR, Westwood JH, Heath G, Macaulay K, Smith AG, MacFarlane SA, Palukaitis P & Carr JP (2013) Regulation of RNA-Dependent RNA Polymerase 1 and Isochorismate Synthase Gene Expression in Arabidopsis. *PLoS One* **8:**

Hussain A, Mun B-G, Imran QM, Lee S-U, Adamu TA, Shahid M, Kim K-M & Yun B-W (2016) Nitric Oxide Mediated Transcriptome Profiling Reveals Activation of Multiple Regulatory Pathways in Arabidopsis thaliana. *Front. Plant Sci.* **7:** 1–18

Hussain A, Yun B-W, Kim JH, Gupta KJ, Hyung N & Loake GJ (2019) Novel and conserved functions of S-nitrosoglutathione reductase (GSNOR) in tomato. *Exp. Biol.*

Igamberdiev AU, Hebelstrup KH, Stasolla C & Hill RD (2016) Regulation and Turnover of Nitric Oxide by Phytoglobins in Plant Cell Responses. *Gasotransmitters in Plants***:** 157–173 Available at: http://link.springer.com/10.1007/978-3-319-40713-5

Jaffrey SR & Snyder SH (2001) The Biotin Switch Method for the Detection of S-Nitrosylated Proteins. *Sci. Signal.* **2001:** pl1–pl1

Jeandroz S, Wipf D, Stuehr DJ, Lamattina L, Melkonian M, Tian Z, Zhu Y, Carpenter EJ, Wong GK & Wendehenne D (2016) Occurrence , structure , and evolution of nitric oxide synthase – like proteins in the plant kingdom. **9:**

Jensen MK & Skriver K (2014) NAC transcription factor gene regulatory and protein-protein interaction networks in plant stress responses and senescence. *IUBMB Life* **66:** 156–166

Jevševar S, Gaberc-Porekar V, Fonda I, Podobnik B, Grdadolnik J & Menart V (2005)

Production of nonclassical inclusion bodies from which correctly folded protein can be extracted. *Biotechnol. Prog.* **21:** 632–639

Kachroo P & Kachroo A (2018) Plants Pack a Quiver Full of Arrows. *Cell Host Microbe* **23:** 573–575

Kachroo P, Lim GH & Kachroo A (2016) Nitric Oxide-Mediated Chemical Signaling during Systemic Acquired Resistance Elsevier Ltd

Karapetyan S & Dong X (2018) Redox and the circadian clock in plant immunity: A balancing act. *Free Radic. Biol. Med.* **119:** 56–61 Available at: https://doi.org/10.1016/j.freeradbiomed.2017.12.024

Kelly LA, Mezulis S, Yates C, Wass M & Sternberg M (2015) The Phyre2 web portal for protein modelling, prediction, and analysis. *Nat. Protoc.* **10:** 845–858

Kidd BN, Edgar CI, Kumar KK, Aitken EA, Schenk PM, Manners JM & Kazan K (2009) The Mediator Complex Subunit PFT1 Is a Key Regulator of Jasmonate-Dependent Defense in Arabidopsis. *Plant Cell Online* **21:** 2237–2252

Kim, YongSig, Karen, Schumaker, Zhu J-K (2006) EMS Mutagenesis of Arabidopsis Seed. *Cold Spring Harb. Protoc.* **2006:** pdb.prot4621-pdb.prot4621

Kim CM, Jang T ho & Park HH (2016) Functional Analysis of CP2-Like Domain and SAM-Like Domain in TFCP2L1, Novel Pluripotency Factor of Embryonic Stem Cells. *Appl. Biochem. Biotechnol.* **179:** 650–658 Available at: http://dx.doi.org/10.1007/s12010-016-2021-z

Kim K, Franceschi VR, Davin LB & Lewis NG (2005) Glucuronidase as Reporter Geneas. *Methods* **323:**

Kneeshaw S, Gelineau S, Tada Y, Loake GJ & Spoel SH (2014) Selective Protein Denitrosylation Activity of Thioredoxin-h5 Modulates Plant Immunity. *Mol. Cell* **56:** 153–162

Kong Q, Sun T, Qu N, Ma J, Li M, Cheng Y, Zhang Q, Wu D, Zhang Z & Zhang Y (2016) Two redundant receptor-like cytoplasmic kinases function downstream of pattern recognition receptors to regulate activation of SA biosynthesis in Arabidopsis. *Plant Physiol.* **171:** pp.01954.2015

Kovacs I, Ageeva A, König E-E & Lindermayr C (2016) S-Nitrosylation of Nuclear Proteins. **77:** 15–39

Kröncke K, Fchsel K, Schidt T, Zenke F, Dasting I, Wesener J, Bettermann H, Breunig K & Kolh-Bachofen V (1994) Nitric Oxide destroys zinc-sulfur clusters inducing zinc release from metallothionein and inhibition of the zinc finger-type yeast transcription activator LAC9. *Biochem. Biophys. Res. Commun.* **200:** 1105–1110

Kumar D (2014) Salicylic acid signaling in disease resistance. *Plant Sci.***:** 1–8

Lai Y-S, Renna L, Yarema J, Ruberti C, He SY & Brandizzi F (2018) Salicylic acid-independent role of NPR1 is required for protection from proteotoxic stress in the plant endoplasmic reticulum. *Proc. Natl. Acad. Sci.* **115:** E5203–E5212

Lamotte O, Bertoldo JB, Besson-Bard A, Rosnoblet C, AimÃ© S, Hichami S, Terenzi H & Wendehenne D (2015) Protein S-nitrosylation: specificity and identification strategies in plants. *Front. Chem.* **2:** 1–10

Lawton K, Weymann K, Friedrich L, Vernooij B, Uknes S & Ryals J (1995) Systemic acquired resistance in Arabidopsis requires salicylic acid but not ethylene. *Mol. plant-microbe Interact.* **8:** 863–70

Lee J-Y, Colinas J, Wang JY, Mace D, Ohler U & Benfey PN (2006) Transcriptional and posttranscriptional regulation of transcription factor expression in Arabidopsis roots. *Proc. Natl. Acad. Sci.* **103:** 6055–6060 Available at: http://www.pnas.org/cgi/doi/10.1073/pnas.0510607103

Lee TY, Chen YJ, Lu TC, Huang H Da & Chen YJ (2011) Snosite: Exploiting maximal dependence decomposition to identify cysteine S-Nitrosylation with substrate site specificity. *PLoS One* **6:**

Leibly DJ, Nguyen TN, Kao LT, Hewitt SN, Barrett LK & van Voorhis WC (2012) Stabilizing Additives Added during Cell Lysis Aid in the Solubilization of Recombinant Proteins. *PLoS One* **7:**

Lewsey MG, Murphy AM, Maclean D, Dalchau N, Westwood JH, Macaulay K, Bennett MH, Moulin M, Hanke DE, Powell G, Smith AG & Carr JP (2010) 2010 - The Cucumber mosaic virus (CMV) 2b counter-defense protein disrupts plant antiviral mechanisms mediated by RNA silencing and salicylic acid (SA)..pdf. **23:** 835–845

Li-Jia Q & Genji Q (2006) Generation and Identifi cation of Arabidopsis EMS Mutants. In *Arabidopsis Protocols* pp 225–239.

Li B, Meng X, Shan L & He P (2016) Transcriptional Regulation of Pattern-Triggered Immunity in Plants. *Cell Host Microbe* **19:** 641–650

Li W-X, Oono Y, Zhu J, He X-J, Wu J-M, Iida K, Lu X-Y, Cui X, Jin H & Zhu J-K (2008) The Arabidopsis NFYA5 Transcription Factor Is Regulated Transcriptionally and Posttranscriptionally to Promote Drought Resistance. *Plant Cell Online* **20:** 2238–2251 Available at: http://www.plantcell.org/cgi/doi/10.1105/tpc.108.059444

Li Y (2015) Redox regulation of saliLi, Y. (2015). Redox regulation of salicylic acid synthesis in plant immunity.cylic acid synthesis in plant immunity

Lieutaud P, Ferron F, Uversky A V., Kurgan L, Uversky VN & Longhi S (2016) How disordered is my protein and what is its disorder for? A guide through the “dark side” of the protein universe. *Intrinsically Disord. Proteins* **4:** e1259708

Lindermayr C, Sell S, Muller B, Leister D & Durner J (2010) Redox Regulation of the NPR1-TGA1 System of Arabidopsis thaliana by Nitric Oxide. *Plant Cell* **22:** 2894–2907

Liu X, Sun Y, Kørner CJ, Du X, Vollmer ME & Pajerowska-Mukhtar KM (2015) Bacterial Leaf Infiltration Assay for Fine Characterization of Plant Defense Responses using the Arabidopsis thaliana-Pseudomonas syringae Pathosystem. *J. Vis. Exp.***:** 1–12

Loake G & Grant M (2007) Salicylic acid in plant defence--the players and protagonists. *Curr. Opin. Plant Biol.* **10:** 466–72

Lobstein J, Emrich CA, Jeans C, Faulkner M, Riggs P & Berkmen M (2012) SHuffle, a novel Escherichia coli protein expression strain capable of correctly folding disulfide bonded proteins in its cytoplasm. *Microb. Cell Fact.* **11:** 1–16

Lukowitz W, Gillmor CS & Scheible W-R (2002) Positional Cloning in Arabidopsis. Why It Feels Good to Have a Genome Initiative Working for You. *Plant Physiol.* **123:** 795–806

Lv F, Zhou J, Zeng L & Xing D (2015) β-cyclocitral upregulates salicylic acid signalling to enhance excess light acclimation in Arabidopsis. *J. Exp. Bot.* **66:** 4719–4732

Ma X, Wang W, Bittner F, Schmidt N, Berkey R, Zhang L, King H, Zhang Y, Feng J, Wen Y, Tan L, Li Y, Zhang Q, Deng Z, Xiong X & Xiao S (2016) Dual and Opposing Roles of Xanthine Dehydrogenase in Defense-Associated Reactive Oxygen Species Metabolism in Arabidopsis. *Plant Cell* **28:** 1108–1126

McPherson A & Gavira JA (2014) Introduction to protein crystallization. *Acta Crystallogr. Sect. FStructural Biol. Commun.* **70:** 2–20

Mengel A, Chaki M, Shekariesfahlan A & Lindermayr C (2013) Effect of nitric oxide on gene transcription – S-nitrosylation of nuclear proteins. *Front. Plant Sci.* **4:** 1–7

Meyer Y, Reichheld JP & Vignols F (2005) Thioredoxins in Arabidopsis and other plants. *Photosynth. Res.* **86:** 419–433

Mittler R (2017) ROS Are Good. *Trends Plant Sci.* **22:** 11–19

Moghaddas Sani H, Hamzeh-Mivehroud M, Silva AP, Walshe JL, Mohammadi SA, Rahbar-Shahrouziasl M, Abbasi M, Jamshidi O, Low JK, Dastmalchi S & Mackay JP (2018) Expression, purification and DNA-binding properties of zinc finger domains of DOF proteins from Arabidopsis thaliana. *BioImpacts* **8:** 167–176

Mou Z, Fan W, Dong X & Carolina N (2003) Inducers of Plant Systemic Acquired Resistance Regulate NPR1 Function through Redox Changes. *Cell* **113:** 935–944

Murray SL, Adams N, Kliebenstein DJ, Loake GJ & Denby KJ (2005) A constitutive PR-1::luciferase expression screen identifies Arabidopsis mutants with differential disease resistance to both biotrophic and necrotrophic pathogens. *Mol. Plant Pathol.* **6:** 31–41

Murray SL, Thomson C, Chini A, Read ND & Loake GJ (2002) Characterization of a novel, defense-related Arabidopsis mutant, cir1, isolated by luciferase imaging. *Mol. Plant. Microbe. Interact.* **15:** 557–566

Nagel DH, Doherty CJ, Pruneda-Paz JL, Schmitz RJ, Ecker JR & Kay SA (2015) Genome-wide identification of CCA1 targets uncovers an expanded clock network in Arabidopsis. *Proc. Natl. Acad. Sci. U. S. A.* **112:** E4802-10 Available at: http://www.ncbi.nlm.nih.gov/pubmed/26261339%0Ahttp://www.pubmedcentral.nih.gov/articlerender.fcgi?artid=PMC4553765

Nakamura T & Lipton SA (2016) Protein S-Nitrosylation as a Therapeutic Target for Neurodegenerative Diseases. *Trends Pharmacol. Sci.* **37:** 73–84 Available at: http://dx.doi.org/10.1016/j.tips.2015.10.002

Nakano M, Nobuta K, Vamaraju K, Singh S, Tej S, Skogen J & Meyers B (2005) Plant MPSS databases: signature-based transcriptional resources for analyses of mRNA and small RNA. *Nucleic Acids Res.* **34:** D731–D735

Navarova H, Bernsdorff F, Doring A-C & Zeier J (2012) Pipecolic Acid, an

Endogenous Mediator of Defense Amplification and Priming, Is a Critical Regulator of Inducible Plant Immunity. *Plant Cell* **24:** 5123–5141 Available at: http://www.plantcell.org/cgi/doi/10.1105/tpc.112.103564

Page DR & Grossniklaus U (2002) the Art and Design of Genetic Screens: Arabidopsis Thaliana. *Nat. Rev. Genet.* **3:** 124–136

Park SW, Liu PP, Forouhar F, Vlot AC, Tong L, Tietjen K & Klessig DF (2009) Use of a synthetic salicylic acid analog to investigate the roles of methyl salicylate and its esterases in plant disease resistance. *J. Biol. Chem.* **284:** 7307–7317

Polverari A, Molesini B, Pezzotti M, Buonaurio R, Marte M, Delledonne M & Scientifico D (2003) Nitric Oxide-Mediated Transcriptional Changes in Arabidopsis thaliana. **16:** 1094–1105

Pruneda-Paz JL, Breton G, Para A & Kay SA (2009) A functional genomics approach reveals CHE as a novel component of the Arabidopsis circadian clock. *Science (80-.).* **323:** 1481–1485

Qi Y, Tsuda K, Joe A, Sato M, Nguyen L V., Glazebrook J, Alfano JR, Cohen JD & Katagiri F (2010) A Putative RNA-Binding Protein Positively Regulates Salicylic Acid–Mediated Immunity in Arabidopsis . *Mol. Plant-Microbe Interact.* **23:** 1573–1583

Qin J, Wang K, Sun L, Xing H, Wang S, Li L, Chen S, Guo H-S & Zhang J (2018) The plant-specific transcription factors CBP60g and SARD1 are targeted by a Verticillium secretory protein VdSCP41 to modulate immunity. *Elife* **7:** 1–25

Rekhter D, Lüdke D, Ding Y, Feussner K, Zienkiewicz K, Lipka V, Wiermer M, Zhang Y & Feussner I (2019) PBS3 is the missing link in plant-specific isochorismate-derived salicylic acid biosynthesis. *bioRxiv***:** 1–10

Reyes LH, Cardona C, Pimentel L, Rodríguez-López A & Alméciga-Díaz CJ (2017) Improvement in the production of the human recombinant enzyme N-acetylgalactosamine-6-sulfatase (rhGALNS) in Escherichia coli using synthetic biology approaches. *Sci. Rep.* **7:** 1–14

Rosano GL & Ceccarelli E a. (2014) Recombinant protein expression in Escherichia coli: Advances and challenges. *Front. Microbiol.* **5:** 1–17

Santolini J, André F, Jeandroz S & Wendehenne D (2017) Nitric oxide synthase in plants: Where do we stand? *Nitric Oxide - Biol. Chem.* **63:** 30–38

Santos CA, Beloti LL, Toledo MAS, Crucello A, Favaro MTP, Mendes JS, Santiago AS, Azzoni AR & Souza AP (2012) A novel protein refolding protocol for the solubilization and purification of recombinant peptidoglycan-associated lipoprotein from Xylella fastidiosa overexpressed in Escherichia coli. *Protein Expr. Purif.* **82:** 284–289

Schneeberger K (2014) Using next-generation sequencing to isolate mutant genes from forward genetic screens. *Nat. Rev. Genet.* **15:** 662–676 Available at: http://dx.doi.org/10.1038/nrg3745

Serpa V, Vernal J, Lamattina L, Grotewold E, Cassia R & Terenzi H (2007) Inhibition of AtMYB2 DNA-binding by nitric oxide involves cysteine S-nitrosylation. *Biochem. Biophys. Res. Commun.* **361:** 1048–1053

Shaikhali J, Davoine C, Brännström K, Rouhier N, Bygdell J, Björklund S & Wingsle

G (2015) Biochemical and redox characterization of the mediator complex and its associated transcription factor GeBPL, a GLABROUS1 enhancer binding protein. *Biochem. J.* **468:** 385–400

Shaikhali J & Wingsle G (2017) Redox-regulated transcription in plants: Emerging concepts. *AIMS Mol. Sci.* **4:** 301–338

Shapiro AD & Zhang C (2001) The Role of NDR1 in Avirulence Gene-Directed Signaling and Control of Programmed Cell Death in Arabidopsis. *Plant Physiolo* **16:** 1089–1101

Sharma A, Hussain A, Mun BG, Imran QM, Falak N, Lee SU, Kim JY, Hong JK, Loake GJ, Ali A & Yun BW (2016) Comprehensive analysis of plant rapid alkalization factor (RALF) genes. *Plant Physiol. Biochem.* **106:** 82–90

Shi H, Ye T, Chen F, Cheng Z, Wang Y, Yang P, Zhang Y & Chan Z (2013) Manipulation of arginase expression modulates abiotic stress tolerance in Arabidopsis: Effect on arginine metabolism and ROS accumulation. *J. Exp. Bot.* **64:** 1367–1379

Shi YF, Wang DL, Wang C, Culler AH, Kreiser MA, Suresh J, Cohen JD, Pan J, Baker B & Liu JZ (2015) Loss of GSNOR1 function leads to compromised auxin signaling and polar auxin transport. *Mol. Plant* **8:** 1350–1365

Shine MB, Xiao X, Kachroo P & Kachroo A (2018) Signaling mechanisms underlying systemic acquired resistance to microbial pathogens. *Plant Sci.***:** 0–1

Singh A, Lim GH & Kachroo P (2017) Transport of chemical signals in systemic acquired resistance. *J. Integr. Plant Biol.* **59:** 336–344

Spadaro D, Yun BW, Spoel SH, Chu C, Wang YQ & Loake GJ (2010) The redox switch: Dynamic regulation of protein function by cysteine modifications. *Physiol. Plant.* **138:** 360–371

Spoel SH & Dong X (2012) How do plants achieve immunity? Defence without specialized immune cells. *Nat. Rev. Immunol.* **12:** 89–100

Spoel SH & van Ooijen G (2013) Circadian Redox Signaling in Plant Immunity and Abiotic Stress. *Antioxid. Redox Signal.* **20:** 3024–3039

Staiger D, Korneli C, Lummer M & Navarro L (2013) Emerging role for RNA-based regulation in plant immunity. *New Phytol.* **197:** 394–404

Stöhr C, Strube F, Marx G, Ullrich WR & Rockel P (2001) A plasma membrane-bound enzyme of tobacco roots catalyses the formation of nitric oxide from nitrite. *Planta* **212:** 835–841

Stubauer G, Giuffrè A & Sarti P (1999) Mechanism of S-nitrosothiol formation and degradation mediated by copper ions. *J. Biol. Chem.* **274:** 28128–28133

Sun T, Busta L, Zhang Q, Ding P, Jetter R & Zhang Y (2018) TGACG-BINDING FACTOR 1 (TGA1) and TGA4 regulate salicylic acid and pipecolic acid biosynthesis by modulating the expression of SYSTEMIC ACQUIRED RESISTANCE DEFICIENT 1 (SARD1) and CALMODULIN-BINDING PROTEIN 60g (CBP60g). *New Phytol.* **217:** 344–354

Sun T, Zhang Y, Li Y, Zhang Q, Ding Y & Zhang Y (2015) ChIP-seq reveals broad roles of SARD1 and CBP60g in regulating plant immunity. *Nat. Commun.* **6:**

10159

Tada Y, Spoel SH, Pajerowska-Mukhtar K, Mou Z, Song J, Wang C, Zuo J & Dong X (2008) Plant immunity requires conformational charges of NPR1 via S-nitrosylation and thioredoxins. *Science (80-.).* **321:** 952–956

Tavares CP & Terenzi H (2016) Biochemical analysis of the interaction between Arabidopsis thaliana AtMYB30 transcription factor and its DNA specific target site. *J. Plant Biochem. Biotechnol.* **25:** 97–103

Tavares CP, Vernal J, Delena RA, Lamattina L, Cassia R & Terenzi H (2014) S-nitrosylation influences the structure and DNA binding activity of AtMYB30 transcription factor from Arabidopsis thaliana. *Biochim. Biophys. Acta - Proteins Proteomics* **1844:** 810–817

Tedman-Jones JD, Lei R, Jay F, Fabro G, Li X, Reiter WD, Brearley C & Jones JDG (2008) Characterization of Arabidopsis mur3 mutations that result in constitutive activation of defence in petioles, but not leaves. *Plant J.* **56:** 691–703

Torrens-spence MP, Bobokalonova A, Carballo V, Christopher M, Shen A & Weng J (2019) PBS3 and EPS1 complete salicylic acid biosynthesis from isochorismate in Arabidopsis. *bioRxiv*

Truman W & Glazebrook J (2012) Co-expression analysis identifies putative targets for CBP60g and SARD1 regulation. *BMC Plant Biol.* **12:** 1

Truman W, Sreekanta S, Lu Y, Bethke G, Tsuda K, Katagiri F & Glazebrook J (2013) The CALMODULIN-BINDING PROTEIN60 family includes both negative and positive regulators of plant immunity. *Plant Physiol.* **163:** 1741–51

Tsuda K, Mine A, Bethke G, Igarashi D, Botanga CJ, Tsuda Y, Glazebrook J, Sato M & Katagiri F (2013) Dual Regulation of Gene Expression Mediated by Extended MAPK Activation and Salicylic Acid Contributes to Robust Innate Immunity in Arabidopsis thaliana. *PLoS Genet.* **9:** e1004015

Uchida N, Sakamoto T, Kurata T & Tasaka M (2011) Identification of EMS-induced causal mutations in a non-reference arabidopsis thaliana accession by whole genome sequencing. *Plant Cell Physiol.* **52:** 716–722

Umbreen S, Lubega J & Loake G (2019) Sulphur: the heart of nitric oxide-dependent redox. *J. Exp. Bot.*

Urquiza-García U & Millar A (2018) Expanding the bioluminescence reporter toolkit for plant chronobiology with NanoLUC. *bioRxiv*

van Verk MC, Bol JF & Linthorst HJM (2011a) Prospecting for Genes involved in transcriptional regulation of plant defenses, a bioinformatics approach. *BMC Plant Biol.* **11:**

van Verk MC, Bol JF & Linthorst HJM (2011b) WRKY transcription factors involved in activation of SA biosynthesis genes. *BMC Plant Biol.* **11:** 89

Vlot a C, Dempsey DA & Klessig DF (2009) Salicylic Acid, a multifaceted hormone to combat disease. *Annu. Rev. Phytopathol.* **47:** 177–206

Walters M (2015) The plant innate immune system. **26:** 8–12

Wang BL, Tang XY, Cheng LY, Zhang AZ, Zhang WH, Zhang FS, Liu JQ, Cao Y,

Allan DL, Vance CP & Shen JB (2010) Nitric oxide is involved in phosphorus deficiency-induced cluster-root development and citrate exudation in white lupin. *New Phytol.* **187:** 1112–1123

Wang C, El-Shetehy M, Shine MB, Yu K, Navarre D, Wendehenne D, Kachroo A & Kachroo P (2014a) Free Radicals Mediate Systemic Acquired Resistance. *Cell Rep.* **7:** 348–355

Wang H, Wang F, Wang W, Yao X, Wei D, Cheng H & Deng Z (2014b) Improving the expression of recombinant proteins in E. coli BL21 (DE3) under acetate stress: An alkaline ph shift approach. *PLoS One* **9:** 1–11

Wang L, Tsuda K, Sato M, Cohen JD, Katagiri F & Glazebrook J (2009a) Arabidopsis CaM binding protein CBP60g contributes to MAMP-induced SA accumulation and is involved in disease resistance against Pseudomonas syringae. *PLoS Pathog.* **5:**

Wang L, Tsuda K, Truman W, Sato M, Nguyen L V., Katagiri F & Glazebrook J (2011a) CBP60g and SARD1 play partially redundant critical roles in salicylic acid signaling. *Plant J.* **67:** 1029–1041

Wang W, Barnaby JY, Tada Y, Li H, Tör M, Caldelari D, Lee DU, Fu XD & Dong X (2011b) Timing of plant immune responses by a central circadian regulator. *Nature* **470:** 110–115

Wang X, Gao J, Zhu Z, Dong X, Wang X, Ren G, Zhou X & Kuai B (2015) TCP transcription factors are critical for the coordinated regulation of *ISOCHORISMATE SYNTHASE 1* expression in *Arabidopsis thaliana*. *Plant J.* **82:** 151–162

Wang YQ, Feechan A, Yun BW, Shafiei R, Hofmann A, Taylor P, Xue P, Yang FQ, Xie ZS, Pallas JA, Chu CC & Loake GJ (2009b) S-nitrosylation of AtSABP3 antagonizes the expression of plant immunity. *J. Biol. Chem.* **284:** 2131–2137

Wildermuth MC, Dewdney J, Wu G & Ausubel FM (2001) Isochorismate synthase is required to synthesize salicylic acid for plant defence. *Nature* **414:** 562–5

Wilkinson JQ & Crawford NM (1991) Identification of the Arabidopsis CHL3 Gene as the Nitrate Reductase Structural Gene NIA2. *Plant Cell* **3:** 461

Wrzaczek M, Brosché M & Kangasjärvi J (2013) ROS signaling loops - production, perception, regulation. *Curr. Opin. Plant Biol.* **16:** 575–82

Yang J, Giles LJ, Ruppelt C, Mendel RR, Bittner F & Kirk ML (2015) Oxyl and hydroxyl radical transfer in mitochondrial amidoxime reducing component-catalyzed nitrite reduction. *J. Am. Chem. Soc.* **137:** 5276–5279

Yarmolinsky D, Brychkova G, Fluhr R & Sagi M (2012) Sulfite Reductase Protects Plants against Sulfite Toxicity. *Plant Physiol.* **161:** 725–743

Yu M, Lamattina L, Spoel SH & Loake GJ (2014) Nitric oxide function in plant biology : a redox cue in deconvolution.

Yu M, Yun BW, Spoel SH & Loake GJ (2012) A sleigh ride through the SNO: Regulation of plant immune function by protein S-nitrosylation. *Curr. Opin. Plant Biol.* **15:** 424–430

Yun BW, Feechan A, Yin M, Saidi NBB, Le Bihan T, Yu M, Moore JW, Kang JG, Kwon

E, Spoel SH, Pallas JA & Loake GJ (2011) S-nitrosylation of NADPH oxidase regulates cell death in plant immunity. *Nature* **478:** 264–268 Available at: http://dx.doi.org/10.1038/nature10427

Yun BW, Skelly MJ, Yin M, Yu M, Mun BG, Lee SU, Hussain A, Spoel SH & Loake GJ (2016) Nitric oxide and S-nitrosoglutathione function additively during plant immunity. *New Phytol.* **211:** 516–526

Zhang C, Xie Q, Anderson RG, Ng G, Seitz NC, Peterson T, McClung CR, McDowell JM, Kong D, Kwak JM & Lu H (2013a) Crosstalk between the Circadian Clock and Innate Immunity in Arabidopsis. *PLoS Pathog.* **9:**

Zhang F, Yao J, Ke J, Zhang L, Lam VQ, Xin XF, Zhou XE, Chen J, Brunzelle J, Griffin PR, Zhou M, Xu HE, Melcher K & He SY (2015) Structural basis of JAZ repression of MYC transcription factors in jasmonate signalling. *Nature* **525:** 269–273

Zhang L, Song G, Xu T, Wu QP, Shao XX, Liu YL, Xu ZG & Guo ZY (2013b) A novel ultrasensitive bioluminescent receptor-binding assay of INSL3 through chemical conjugation with nanoluciferase. *Biochimie* **95:** 2454–2459

Zhang X, Wang C, Zhang Y, Sun Y & Mou Z (2012) The Arabidopsis Mediator Complex Subunit16 Positively Regulates Salicylate-Mediated Systemic Acquired Resistance and Jasmonate/Ethylene-Induced Defense Pathways. *Plant Cell* **24:** 4294–4309

Zhang X, Yao J, Zhang Y, Sun Y & Mou Z (2013c) The Arabidopsis Mediator complex subunits MED14/SWP and MED16/SFR6/IEN1 differentially regulate defense gene expression in plant immune responses. *Plant J.* **75:** 484–497

Zhang Y, Boguslaw S & Godzik A (2007) Between order and disorder in protein structures – analysis of “dual personality” fragments in proteins. *Magn Reson Imaging* **15:** 1141–1147

Zhang Y, Xu S, Ding P, Wang D, Cheng YT, He J, Gao M, Xu F, Li Y, Zhu Z & Li X (2010) Control of salicylic acid synthesis and systemic acquired resistance by two members of a plant-specific family of transcription factors. *Proc Natl Acad Sci U S A* **107:** 18220–18225

Zheng X, Spivey NW, Zeng W, Liu P-P, Fu ZQ, Klessig DF, He SY & Dong X (2012a) Coronatine Promotes Pseudomonas syringae Virulence in Plants by Activating a Signaling Cascade that Inhibits Salicylic Acid Accumulation. *Cell Host Microbe* **11:** 587–596

Zheng X, Zhou M, Yoo H, Pruneda-Paz JL, Spivey NW, Kay S a. & Dong X (2015) Spatial and temporal regulation of biosynthesis of the plant immune signal salicylic acid. *Proc. Natl. Acad. Sci.* **112:** 201511182

Zheng XY, Spivey NW, Zeng W, Liu PP, Fu ZQ, Klessig DF, He SY & Dong X (2012b) Coronatine promotes pseudomonas syringae virulence in plants by activating a signaling cascade that inhibits salicylic acid accumulation. *Cell Host Microbe* **11:** 587–596

Zhou C, Liu Z, Zhu L, Ma Z, Wang J & Zhu J (2016) Exogenous melatonin improves plant iron deficiency tolerance via increased accumulation of polyamine-mediated nitric oxide. *Int. J. Mol. Sci.* **17:**

Zhou M, Wang W, Karapetyan S, Mwimba M, Marqués J, Buchler NE & Dong X (2015) Redox rhythm reinforces the circadian clock to gate immune response. *Nature* **523:** 472–476